

See discussions, stats, and author profiles for this publication at: <https://www.researchgate.net/publication/258640667>

Catalytic Oxidation of Light Alkanes (C-1-C-4) by Heteropoly Compounds

ARTICLE *in* CHEMICAL REVIEWS · NOVEMBER 2013

Impact Factor: 46.57 · DOI: 10.1021/cr300302b · Source: PubMed

CITATIONS

36

READS

115

7 AUTHORS, INCLUDING:



Miao Sun

Saudi Arabian Oil Company

11 PUBLICATIONS 184 CITATIONS

[SEE PROFILE](#)



Frédéric Lefebvre

French National Centre for Scientific Research

279 PUBLICATIONS 4,707 CITATIONS

[SEE PROFILE](#)



Jean marie Basset

King Abdullah University of Science and Techn...

479 PUBLICATIONS 10,653 CITATIONS

[SEE PROFILE](#)

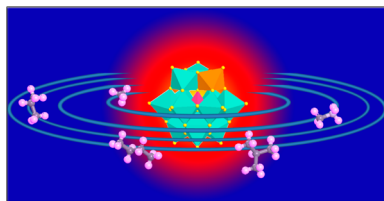
Catalytic Oxidation of Light Alkanes (C_1 – C_4) by Heteropoly Compounds

Miao Sun,*[†] Jizhe Zhang,[‡] Piotr Putaj,^{||} Valerie Caps,[§] Frédéric Lefebvre,^{||} Jeremie Pelletier,[§] and Jean-Marie Basset*,[§]

[†]Research and Development Center, Saudi Aramco Oil Company, Dhahran 31311, Saudi Arabia

[‡]Division of Chemical and Life Sciences and Engineering, and [§]KAUST Catalysis Center, King Abdullah University of Science and Technology, Thuwal 23955-6900, Saudi Arabia

^{||}Laboratoire de Chimie Organométallique de Surface, CPE Lyon, 43 Bd du 11 Novembre 1918, 69622 Villeurbanne, France



CONTENTS

1. Introduction and Scope	982	6.2.3. Selective Oxidation of Ethane to Ethylene and Acetic Acid	995
2. Selective Oxidation of Light Alkanes	982	6.3. Conclusion	998
2.1. Economic Incentives: Cheaper Feedstocks	983	7. Selective Oxidation of Propane	998
2.2. Scientific Trends: C–H Activation at the Lowest Temperature	984	7.1. Oxidative Dehydrogenation (ODH) of Propane to Propylene	998
3. Heteropoly Compounds	985	7.1.1. General Mechanisms for Propane ODH to Propylene Reaction	999
4. General Aspect of Light Alkane Oxidation Mechanism	986	7.1.2. ODH of Propane to Propylene over HPC Catalysts	999
5. Selective Oxidation of Methane	987	7.2. Selective Oxidation of Propane to Acrolein and Acrylic Acid	1001
5.1. General Mechanisms for Methane Selective Oxidation to Oxygenates	988	7.2.1. General Mechanisms for Selective Oxidation of Propane to Acrolein and Acrylic Acid	1001
5.2. Selective Oxidation of Methane over HPC Catalysts	988	7.2.2. Selective Oxidation of Propane to Acrolein and Acrylic Acid over HPC Catalysts	1002
5.2.1. Selective Oxidation of Methane to Methanol and Formaldehyde at High Temperature	988	7.3. Conclusion	1006
5.2.2. Selective Oxidation of Methane to Formic Acid at Low Temperature	989	8. Selective Oxidation of Butane	1008
5.2.3. Selective Oxidation of Methane to Methyl Formate and Methyl Trifluoroacetate at Low Temperature	990	8.1. Selective Oxidation of <i>n</i> -Butane to Maleic Acid or Maleic Anhydride	1008
5.2.4. Selective Oxidation of Methane to Methyl Acetate and Methyl Trifluoroacetate at Low Temperature	990	8.1.1. General Mechanisms for Selective Oxidation of <i>n</i> -Butane to Maleic Anhydride or Maleic Acid	1008
5.2.5. Selective Oxidation of Methane to Methanol at Low Temperature	991	8.1.2. Selective Oxidation of <i>n</i> -Butane to Maleic Acid or Maleic Anhydride over HPC Catalysts	1008
6. Selective Oxidation of Ethane	992	8.2. Oxidative Dehydrogenation of Iso-butane to Iso-butene	1008
6.1. General Mechanisms for Ethane Selective Oxidation to Ethylene and Oxygenates	993	8.3. Selective Oxidation of Iso-butane to Methacrolein and Methacrylic Acid	1010
6.2. Selective Oxidation of Ethane over HPC Catalysts	993	8.3.1. General Mechanisms for Selective Oxidation of Iso-butane to Methacrolein and Methacrylic Acid	1010
6.2.1. Oxidative Dehydrogenation of Ethane to Ethylene	993	8.3.2. Selective Oxidation of Iso-butane to Methacrolein and Methacrylic Acid over HPC Catalysts	1010
6.2.2. Selective Oxidation of Ethane to Ethylene and Acetaldehyde	995	9. Conclusion	1014
		Author Information	1014
		Corresponding Authors Notes	1014
			1015

Received: May 23, 2011

Published: November 18, 2013

Biographies	1015
Abbreviations	1016
References	1017

1. INTRODUCTION AND SCOPE

Heteropoly compounds (HPC) occupy a singular position in the catalysis arena, for their composition is akin to that of the many metal oxide-based catalysts used in heterogeneous processes. One type of transformation that has long resisted research efforts toward commercial processes is the selective oxidation of light alkanes (C_1-C_4). In this respect, HPC can be designed rationally and conveniently prepared so as to modify the catalyst in a controlled way inaccessible with common metal-oxide catalysis. Not only do their smaller size and their stability render them structurally more defined, but several have displayed remarkable performance for catalytic conversions. Their availability and low cost make them particularly interesting as substrates to supply chemical feedstock. As a result, the performance of a large series of HPC has been investigated for the oxidation of light alkanes. Considering that under the conditions employed (elevated temperature, strong oxidant) those substrates are prone to complete oxidation, catalysts directing selectively the reaction toward partially oxidized product remain an open challenge.

In a broader context, understanding catalysis is crucial for the development of industrial applications absolutely necessary for making the future sustainable. In essence, catalysis is a molecular phenomenon in which substrates are transformed into product under the direction of a minor amount of the catalyst, a molecule, a biomolecule, or a solid. In heterogeneous catalysis, which is still dominating in industrial processes, oxides and mixed oxides have been used for decades in acid–base and in oxidation catalysis. Development of heterogeneous catalysis has generally been an iterative strategy resulting from trial and error. Mixed oxides are still the most efficient way to achieve the best production but remain poorly understood for the many reactions they promote. For instance, more than eight different elements in the most active and selective oxidation catalyst have been identified.^{1–5}

Unfortunately, this mixed composition is a real obstacle for rationalizing the catalytic phenomena at the molecular level. Undoubtedly, in the long term, there must be a molecular understanding to establish accurately the structure–activity relationships and predict a more rational approach of heterogeneous catalysis.

In this context, heteropoly compounds have attracted a huge interest not only in acid–base but also in oxidation catalysis. Those compounds are a large class of nanosized clusters containing transition metals, main group elements, plus a certain amount of protons and/or water molecules. Their structure, size, and properties correspond to a unique situation between molecules and oxides, which allows, in principle, molecular chemists and surface science chemists to find a common field of discussion. They are already used commercially in acid-based catalysis because of their acidic properties, which can be monitored at will.⁶ The interest of these “oxide molecules” is their molecular structure, which reaches the nanoscale range and makes us suggest an easier molecular understanding of mechanism: are HPC good models of heterogeneous catalysis, are they good precursors of heterogeneous catalyst with a kind of controlled composition, and are they real catalysts by themselves either supported or

Table 1. Processes under Study or Development for the Oxyfunctionalization of Light Alkanes (C_1-C_4) in the Petrochemical Industry^{18 a}

raw material	product	phase	development stage
methane	methanol	gas, het./hom.	pilot plan
methane	syngas	gas, het./hom.	pilot plan
methane	ethylene	gas, het./hom.	pilot plan
ethane	acetic acid	gas, heterog.	industrial
ethane	ethylene	gas, het./hom.	research
propane	acrylic acid	gas or liquid	research
propane	propyl alcohol	liquid, homog.	research
propane	acrylonitrile	gas, heterog.	industrial
propane	propylene	gas, heterog.	research
n-butane	acetic acid	liquid, homog.	industrial
n-butane	maleic anhydride	gas, heterog.	industrial
n-butane	butadiene	gas, heterog.	industrial abandoned
iso-butane	methacrylic acid	gas, heterog.	pilot plan
iso-butane	iso-butene	gas, heterog.	research
iso-butane	t-butyl alcohol	liquid, het. or hom.	research

^aThe het./hom. indicates the likely presence of a mechanism initiated on the catalyst surface and transferred to the gas phase.

unsupported? All of these questions boosted this area in the last 20 years and have made the heteropoly acid (HPA) ideal for trying to rationalize oxidation catalysts.

The scope of this work is to review HPC-based catalysts used in catalytic oxidation of light alkanes (C_1-C_4). Even though classic mixed oxides catalysts such as Mo–V–Te–Nb(Sb)–O show outstanding performance in alkanes oxidation, they are technically different from HPC catalysts and have already been systematically reviewed by many expert scientists.^{7–11} Therefore, in this Review, only HPC catalysts have been focused so as to provide an overview of other efficient approaches toward selective oxidation of light alkanes (C_1-C_4). In a first part, economic background of alkane transformation is tackled prior to a concise scientific description of the selective oxidation of alkane. An overview of the properties of HPC is then given with emphasis being placed on their effect over catalysis. The next sections examine the various HPC according to the reaction they achieve on substrate beginning with methane and concluding with iso-butane. Solid mechanism studies appear difficult to propose, but are very likely to draw similarity to the existing oxidation process. Nonetheless, the rich library available of HPC with their tailored formula and structure is undoubtedly a valuable tool to the understanding of this chemistry.

This Review does not draw a structure activity relationship in HPC, which still appears to be difficult, but rather outlines a picture of the situation taken from the numerous examples given in the literature.

2. SELECTIVE OXIDATION OF LIGHT ALKANES

The development of new catalysis for the selective oxidation of alkane is at the intersection between strong economic interests for optimizing the manufacture of chemical building blocks and the enduring scientific challenge to activate these very inert compounds to functionalize them.

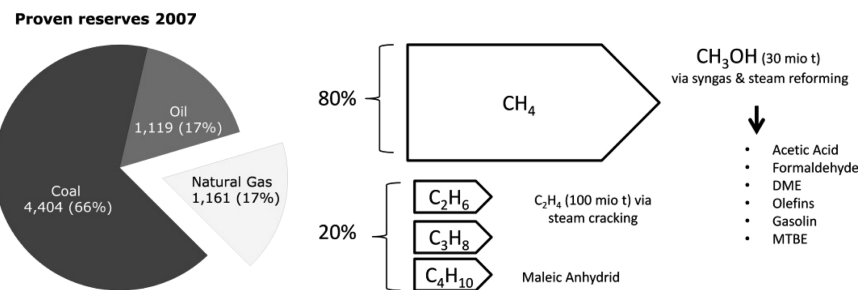
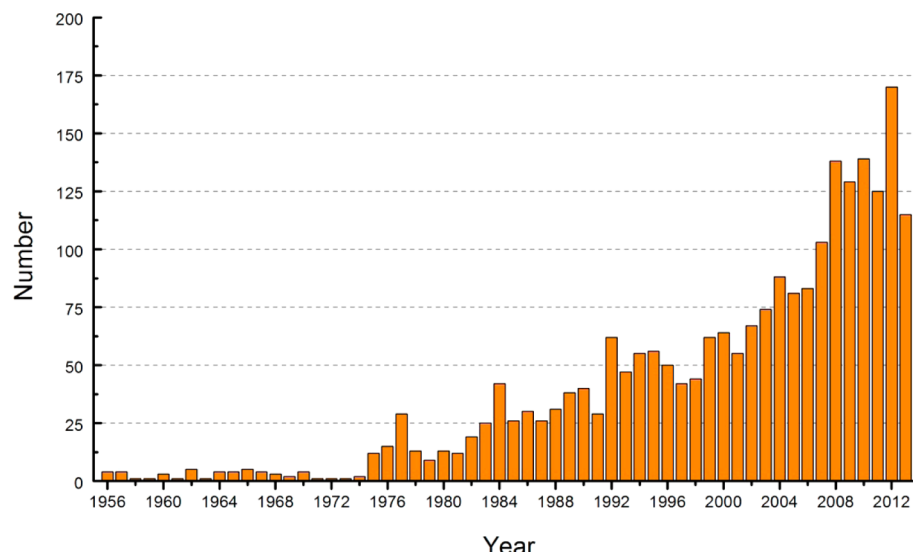


Figure 1. Natural gas overview as a chemical feedstock. Energetic use is not represented.

Chart 1. Number of Patents Filled for Processes Using Heteropoly Acid as Catalysts per Year with the Keywords “Heteropoly Acid” and “Catalyst”^a



^aStatistical data from SciFinder.

Light alkanes are found in abundance in natural gas, with methane being the prime component 80–98% far ahead of ethane, propane, and butane.¹² Exploiting their energetic content for heating, electricity, and transportation surpasses largely other applications such as chemical feedstock. In addition, natural gas extraction has become increasingly significant as compared to other fossil energies for its supplies are expected to last longer than oil (roughly 200 years in the Middle East taking into account current known reserve and consumption).¹³ Recent interests have been fueled by the emerging of shale gas, abundant and more spread worldwide than traditional natural gas basins. Transforming methane or the next higher alkanes near the extraction sites is also desirable to facilitate transportation or storage.

Utilization of natural gas as a chemical feedstock is known for a few processes (Figure 1). It generally requires elevated pressure and temperature (above 500 °C). Ethane can lead to ethylene by steam cracking, while methane can be used to produce syngas ($\text{CO}+\text{H}_2$) by steam reforming, the latter being a starting material to manufacture many chemicals (via Fischer–Tropsch) including methanol, a pivotal building block for formaldehyde, acetic acid, and MTBE (methyl tertiary butyl ether).¹⁴ To our knowledge, the commercial examples for the selective oxidation of alkane are the direct conversion of butane into acetic acid, butane into maleic anhydride, propane to acrylic acid, and butane to butadiene.^{15,16}

2.1. Economic Incentives: Cheaper Feedstocks

Producing commodity chemicals directly from alkane feedstocks with the view to replace more expensive building blocks (e.g., methanol, olefin/alkenes, etc.) is hardly a new notion. A few decades ago, interests on the subject rose alongside oil prices before fading due to the difficulty to design economically relevant and industrially practical processes. Several attempts were found to be unsuccessful. For example, Du Pont has developed a technology for the production of maleic anhydride from oxidation of butane, using a transport bed reactor (also referred to as a circulating-fluidized-bed reactor, CFBR). The process was commercialized in 1996 in Gijon, Spain. However, due to various operational problems, the plant was closed in 2004 and later dismantled.¹⁷ This is unfortunate because the plant was designed as a consequence of a well-known redox mechanism! Yet the potential economic benefits, largely impacted by reducing oil supply in the long term, are pushing again research and development efforts toward this end.

Considering all oxidative dehydrogenation products of interest for the chemical industry, three categories can be distinguished: (i) alkenes, that is, ethylene and propylene; (ii) oxygenates; and (iii) heterocompounds. These chemicals are generally manufactured by high-temperature, endothermic processes, such as cracking, dehydrogenation, and reforming, starting from petroleum or natural gas.

Table 2. Industrial Processes Catalyzed by Heteropoly Acids²⁵

reaction	reaction type	catalyst	start (ref)
$\text{CH}_2=\text{CHCH}_3 + \text{H}_2\text{O} \rightarrow \text{CH}_3\text{CH}(\text{OH})\text{CH}_3$	homogeneous	$\text{H}_4\text{SiW}_{12}\text{O}_{40}$	1972 (26)
$2\text{CH}_2=\text{C}(\text{CH}_3)\text{CHO} + \text{O}_2 \rightarrow 2\text{CH}_2=\text{C}(\text{CH}_3)\text{COOH}$	heterogeneous	Mo–V–P–HPA	1982 (20)
$\text{CH}_2=\text{C}(\text{CH}_3)_2 + \text{H}_2\text{O} \rightarrow (\text{CH}_3)_3\text{COH}$	homogeneous	$\text{H}_3\text{PMo}_2\text{O}_{40}$	1984 (20)
$n\text{THF} + \text{H}_2\text{O} \rightarrow \text{HO}-[-(\text{CH}_2)_4-\text{O}-]_n-\text{H}$	biphasic	$\text{H}_3\text{PW}_{12}\text{O}_{40}$	1985 (21,27)
$\text{CH}_3\text{CH}=\text{CHCH}_3 + \text{H}_2\text{O} \rightarrow \text{CH}_3\text{CH}(\text{OH})\text{CH}_2\text{CH}_3$	homogeneous	$\text{H}_3\text{PMo}_2\text{O}_{40}$	1989 (22)
ketone amination to imine	heterogeneous	supported HPA	1996 (24)
$\text{CH}_2=\text{CH}_2 + \text{O}_2 \rightarrow \text{CH}_3\text{COOH}$	heterogeneous	$\text{Pd}-\text{H}_4\text{SiW}_{12}\text{O}_{40}/\text{SiO}_2$	1997 (28)
$\text{CH}_2=\text{CH}_2 + \text{CH}_3\text{COOH} \rightarrow \text{CH}_3\text{CH}_2\text{O}_2\text{CCH}_3$	heterogeneous	$\text{H}_4\text{SiW}_{12}\text{O}_{40}/\text{SiO}_2$	2001 (29)

For (i), the incentive is not feedstock replacement but improvement in process economics through higher yield and/or lower capital cost. Regarding (ii) and (iii), these consist of chemical intermediates currently produced from feedstocks that are more expensive than alkanes. This is more challenging technically as almost no commercial applications consuming the alkane feedstock currently operate. Any new production chains will have to be optimized to be competitive against already established supplies regarding activity, selectivity, and lifetime. This may also be highly rewarding economically as alkanes are significantly cheaper than the actual feedstocks (olefins, aromatics).¹⁹ Research efforts have been directed toward many different products so as to implement new commercial processes (Table 1).¹⁸ Most are still in the research stage, but at least five of the processes listed have been commercialized. It should be noted that adjusting processes regarding activity, selectivity, and reusability to strike the right balance is difficult.

Heteropolyanion-based catalysis is the subject of increasing attention (Chart 1) from the industrial world and found use in several commercial processes, with Japan being the world leader.^{20–22} Presently, over 80% of the patent applications concerning polyoxometalates are related to catalysis.²³

After first successful industrial application of heteropoly acid as a homogeneous catalysts for the hydration of propylene (Tokuyama process) in 1972,^{20,22} several new large-scale processes have been developed employing heteropoly acids or their salts as acid or oxidation catalysts (Table 2). Among them are the hydration of olefins, the vapor-phase oxidation of methacrolein to methacrylic acid and of ethylene to acetic acid, and the gas-phase synthesis of ethyl acetate from ethanol and acetic acid. On a smaller scale, heteropoly acids are used as acid catalysts for the polymerization of tetrahydrofuran in a liquid/liquid biphasic system and synthesis of glycosides in a homogeneous system.²⁰ Armor et al.²⁴ reviewed recent industrial applications of heteropoly acid catalysts in the U.S., which include the continuous amination of a ketone to imine over a supported HPA in the synthesis of isophorone nitrileimine by DuPont (1996 start).

2.2. Scientific Trends: C–H Activation at the Lowest Temperature

Regardless of the considered transformation of any alkane, selective oxidation presents at least two issues requiring the attention of the catalysis chemists: (i) how to activate C–H bonds using the lowest amount of energy possible to initiate the transformation; and (ii) how to harness the oxidation reaction to product selectively targeted compounds. Many factors are affecting these reactions, some related to the chemical properties of the feed and products, and others related to the catalyst employed.

Several problems are directly connected to the inertness of light alkanes. First, light compounds, in particular methane, are difficult to physisorb on solid catalysts. The “stickiness” of an

Table 3. Representative C–H Bond Dissociation Energies³¹

bond type	bond dissociation energy (kcal mol ⁻¹) ^a
H–CH ₃	105
H–CH ₂ R	98–101
H–CHR ₂	95–99
H–CR ₃	93–95
H–CH=CH ₂	104–111
H–CH ₂ CH=CH ₂	86
H–C≡CH	132–133
H–CH ₂ C≡CH	89
H–C ₆ H ₅	111–113
H–CH ₂ C ₆ H ₅	88–90
H–CH ₂ OH	94–96
H–C(=O)R	86–88
H–CH ₂ C(=O)R	92–98
H–CH ₂ CO ₂ H	97–99

^aWhere ranges are displayed, they represent disagreements between the three compendia used, which may amount to as much as 5 kcal/mol, but the basic relationships between the various types of bond energies are consistent.

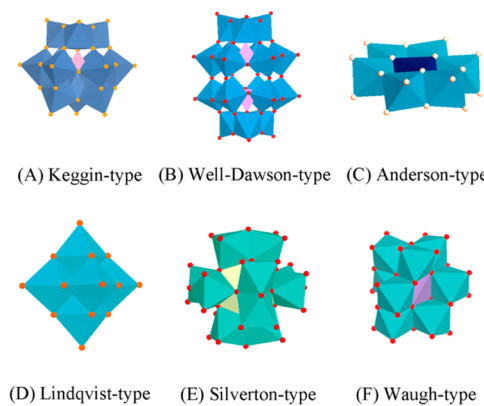


Figure 2. Basic heteropolyanion structures in polyhedral representation: (A) Keggin-type; (B) Well–Dawson-type; (C) Anderson-type; (D) Lindqvist-type; (E) Silverton-type; and (F) Waugh-type.

alkane molecule to an oxidized surface depends on its size; a larger molecule can be physisorbed much more effectively in a predissociative state than a small molecule.³⁰ Second, the activation of a C–H bond is generally the difficult and rate-determining step. This is perhaps due to the high strength as indicated by the bond dissociation energy (see Table 3).³¹

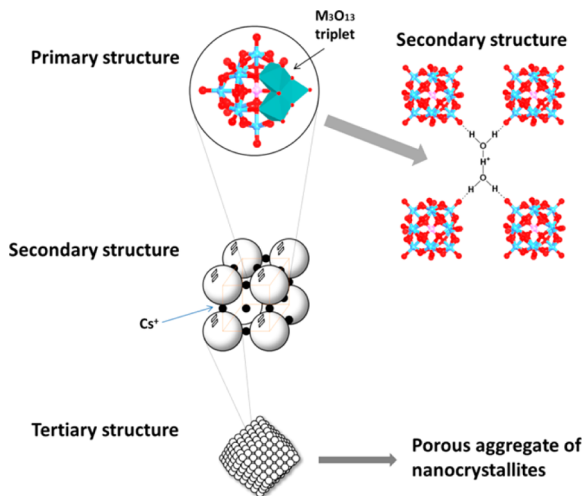


Figure 3. Primary, secondary, and tertiary structures of heteropoly compounds.⁶

Once the substrate is activated, controlling the selectivity of the oxidation has proven challenging. Under the operating conditions, high pressure and high temperature, all of the products are usually more reactive than the reactants and prone toward total combustion to CO_2 . High selectivity for oxidation of alkane can be achieved for very specific substrates, specifically those yielding relatively stable products, for example, propane to acrylic acid, butane to maleic anhydride, etc. The most noteworthy example, and commercially employed, of this series is probably the direct conversion of butane into maleic anhydride with high selectivities (up to 97% at 65% conversion).³²

Several different types of catalysts (e.g., nonreducible oxides, reducible oxides, metals) are capable of oxidizing saturated hydrocarbons with varying efficiencies. As usual with solid catalysts employed to treat gas or liquid feeds, the identification of the elementary steps and the observation of the intermediates are difficult. The strong conditions (e.g., high temperature and high pressure) are also making *in situ* studies more complicated. Finally, metal oxides-based catalysts are believed to display a variety of sites, each with potentially different affinities for the transformation considered. There is an obvious need for catalytic systems that can be modified on purpose at the molecular level so as to simplify *in situ* studies.

Heteropoly acids (HPA) can be envisaged as a key compound to comprehend the catalysis of metal oxide. Arguably, they are small and are significantly more defined than their heterogeneous catalyst counterparts. Heteropoly compounds are frequently used as model systems for fundamental research, providing unique opportunities for mechanistic studies on the molecular level (vide infra).²⁵

3. HETEROPOLY COMPOUNDS

Heteropoly compounds (HPC) belong to a large family of anionic transition metal–oxygen clusters that includes heteropoly acids (e.g., $\text{H}_3\text{PW}_{12}\text{O}_{40}$), salts of heteropoly acids (e.g., $\text{Cs}_3\text{PW}_{12}\text{O}_{40}$), and transition-metal-substituted polyoxometalates (e.g., $\text{PVMo}_{11}\text{O}_{40}^{4-}$, $[\gamma\text{-SiW}_{10}\{\text{Fe}(\text{OH}_2)\}_2\text{O}_{38}]^{6-}$). Because of the unique bifunctional redox and acidic properties of HPC (vide infra), their performance as catalysts for the partial oxidation of organic compounds has attracted much attention in the last four decades. It is still a rapidly expanding

area, in both homogeneous and heterogeneous systems, due to their unusual versatility and compatibility with environmentally friendly conditions (employing oxidants such as O_2 and H_2O_2).

HPC, unlike metal oxides and zeolites that have metal oxygen lattices (vide supra), consist of discrete anionic units of metal oxide that are the primary structure of the material. They can be deconstructed as metal–oxygen polyhedrons (e.g., usually Mo^{6+} or W^{6+} , but other metals have been reported, such as V, Nb, or Fe named “addenda”) units organized by at least one central atom being referred to as the “heteroatom” (e.g., Si^{4+} , Ge^{4+} , P^{5+} , As^{5+} , B^{3+} , etc.) (Figure 2).

While heteropolyanions can adopt many structural configurations, Keggin, Anderson, and Wells–Dawson structures, respectively, $[\text{XM}_{12}\text{O}_{40}]^{n-}$, $[\text{XM}_6\text{O}_{24}]^{n-}$, and $[\text{X}_2\text{M}_{18}\text{O}_{62}]^{n-}$, have been the most extensively investigated for catalytic applications due mainly to their relatively high stability and ease of accessibility.^{6,25,33–37}

The primary structures form a secondary structure by being associated by interstitial guest species (e.g., water, Cs^+) to arrange into crystals; organic guest species (e.g., alcohols, ethers, amines) may also be incorporated. Aggregates of the secondary structures form a tertiary structure that describes the physical characteristics of the material (e.g., porosity, particle size, and surface area).

Using Keggin-type heteropolyanion as an illustration, the primary, secondary, and tertiary structures of HPC are depicted in Figure 3.^{6,25,34}

Variations in the structure and chemical composition modify the acidic and oxidative properties of HPC and thereby affect their catalytic performances in oxidation reactions. HPC have several properties attractive for oxidation catalysis,⁶ the most important being their multifunctionality and structural mobility. On the one hand, they possess a very strong Brønsted acidity and are efficient oxidants, exhibiting fast reversible multi-electron redox transformations under mild conditions. Their acid–base and redox properties can be varied over a wide range by changing the chemical composition. On the other hand, solid heteropoly compounds possess a discrete ionic structure, comprising fairly mobile structural unites, heteropolyanions and counter-cations, unlike the network structure of, for example, zeolites and metal oxides. The structure is frequently preserved upon substitution or oxidation/reduction and manifests itself to exhibit extremely high proton mobility and a “pseudoliquid phase”. Moreover, many HPC have a very high solubility in polar solvents and fairly high thermal stability in the solid state.²⁵

Catalysis can be performed in homogeneous as well as in heterogeneous systems (gas–solid, liquid–solid, or biphasic liquid–liquid) systems. HPC can be used in various phases, as homogeneous liquids, two-phase liquids (in phase-transfer

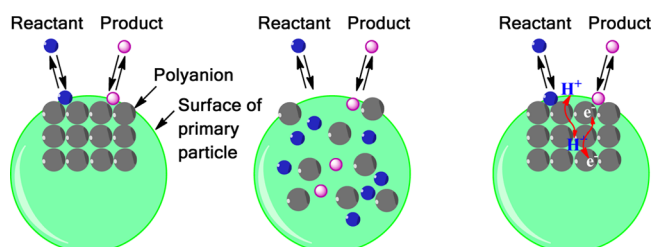


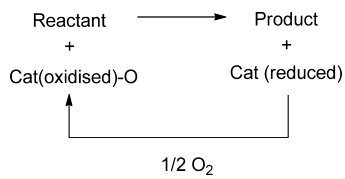
Figure 4. Three types of catalysis by HPC: (a) surface-type; (b) bulk-type (I) (or pseudoliquid); and (c) bulk-type (II).⁶

catalysis), liquid–solid combinations, and gas–solid combinations, etc. Three classes of catalysis are understood to happen in liquid–solid and gas–solid combinations (Figure 4): (a) surface-type catalysis; (b) bulk-type (I), or pseudoliquid, catalysis; and (c) bulk-type (II) catalysis. Surface-type catalysis (a) is similar to heterogeneous catalysis, whereby the reactions occur on the outer surface and pore walls of solid catalysts. The reaction rate is thus related to the catalytic surface area. Bulk-type I catalysis (b) was observed in acid catalysis at relatively low temperatures with heteropolyanions, as a salt or in their acid forms. The reactant molecules are absorbed in the ionic crystal between the polyanions, as opposed to inside them, by replacing crystallization water or by expanding lattices. The polyanion structure itself remains intact. This catalysis has been coined “pseudoliquid” for the solid phase behaves like a solution; in the ideal case, the reaction rate is correlated to the volume of the catalyst. For the acid-catalyzed reaction, the rate is directly connected to the total number of acidic groups in the solid bulk. Bulk-type II catalysis (c) was documented for some oxidation reactions at high temperatures. Although the principal reaction may proceed on the surface, the whole solid bulk takes part in redox catalysis due to the rapid migration into the bulk of redox carriers such as protons and electrons.⁶

4. GENERAL ASPECT OF LIGHT ALKANE OXIDATION MECHANISM

In heterogeneous catalysis, it is accepted that catalytic transformation of gas or liquid occurs at the surface of solid catalysts following a well-documented sequence: interaction and binding of a surface site with an adsorbate, resulting bonds changes, reactions between reactants, and the final desorption process. Consequently, the identification of the active sites, their properties, and the influence of their geometric and chemical environment is paramount.³⁸ In principle, several competing mechanisms can occur simultaneously, and unambiguous determination remains challenging. In practice, the effects of solvent, counterions, aggregates, or surface inhomogeneities are still lacking certain understanding, which lead to the identification of reaction centers and of their intrinsic properties as a reactive intermediate even more complicated to apprehend.³⁹ Light alkanes are generally difficult to activate caused by their stable chemical properties including significant energies required for both homo- and heterolytic C–H bond cleavages, the negligibly small (if not negative) electron

Scheme 1. Simplified Scheme of Mars–Van Krevelen Mechanism



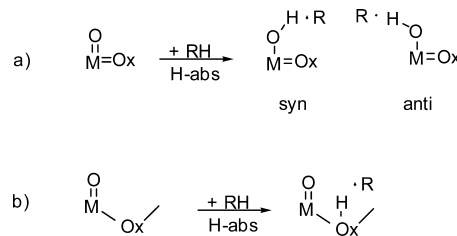
affinity, the large ionization energy, the huge HOMO–LUMO gap, the extremely high pK_a value, the absence of a dipole moment, and the rather small polarizability.³⁹

In the case of metal oxide catalysts, the metal atoms, usually in high oxidation states, are bound by oxygens, either terminal or bridging. The oxidation of alkane is believed to globally follow the classic Mars–Van Krevelen mechanism (Scheme 1) in which the oxygen atoms from surface are activating the

substrate before undergoing further chemical transformation. The catalytic reduced metal sites can then be regenerated by molecular oxidants such as O₂. The real process occurring is a very complex mechanism in which surface oxygens and bulk oxygens play different roles. The extent to which the alkane is oxidized depends on many factors including the conditions, temperature, pressure, and the catalyst employed (precatalysts, oxidant).

Oxidation of light alkanes does necessarily pass via a C–H activation step; several mechanisms^{40–44} have been proposed

Scheme 2. C–H Bond Activation of Alkanes on Surface Metal Oxo Species⁴⁵

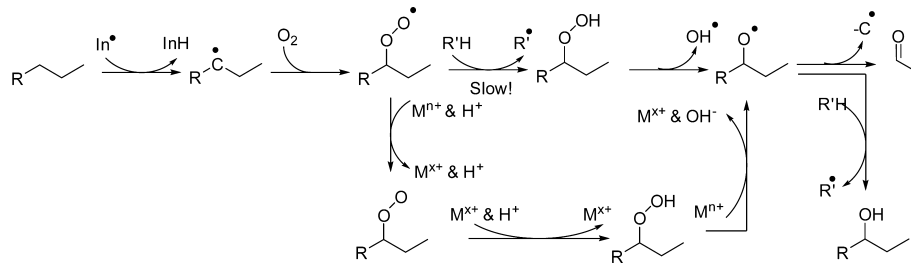


for that particular step without a strong consensus being agreed on, although it is accepted that terminal oxygen are more reactive than bridging ones, thus being the center of the reaction.⁴⁵ According to those reported theories, terminal oxygen or bridging oxygens can interact with the alkane to generate free radicals (Scheme 2). Density functional theory (DFT) calculation supports the H-abstraction pathways generating radical intermediates, which are further transformed into the products via recoordination of the free radical to the surface M–OH (rebound mechanism). The result of this multiple-steps reaction can lead the surface oxygens to desorb leaving the vacancy behind. Surface vacancy may change the electronic structure of the metal and lead to new types of sites. For example, vanadia catalysts have shown interesting performance and have been particularly investigated for the oxidation of alkanes. Hypothetical active sites including terminal oxygen (V=O) and bridging oxygen (V–O–V) are proposed;^{40,41,45} however, the actual active species on the catalyst surface plane remain nevertheless structurally still ill defined. Several pathways derived from organometallic chemistry can be envisaged. In each case, the catalyst active site, M=O or M–O–M, is reduced during reaction and needs to be reoxidized.

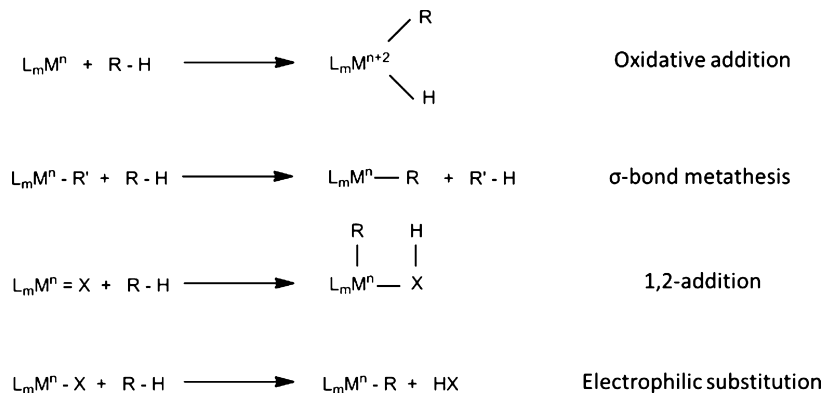
Acid–base properties of the solid are also an important feature, as they play a determining role in the activation of the reactants and in desorption of the intermediate compounds. For instance, an acid surface will favor desorption of acid products, thus avoiding further overoxidation, while a basic surface will favor desorption of basic products.

A free radical mechanism can also occur in which the alkane produces, at the surface of metal active sites, a radical that propagates in the liquid or gas phase and then reacts with dissolved or gas-phase oxygen to give a peroxy radical species (Scheme 3). A typical example in the liquid phase is the selective oxidation of cyclohexane with zeolites substituted by cobalt ions believed to act as a free radical initiator.

For the oxidation reactions, mono-, di-, and polynuclear sites of various catalysts such as well-defined molecular catalysts and biomimetic organometallic catalysts relating to the heme enzyme of cytochrome P-450 and the nonheme enzyme of methane monooxygenase can effectively activate oxidants and/

Scheme 3. Free Radical Mechanism of Direct Oxidation of Saturated Hydrocarbons^a

^aM = Fe, Mn, Co, Cr, Ni, etc.^{31,46}

Scheme 4. Various Mechanisms Belonging to the So-Called Organometallic C–H Bond Activation⁴⁴

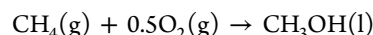
or substrates, resulting in specific activity and selectivity.^{46–58} The mechanism of C–H activation by molecular complexes for homogeneous processes has been extensively investigated; four mechanisms involving at least one metal center have been documented: oxidative addition (usually for late transition metal), σ -bond metathesis for their early counterparts, and, in a few cases, 1,2-addition or electrophilic activation (Scheme 4).⁵⁹ However, degradation of organic ligands invariably occurs under oxidative conditions, and their catalytic activity and lifetime are frequently limited. Therefore, “inorganic catalysts” with structurally well-defined active sites at the atomic or molecular level can contribute to the development of efficient, green, and long-lived oxidation processes.³³

In the following sections, selected mechanisms proposed for selective oxidation of each light alkane have been discussed, and selected results obtained on HPC-based catalysts have been first categorized by feed: methane, ethane, propane, *n*-butane, and iso-butane. For most substrates subjected to oxidation, a distribution of products is obtained with carbon monoxide and carbon dioxide (from now on referred to as CO_x) usually prevailing. Both the conditions and the catalysts employed can direct the reaction toward partially oxidation products. Selectivity toward given products has been used to organize and discuss further. Unless stated otherwise, all heteropoly acids belong to the Keggin class.

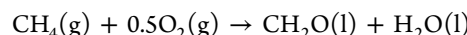
5. SELECTIVE OXIDATION OF METHANE

Methane is the most abundant component of natural gas and is also the most difficult alkane to convert. The intrinsic properties of methane explain the challenge to accomplish its activation prior to any ordinary redox or acid–base chemistry. Provided its direct oxidation is selective enough, several products with increased added values (e.g., methanol, form-

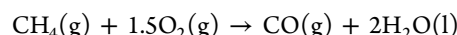
aldehyde) can be obtained. The main issue regarding the yield of this reaction is the overoxidation to CO or CO₂ (vide infra).



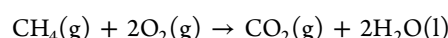
$$\Delta G^\circ = -27.7 \text{ kcal mol}^{-1}$$



$$\Delta G^\circ = -69.1 \text{ kcal mol}^{-1}$$



$$\Delta G^\circ = -134.0 \text{ kcal mol}^{-1}$$

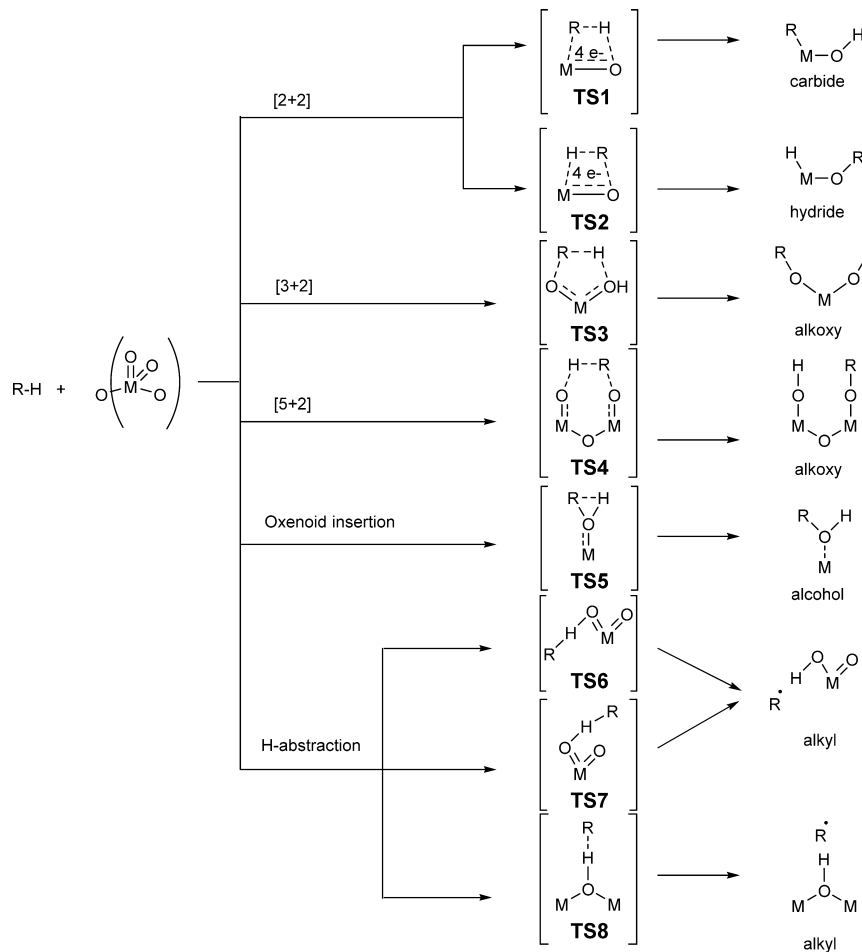


$$\Delta G^\circ = -195.5 \text{ kcal mol}^{-1}$$

Two extreme types of conditions can be distinguished by their temperature, their pressure, and their experimental setup. At high temperature (500 °C and above), the catalytic reaction occurs between a solid and the feed, with the products being in the gas phase and low pressure. At lower temperature, a solvent is added to mediate the reaction and can also be involved in the chemical transformation. Moreover, the pressure applied is much higher. The methane conversion, the products generated, and the selectivity will be examined in the following subsections.

5.1. General Mechanisms for Methane Selective Oxidation to Oxygenates

Selective oxidation of methane to oxygenates including methanol and formaldehyde is one of the most challenging goals in catalysis. The key issues are to surmount the chemical inertness of methane as illustrated by the high C–H bond strength (440 kJ/mol),⁶⁰ high ionization potential (12.5 eV),

Scheme 5. Schematic Representation of Transition States during C–H Activation⁴⁴

low proton affinity (4.4 eV), and low acidity ($pK_a = 48$)⁶¹ of the molecule and to conquer the propensity for full oxidation in the presence of oxygen driven by thermodynamics.

Derivation of methane has been extensively investigated with significant attention being paid to C–H activation, the necessary and determining first step toward more functionalization. A variety of catalysts, mostly based on metal oxides, have been tested. By comparison, HPC-based catalysts have been studied less extensively and in less depth.

Scheme 5 summarizes the possible mechanisms for the activation of methane C–H bond, which were calculated on the basis of model catalysts: $V_3O_6Cl_3$, Cr_3O_9 , Mo_3O_9 , and W_3O_9 .^{42,44} At least eight transition states can be outlined, depending of the type of interaction and the number of electron involved. TS1 and TS2 are obtained from (2 + 2) additions, which lead to the carbide and the hydride formation, respectively; for the valence of the metal center is not changed during the reaction, it may be considered as an acid–base reaction. A two-electron (2 e) oxidation process can also occur with the metal center being reduced formally by two units; TS3 and TS4 correspond to the (3 + 2) and TS5 to the (5 + 2) pathways. All conduct to the formation of hydroxyl and alkoxy directly. Formation of TS5 has been coined as oxenoid insertion and leads directly to the formation of alcohol. H abstraction is a 1e process, which involves radical formation with the metal center being reduced formally by one unit. Both terminal oxygens (TS6 and TS7) and bridging oxygens (TS8) were considered. It is accepted that the hydrogen abstraction

leading to the formation of methyl radical is the favored pathway. However, the elemental steps involved in this process remain ill-defined and somehow controversial.⁶²

5.2. Selective Oxidation of Methane over HPC Catalysts

5.2.1. Selective Oxidation of Methane to Methanol and Formaldehyde at High Temperature.

The main

Scheme 6. General Conditions Employed for the Oxidation of Methane to Methanol and Formaldehyde^a

^aOxidant: N_2O and O_2 ; $T = 570$ – 750 °C.

parameters investigated in the oxidation reactions at high temperature have been the formulation of the HPC catalyst, the oxidant, the pressure, and the temperature. The products such as methanol and formaldehyde were generated (Scheme 6).

The oxidation of methane over supported heteropolyoxometalates was investigated in the late 1980s by Moffat and co-workers.^{63–73} A variety of silica-supported HPC (viz., $HSiMo_{12}$, $HPMo_{12}$, $HMn_{10}V_2$, HPW_{12} , $HSiW_{12}$) were screened at temperature between 520 and 570 °C and atmospheric pressure using nitrous oxide or oxygen as oxidant. Small conversions of methane were reported, and the reaction yielded mainly CO and CO_2 with significantly smaller amounts of

Table 4. Selective Oxidation from Methane to Methanol and Formaldehyde^{63 a}

precatalyst	oxidant	temp (°C)	CH ₄ conversion (%)	selectivity (%)			yield (%)		ref
				CO _x	HCHO	CH ₃ OH	HCHO	CH ₃ OH	
20 wt % H ₃ PMo ₁₂ O ₄₀ /SiO ₂	N ₂ O	570	5.1	87.5	12	0.5	0.61	0.03	63
20.4 wt % H ₃ PV ₂ Mo ₁₀ O ₄₀ /SiO ₂	N ₂ O	570	4.2	88.5	11	0.5	0.46	0.02	63
19.9 wt % H ₄ SiMo ₁₂ O ₄₀ on SiO ₂	N ₂ O	570	2.5	90.9	9	0.4	0.23	0.01	63
26.2 wt % H ₃ PW ₁₂ O ₄₀ on SiO ₂	N ₂ O	570	0.4	100	tr	0	0.00	0.00	63
26.2 wt % H ₄ SiW ₁₂ O ₄₀ on SiO ₂	N ₂ O	570	0.4	100	tr	0	0.00	0.00	63

^aReaction conditions: catalyst, 0.35 g; total flow rate, 30 mL min⁻¹; CH₄ (67%), N₂O (33%).

formaldehyde and traces of methanol (Table 4). These seminal studies highlighted the capacity of HPA to promote selective oxidation. The composition of the HPC was pivotal upon the catalytic performance. Only HPC with molybdenum-based addenda were converting methane, while their tungsten counterparts were inactive under the same condition. Phosphorus as a central atom was also more performing than silicon. The central atom and the addenda with the latter were outweighing the former.^{74–78} The silica support is understood to increase both the thermal stability and the surface area of the HPC available for reaction. Surprisingly, they also found that the addition of very small quantities (less than 1 mol %) of dichloro- or tetrachloro-methane in the feed stream strongly modified the repartition of the reaction products and the activity.⁷⁶

He et al. synthesized a mesoporous silica containing phosphorus, vanadium, and molybdenum by adding, during the sol–gel preparation, variable amounts of H₃PMo₁₀V₂O₄₀ to Si(OEt)₄ and a template (P123).⁷⁹ After aging and calcination at 600 °C, the polyoxometalate structure was destroyed, and the sample could be better described as P–Mo–V mixed oxide species included in the silica matrix. These materials were then used in the gas-phase selective oxidation of methane with only O₂ at atmospheric pressure. Their catalyst led only to the formation of formaldehyde (together with CO and CO₂) (Table 5). The highest space-time yield of HCHO (330 g(HCHO) kg_{cat}⁻¹ h⁻¹) was obtained on the 3.40PMoV-mesoSiO₂ (3.40 stands for the actual mass loading percentage of P–Mo–V mixed oxide) catalyst at 640 °C. This value is higher than those obtained with classical molybdenum oxide and vanadium oxide catalysts under similar reaction conditions^{80,81} and much higher than that achieved with a conventional P–Mo–V mixed oxide prepared by impregnation.

Highest yields were obtained on 3.40 PMoV-mesoSiO₂ at 640 °C. Largest incorporation of HPC did not lead to improvement in the catalysis performance. To note, comparison with Moffat result is possible and suggests strongly that the lower amount of HPC and higher temperature leads to better results. The nature of the catalytic site remains poorly understood as the HPC has been restructured during the catalyst preparation. In addition, preparation of HPC using classic impregnation method yields a significantly lower yield for similar loading and temperature (about 1%). So the most active species must differ from the classical Keggin unit. It should be noted that conversion increases with the temperature, regardless of the loading, while the selectivity decreases. Hence, the temperature is optimal around 640 °C when considering only the yield (see Figure 5).

Benlounes et al. studied the partial oxidation of methane with O₂ or N₂O over PMoV, PMoFe, and SiMoFe mixed oxide catalysts at atmospheric pressure in the 700–750 °C temperature range (Table 6).⁸² In their experiments, they also used

HPC (H₄PMo₁₁VO₄₀, (NH₄)₆HSiMo₁₁FeO₄₀, and (NH₄)₄PMo₁₁FeO₃₉) as precursors to make the highly dispersed iron-containing or vanadium-containing mixed oxides. The main oxygenate products on these catalysts were formaldehyde, methanol, CO, and CO₂. The (NH₄)₄PMo₁₁FeO₃₉ catalyst was the most selective and active system: at 750 °C under O₂, a methane conversion of 23% could be obtained, and the total selectivity in formaldehyde (26%) and methanol (10%) could reach more than 36%. However, as in the above case, the true catalyst was not the polyoxometalate but a kind of mixed oxides formed after its decomposition, making structure–activity relationships very difficult to establish.

Some trends can be outlined regarding the conversion of methane to methanol and formaldehyde at high temperature. Temperature and conversion appear to be correlated with feeble conversion being observed even at 200 °C. Completely oxidized products (CO_x) are obtained at selectivity higher than 50% in most cases. Formaldehyde is the main partially oxidized product with selectivity as high as 63% (3.40 PMoV-meso). Methanol is obtained only with N₂O as oxidant and higher temperature. Oxygen is the best oxidant at high temperature only; it is inefficient at low temperature.

Modification of the classic formula of HPC has been prepared and screened and revealed a few trends. Tungstic acid has shown very poor efficiency, and most effort has been directed toward improving molybdenum-based HPC. Both the primary and the secondary structures have been altered by incorporation of counteraction different from proton (Pd²⁺, Cs⁺, NH₄⁺) or alternative addenda metal to molybdenum (Fe³⁺, V⁵⁺) as counterions Cs⁺ and NH₄⁺ can improve dramatically the conversion as compared to proton including that metal can direct the reaction by promoting the generation in situ of peroxide fragment. The role of the central atom remains unclear: phosphorus is generally more efficient with MoV HPC, while iron forms a superior couple with Si.

5.2.2. Selective Oxidation of Methane to Formic Acid at Low Temperature. Mizuno and co-workers have studied HPC substituting Cs for proton and transition metal additives; the general formula is M_xCs_{2.5}H_{0.5–2x+y}PV_yMo_{12–y}O₄₀ with (M = Pd²⁺, Rh²⁺, Ru²⁺, Pt²⁺, Mn²⁺, Hg²⁺, Fe³⁺, Co²⁺, Cu²⁺; x = 0–3, y = 0–3) (Scheme 7).^{83,84} The cesium atoms are understood to enhance the acidity of the active sites and extend the surface area as compared to their proton counterparts.

At the low-temperature comprised between 200 and 300 °C under atmospheric pressure, the methane conversion is very low but yields formic acid, methanol, CO, and CO₂ with varying proportions depending on the parameters studied (i.e., reaction temperature, the partial pressures of O₂ and H₂, the vanadium substitution, and the addition of transition metal ions (Pd, Pt, Cu, etc.)). Under those conditions, the reaction affords formic acid as the major product. The most selective catalyst

Table 5. Selective Oxidation from Methane to Formaldehyde^{79a}

precatalyst	oxidant	temp (°C)	CH ₄ conversion (%)	selectivity (%)		yield (%)
				CO _x	HCHO	
3.40 PMoV-mesoSiO ₂	O ₂	640	5.9	48	52	3.07
6.68 PMoV-mesoSiO ₂	O ₂	640	6.4	56	44	2.82
3.40 PMoV-mesoSiO ₂	O ₂	620	4.4	45	55	2.42
3.40 PMoV-mesoSiO ₂	O ₂	660	7.6	69	31	2.36
1.35 PMoV-mesoSiO ₂	O ₂	620	4.1	44	56	2.30
1.35 PMoV-mesoSiO ₂	O ₂	640	5.4	58	42	2.27
1.35 PMoV-mesoSiO ₂	O ₂	660	6.5	67	33	2.15
6.68 PMoV-mesoSiO ₂	O ₂	620	4.5	53	47	2.12
3.53 PMoV(im)-mesoSiO ₂	O ₂	620	4.6	55	45	2.07
14.1 PMoV-mesoSiO ₂	O ₂	640	6.7	70	30	2.01
6.68 PMoV-mesoSiO ₂	O ₂	600	4	50	50	2.00
3.53 PMoV(im)-mesoSiO ₂	O ₂	640	4.8	60	40	1.92
3.40 PMoV-mesoSiO ₂	O ₂	600	3.1	38	62	1.92
6.68 PMoV-mesoSiO ₂	O ₂	660	8	78	22	1.76
14.1 PMoV-mesoSiO ₂	O ₂	620	4.3	62	38	1.63
1.35 PMoV-mesoSiO ₂	O ₂	600	2.5	37	63	1.58
3.53 PMoV(im)-mesoSiO ₂	O ₂	600	3.1	52	48	1.49
14.1 PMoV-mesoSiO ₂	O ₂	600	3	58	42	1.26
3.53 PMoV(im)-mesoSiO ₂	O ₂	660	6.7	69	16	1.07
14.1 PMoV-mesoSiO ₂	O ₂	660	7.9	88	12	0.95
meso SiO ₂	O ₂	660	1.6	100	0	0
meso SiO ₂	O ₂	640	0.3	100	0	0
meso SiO ₂	O ₂	620	0.1	100	0	0
meso SiO ₂	O ₂	600	0	100	0	0

^aReaction conditions: catalyst, 0.1 g; GHSV (gas hourly space velocity), 36 200 L kg⁻¹ h⁻¹, CH₄/O₂/N₂ = 2/1/7. meso: Mesoporous. im: Conventional P–Mo–V mixed oxide prepared using classic impregnation method.

Pd_{0.08}Cs_{2.5}H_{2.34}PV₂Mo₁₀O₄₀ converted 0.10% of methane to formic acid (76%) at 300 °C, a result reminiscent of that of Moffat (see previous paragraph) for the conversion of methane by HPC including molybdenum and vanadium atoms. It is noteworthy that the incorporation of vanadium increased the conversion with each additional atom but saw a peak in selectivity at 2. Noble metals were the most efficient with palladium offering the best yield of formic acid.

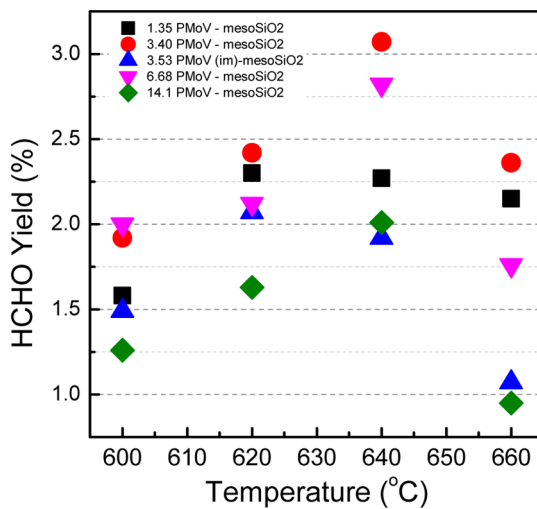


Figure 5. Comparison of the catalytic performance of PMoV-mesoSiO₂ catalysts with different mass loading percentages of P–Mo–V mixed oxide at different reaction temperatures.

The role played by the counter cationic transition metal (viz., Pd) was outlined to be a catalyst for the *in situ* formation of hydrogen peroxide (Scheme 8), which subsequently oxidizes the methane already coordinated as a methyl fragment.^{85–88} This was confirmed by modifying the composition of the oxidant employed; using H₂O₂ gave results similar to those of the combination H₂ and O₂, while selective oxidation products were not obtained with O₂ or H₂ alone (Table 7).

5.2.3. Selective Oxidation of Methane to Methyl Formate and Methyl Trifluoroacetate at Low Temperature. Mizuno et al. performed a large amount of studies on the liquid-phase selective oxidation of methane over heteropoly compound catalysts^{89–93} in highly acidic media. They first reported the one-step oxygenation of methane with hydrogen peroxide in the presence of H₄PVMo₁₁O₄₀ in (CF₃CO)₂O solvent at 80 °C and 50 atm.^{92,93} Methyl formate was the main product alongside formic acid, methyl trifluoroacetate, methanol, and carbon dioxide (Scheme 9).

After 24 h of reaction, a 33% conversion of CH₄ could be achieved, with a yield of methyl formate of 2.4% (Scheme 10). Kinetic experiments⁹¹ led to the following conclusions: (i) the H₄PVMo₁₁O₄₀ precursor decomposes to form VO(O₂)⁺ and PMo₁₁O₃₉⁷⁻ during the catalytic test; (ii) VO(O₂)⁺ is a catalytically active species for the reaction; and (iii) the oxidation proceeds mainly via a radical-chain mechanism in which the rate-determining step is the activation of methane.

On comparison with other HPC, H₄PVMo₁₁O₄₀ was found to be the most active and efficient catalyst (Table 8).⁹⁰ Inorganic and organic salts of di-iron-substituted silicotungstates were tested under milder conditions using water as a solvent.⁹⁴ These precatalysts were designed by analogy with the active center of methane monooxygenase.^{95,96} Only the isomer of the polyoxometalate ([γ-SiW₁₀{Fe(OH₂)₂O₃₈}⁶⁻]) revealed some activity toward methyl formate. Replacement of the organic cations by inorganic ones (typically potassium) allowed performing the reaction in water. Methyl formate was formed in selectivity of 54% with a turnover number (TON) of 23 after 48 h of reaction at 80 °C (Table 8).

5.2.4. Selective Oxidation of Methane to Methyl Acetate and Methyl Trifluoroacetate at Low Temperature. Kitamura et al. reported in 1998 the partial oxidation of

Table 6. Selective Oxidation from Methane to Methanol and Formaldehyde⁸²

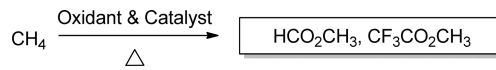
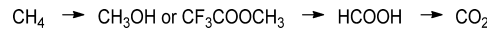
precatalyst	oxidant	temp (°C)	CH ₄ conversion (%)	selectivity (%)			yield (%)	
				CO _x	HCHO	CH ₃ OH	HCHO	CH ₃ OH
(NH ₄) ₆ HSiMo ₁₁ FeO ₄₀	O ₂	750	32	72	20	8	6.40	2.56
(NH ₄) ₄ PMo ₁₁ FeO ₃₉ ^a	O ₂	750	23	63	26	11	5.98	2.53
(NH ₄) ₆ HSiMo ₁₁ FeO ₄₀ ^a	N ₂ O	750	13	63	21	16	2.73	2.08
(NH ₄) ₄ PMo ₁₁ FeO ₃₉ ^a	N ₂ O	750	8	64	14	22	1.12	1.76
H ₄ PMo ₁₁ VO ₄₀ ^a	O ₂	750	13	72	16	12	2.08	1.56
(NH ₄) ₆ HSiMo ₁₁ FeO ₄₀ ^a	N ₂ O	700	6	67	10	23	0.60	1.38
H ₄ PMo ₁₁ VO ₄₀ ^a	N ₂ O	750	6	78	5	17	0.3	1.02
(NH ₄) ₄ PMo ₁₁ FeO ₃₉ ^a	O ₂	700	4	63	13	24	0.52	0.96
(NH ₄) ₆ HSiMo ₁₁ FeO ₄₀ ^a	O ₂	700	4	70	8	22	0.32	0.88
(NH ₄) ₄ PMo ₁₁ FeO ₃₉ ^a	N ₂ O	700	2	69		31	0.00	0.62
H ₄ PMo ₁₁ VO ₄₀ ^a	O ₂	700	3	73	7	20	0.21	0.6
H ₄ PMo ₁₁ VO ₄₀ ^a	N ₂ O	700	2	77		23	0.00	0.46

^aReaction conditions: catalyst, 0.2 g; CH₄/O₂ or CH₄/N₂O = 2.5.Scheme 7. General Conditions Employed for the Oxidation of Methane to Formic Acid^a^aOxidant: O₂, H₂, H₂O₂, and H₂ + O₂; T = 200–300 °C.

methane catalyzed by a series of heteropoly acids whose formulation includes different proportion of addenda between W, Mo, and V (see Table 9). In a typical experiment, a small amount of catalyst was subjected to a pressure of 20 atm in trifluoroacetic acid solvent at 80 °C for 20 h (Scheme 11).^{97,98}

Several oxidants were screened, and K₂S₂O₈ was found to surpass Na₂S₂O₈, (NH₄)₂S₂O₈, MnO₂, KMnO₄, and H₂O₂. Methyl trifluoroacetate was the main product in most cases with a smaller amount of methyl acetate. Polyoxometalates based on molybdenum gave lower yields of oxidation products. A turnover number of 241 was achieved when using H₅PV₂W₁₀O₄₀ as the catalyst with a methyl trifluoroacetate to methyl acetate ratio of 73/27. The highest TON (490) was obtained when reducing the catalyst amount to 0.013 mmol. The inclusion of vanadium addenda appears to be required for improved productivity.

The mechanism proposed by the authors (Scheme 12) for the formation of methyl trifluoroacetate involves vanadium oxo as the catalytic site. The key step is the abstraction of one proton from methane with formation of CH₃[•] radicals with concomitant reduction of vanadium from (V) to (IV). This is reminiscent of the radical formation in the biological transformation of methane to methanol by methane monooxygenase.⁹⁹ In a subsequent step, the CH₃[•] radical is then transformed into a CH₃⁺ species, which reacts with the trifluoroacetate anion. However, as tungstic heteropoly acids are more efficient than molybdic ones, it seems more reasonable to propose that methane reacts with the heteropoly acid to lead to the evolution of hydrogen and the formation of the CH₃⁺ cation. The formation of the methyl acetate

Scheme 9. General Conditions Employed for the Oxidation of Methane to Methyl Formate and Methyl Trifluoroacetate^a^aOxidant: H₂O₂; T = 80 °C.Scheme 10. Proposed Reaction Scheme for Oxidation of Methane in a H₄PMo₁₁O₄₀ + H₂O₂ + (CF₃CO)₂O System

byproduct (sometimes in a higher amount than methyl trifluoroacetate) is also intriguing. The authors proposed that it is formed via ester exchange between methyl trifluoroacetate and acetic acid; the latter would be obtained from the reaction of CH₄ and CO derived from the decomposition of trifluoroacetic acid or trifluoroacetic anhydride.

In conclusion, oxidation of methane at low temperature and high pressure resulted in lower and slower conversion as compared to the higher temperature and low pressure discussed in the previous subsection, –6.4% in 20 h for H₅PV₂W₁₀O₄₀.

Tungsten-based HPC have demonstrated relatively high conversion provided they contain vanadium addenda. Vanadium centers appear to promote the reaction and are believed to go through a radical mechanism. Under these conditions, the intermediates are reacting significantly with the solvent to yield methyl trifluoroacetate.

5.2.5. Selective Oxidation of Methane to Methanol at Low Temperature. Very low conversion of methane has been reported at low to ambient temperature by a few groups under exotic conditions. Mizuno designed HPA inspired by the monooxygenase^{95,96} enzyme, while Neumann employed highly oxidizing conditions (Table 10).

Tetrabutylammonium salt of di-iron-substituted silicotungstate $\left[\left(\text{C}_4\text{H}_9\right)_4\text{N}\right]_{3.5}\text{H}_{2.5}\left[\gamma\text{-SiW}_{10}\{\text{Fe(OH}_2\}\}_2\text{O}_{38}\right]$ was found by Mizuno and co-workers to be active in the low temperature

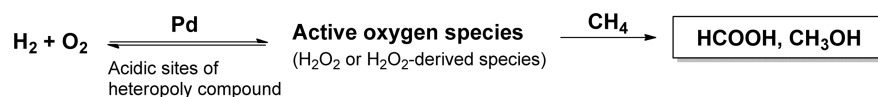
Scheme 8. Proposed Reaction Scheme of Methane Selective Oxidation to Formic Acid Catalyzed by Pd-Containing HPC Catalyst⁸³

Table 7. Selective Oxidation from Methane to Formic Acid⁸³

precatalyst	oxidant	temp (°C)	CH ₄ conversion (%)	selectivity (%)			yield (%)
				CO _x	CH ₃ OH	HCOOH	
Pd _{0.08} Cs _{2.5} H _{3.34} PV ₃ Mo ₉ O ₄₀	O ₂	300	0.14			60	0.084
Pd _{0.08} Cs _{2.5} H _{2.34} PV ₂ Mo ₁₀ O ₄₀	O ₂	300	0.10			76	0.076
Pd _{0.08} Cs _{2.5} H _{1.34} PVMo ₁₁ O ₄₀	H ₂ +O ₂ +H ₂ O ^b	300	0.077	15	0	85	0.065
Pd _{0.08} Cs _{2.5} H _{0.34} PMo ₁₂ O ₄₀	O ₂	200	0.087	25	0	75	0.065
Pt _{0.08} Cs _{2.5} H _{0.34} PMo ₁₂ O ₄₀	O ₂	200	0.067	15	2	83	0.056
Pd _{0.08} Cs _{2.5} H _{1.34} PVMo ₁₁ O ₄₀	O ₂	300	0.08			70	0.056
Pd _{0.08} Cs _{2.5} H _{1.34} PVMo ₁₁ O ₄₀	H ₂ O ₂ +H ₂ O ^a	300	0.075	38	13	49	0.037
Pd _{0.08} Cs _{2.5} H _{0.34} PMo ₁₂ O ₄₀	O ₂	300	0.08			46	0.037
Rh _{0.08} Cs _{2.5} H _{0.34} PMo ₁₂ O ₄₀	O ₂	200	0.041	34	0	66	0.027
Ru _{0.08} Cs _{2.5} H _{0.34} PMo ₁₂ O ₄₀	O ₂	200	0.156	98	0	2	0.003
Co _{0.08} Cs _{2.5} H _{0.34} PMo ₁₂ O ₄₀	O ₂	200	0.062	97	0	3	0.002
Mn _{0.08} Cs _{2.5} H _{0.34} PMo ₁₂ O ₄₀	O ₂	200	0.06	97	0	3	0.002
Fe _{0.08} Cs _{2.5} H _{0.26} PMo ₁₂ O ₄₀	O ₂	200	0.063	98	0	1	0.001
Cu _{0.08} Cs _{2.5} H _{0.34} PMo ₁₂ O ₄₀	O ₂	200	0.049	97	0	3	0.001
Hg _{0.08} Cs _{2.5} H _{0.34} PMo ₁₂ O ₄₀	O ₂	200	0.044	100	0	0	0.000
Cs _{2.5} H _{0.5} PMo ₁₂ O ₄₀	O ₂	200	0	0	0	0	0.000

^aH₂O₂, 1.5 kPa; H₂O, 9 kPa. ^bH₂, 33 kPa; O₂, 14 kPa; H₂O, 9 kPa.

Table 8. Selective Oxidation from Methane to Methyl Formate

precatalyst	CH ₄ conversion (%)	selectivity (%)						yield ^c (%)	ref
		CO _x	HCOOCH ₃	HCOOH	CH ₃ OH	CF ₃ COOCH ₃	C ₂ H ₆		
[γ-SiW ₁₀ {Fe(OH ₂) ₂ O ₃₈ } ⁶⁻] ^a	40	44	54	1	1			22.4	94
H ₄ PVMo ₁₁ O ₄₀ ^b	4.7	7	72	15	1	5	tr	4.4	90
H ₄ PVV ₁₁ O ₄₀ ^b	10.2	56	23	tr	tr	7	14	3.1	90
H ₅ SiVMo ₁₁ O ₄₀ ^b	5.8	63	28	0	tr	9	0	2.1	90
H ₆ PVMo ₉ O ₄₀ ^b	1.6	42	41	0	0	17	0	0.9	90
H ₅ PV ₂ Mo ₁₀ O ₄₀ ^b	3	67	24	0	0	7	2	0.9	90
H ₃ PMo ₁₂ O ₄₀ ^b	2.7	86	0	0	0	14	tr	0.4	90

^aReaction conditions: solvent, H₂O, 1.8 mL; CH₄, 50 atm; H₂O₂, 2.4 mmol; catalyst, 5 μmol; reaction temperature, 80 °C; reaction time, 48 h.

^bReaction conditions: oxidant, H₂O₂; solvent, (CF₃CO)₂O, 1.8 mL; CH₄, 50 atm; H₂O₂, 2.4 mmol; catalyst, 5 μmol; reaction temperature, 80 °C; reaction time, 24 h. ^cSum of yields of selective oxygenates, that is, CH₃OH, HCOOH, HCOOCH₃ and CF₃COOCH₃; tr: trace.

selective oxidation of methane to methanol.^{89,100} The reaction was carried out under high pressure (50 atm of CH₄) in acetonitrile at 32 °C with hydrogen peroxide. The selectivities to methanol and carbon dioxide were 73% and 27%, respectively, after 24 h of reaction, and a turnover number of 25 was achieved.

Neumann et al. studied the aerobic partial oxidation of methane in water¹⁰¹ catalyzed by using a system supporting a bipyrimidinylplatinum-polyoxometalate (H₅PV₂Mo₁₀O₄₀) hybrid complex on silica. The bipyrimidinyl ligand was methylated on one of its nitrogens, allowing the formation of a platinum cationic complex that was substituted to one proton of H₅PV₂Mo₁₀O₄₀. The resulting hybrid material was supported on silica. They added a polyoxometalate (H₅PV₂Mo₁₀O₄₀) both on the silica support (to favor the reoxidation of platinum in the catalytic cycle) and in aqueous media (to increase the acidity of the medium). The reactions were carried out at 50 °C under a pressure of 30 bar methane and 2 bar O₂, and the TON reached 33.

It is believed that phosphovanadomolybdates act essentially as cocatalysts.¹⁰² The presence of the polyoxometalate in the [Pt(Mebipym)-Cl₂]⁺[H₄PV₂Mo₁₀O₄₀]⁻ hybrid catalyst is believed to facilitate both (a) oxidation of Pt(II) to Pt(IV) intermediates and (b) the addition of methane (also methanol) to a Pt(II) center by providing a conduit for improved oxidation of intermediate hydride species.

5.3. Conclusions. Large numbers of HPC have been screened for the selective oxidation of methane to methanol, formaldehyde, and formic acid. The conversion seems to be more or less correlated to the temperature of the reactions. The selectivity toward one or more given products is controlled by the formulation of the HPC coupled to the nature of the oxidant employed. Yet the actual structure of the active species remains elusive as reorganization of the catalyst is likely to occur at the higher temperature. The inclusion of vanadium or iron addenda into the structure of heteropolyanion has allowed one to reach improved conversion and selectivity.

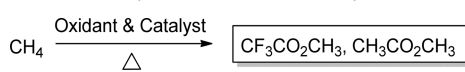
6. SELECTIVE OXIDATION OF ETHANE

The heterogeneous selective oxidation of cheap and abundant ethane to ethylene and other value-added oxygenates has been a focus for decades. The C–H bond energy in ethane is 420 kJ/mol.¹⁰³ Thus, similar to methane, ethane is also one of the most difficult organic molecules to be activated. In this subsection, general mechanisms for ethane oxidation and catalytic studies using HPC to transform ethane are discussed. Ethylene is the preeminent product from selective oxidation in most cases. Minor amounts of acetaldehyde and acetic acid were also observed albeit not concomitantly, and thus will be examined separately. Some of the studies reported are directly inspired by that on methane transformations (i.e., Moffat, Misono; see

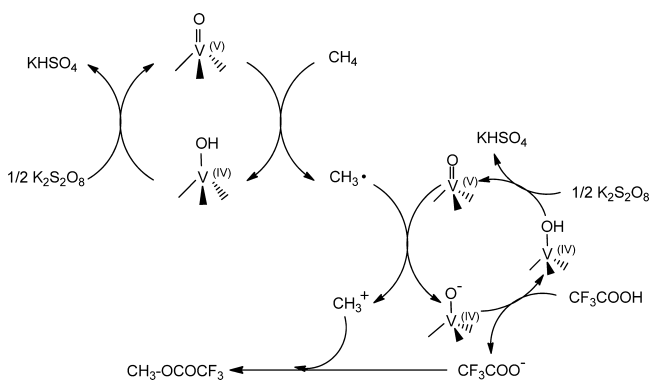
Table 9. Selective Oxidation from Methane to Methyl Trifluoroacetate and Methyl Acetate^a

precatalyst	oxidant	temp (°C)	pressure (atm)	CF ₃ COOCH ₃ /CH ₃ COOCH ₃ ratio	TON	yield (%) ^b
H ₅ PV ₂ W ₁₀ O ₄₀	K ₂ S ₂ O ₈	80	20	73/27	241	6.4
H ₅ PV ₂ Mo ₁₀ O ₄₀	K ₂ S ₂ O ₈	80	20	88/12	161	4.7
H ₅ SiVW ₁₁ O ₄₀	K ₂ S ₂ O ₈	80	20	73/27	161	3.5
H ₆ PV ₃ W ₉ O ₄₀	K ₂ S ₂ O ₈	80	20	55/45	139	3.3
H ₆ PV ₃ Mo ₉ O ₄₀	K ₂ S ₂ O ₈	80	20	86/14	92	2.8
H ₄ PVMo ₁₁ O ₄₀	K ₂ S ₂ O ₈	80	20	83/17	80	2.4
H ₇ PV ₃ Mo ₉ O ₄₀	K ₂ S ₂ O ₈	80	20	73/27	76	2.1
H ₈ PV ₃ Mo ₉ O ₄₀	K ₂ S ₂ O ₈	80	20	67/33	62	1.8
H ₄ PVV ₁₁ O ₄₀	K ₂ S ₂ O ₈	80	20	76/24	50	1.0
H ₄ SiW ₆ Mo ₆ O ₄₀	K ₂ S ₂ O ₈	80	20	56/44	32	0.8
H ₃ PW ₁₂ O ₄₀	K ₂ S ₂ O ₈	80	20	76/24	22	0.5
H ₄ SiMo ₁₂ O ₄₀	K ₂ S ₂ O ₈	80	20	74/26	19	0.5
none	K ₂ S ₂ O ₈	80	20	79/21		0.4
H ₄ SiW ₁₂ O ₄₀	K ₂ S ₂ O ₈	80	20	72/28	15	0.4
H ₄ SiW ₉ Mo ₃ O ₄₀	K ₂ S ₂ O ₈	80	20	59/41	18	0.4
H ₃ PW ₆ MO ₆ O ₄₀	K ₂ S ₂ O ₈	80	20	73/27	17	0.4
H ₃ PW ₈ Mo ₄ O ₄₀	K ₂ S ₂ O ₈	80	20	54/46	14	0.3
H ₃ PW ₁₀ Mo ₂ O ₄₀	K ₂ S ₂ O ₈	80	20	72/28	12	0.3
H ₃ PW ₄ Mo ₈ O ₄₀	K ₂ S ₂ O ₈	80	20	90/10	8	0.2
H ₃ PMo ₁₂ O ₄₀	K ₂ S ₂ O ₈	80	20	76/24	5	0.1
H ₃ PW ₂ Mo ₁₀ O ₄₀	K ₂ S ₂ O ₈	80	20	83/17	4	0.1
H ₄ SiW ₄ Mo ₈ O ₄₀	K ₂ S ₂ O ₈	80	20	80/20	6	0.1

^aReaction conditions: CH₄, 20 atm; catalyst, 50 mg; K₂S₂O₈, 5.00 mmol; CF₃COOH, 10.0 mmol; (CF₃CO)₂O, 5.0 mL; 80 °C; 20 h. ^bGLC yield of methyl trifluoroacetate and methyl acetate based on CH₄.

Scheme 11. General Conditions Employed for the Oxidation of Methane to Methyl Acetate and Methyl Trifluoroacetate^a

^aOxidant: K₂S₂O₈, Na₂S₂O₈, (NH₄)₂S₂O₈, MnO₂, KMnO₄, H₂O₂, and (CF₃CO)₂O; P = 20 atm; T = 80 °C.

Scheme 12. Proposed Mechanism for the Formation of Methyl Trifluoroacetate from Methane over Vanadium-Containing Heteropoly Acids⁹⁷

section 5.2), and the same parameters have been scrutinized: the HPC formulation, the oxidant, the temperature, and so on.

6.1. General Mechanisms for Ethane Selective Oxidation to Ethylene and Oxygenates

The selective oxidation of ethane has been reported to yield ethylene, acetaldehyde, and acetic acid. Ethylene is one of the most important building blocks in the chemical industry, which is mainly used in producing polyethylene, ethylene dichloride, ethylbenzene, and so on. Acetaldehyde has been used in

Table 10. Selective Oxidation from Methane to Methanol Catalyzed by [Pt(Mebipym)Cl₂]⁺[H₄PV₂Mo₁₀O₄₀]⁻/SiO₂^{101 a}

acid (μmol)	CH ₃ OH (μmol)	HCHO (μmol)	CH ₃ CHO (μmol)	TON ^b
none	0	14	tr	6
H ₂ SO ₄ (150)	1	5	tr	31
H ₄ PV ₂ Mo ₁₀ O ₄₀ (60)	0	7	2	32
H ₄ PV ₂ Mo ₁₀ O ₄₀ (30)	0	17	0	33

^aReaction conditions: 2.88 μmol of catalyst; 2 mL of H₂O, 0–150 μmol of acid; 30 bar CH₄, 2 bar O₂; 50 °C. ^bTON: moles of product per mole of catalyst.

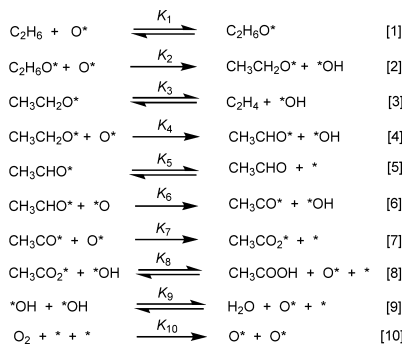
synthesizing acetic acid, while acetic acid is normally used for the production of vinyl acetate, acetic anhydride, and solvent ester.

Similar to methane, the most dominant mechanism proposed for ethane C–H activation is the hydrogen abstraction leading to the formation of ethyl radical, and most of the theoretical calculations are based on metal oxide catalysts. Scheme 13 shows the sequence of reduction–oxidation elementary steps for ethane oxidation to ethylene, acetaldehyde, and acetic acid on Mo–V–Nb oxide catalysts.¹⁰⁴ The mechanism hypothesis proposed for ethane selective oxidation catalyzed by HPC catalysts agrees with this radical mechanism.¹⁰⁵

6.2. Selective Oxidation of Ethane over HPC Catalysts

6.2.1. Oxidative Dehydrogenation of Ethane to Ethylene. Oxidative dehydrogenation (ODH) of ethane is a novel route currently proposed for the exploitation of abundant ethane as a raw material for much higher priced ethylene (Scheme 14). It takes place at lower temperature than the conventional dehydrogenation process and releases heat as well. Also, the heat released from the reaction and the presence of

Scheme 13. Mars–van Krevelen Redox Cycle for Ethane Oxidation to Ethylene, Acetaldehyde, and Acetic Acid^a



^a O^* represents a surface lattice oxygen ($\text{M}_i=\text{O}$ or $\text{M}_i-\text{O}-\text{M}_j$, where M_i and M_j can be Mo^{6+} , V^{5+} , or Nb^{5+}), $\text{CH}_3\text{CH}_2\text{O}^*$ is an ethoxide species attached to an M_i cation ($\text{C}_2\text{H}_5-\text{O}-\text{M}_i$), and CH_3CHO^* and CH_3CO_2^* are adsorbed acetaldehyde and acetate species, respectively. $\cdot\text{OH}$ denotes a hydroxyl group, and \cdot^* represents an oxygen vacancy and its associated reduced center.¹⁰⁴

Scheme 14. General Conditions Employed for the Oxidative Dehydrogenation of Ethane to Ethylene^a



^aOxidant: O_2 ; $T = 400\text{--}540\text{ }^\circ\text{C}$.

oxygen inhibit the coke deposition, thus preventing a loss of catalytic activity. However, the key point in ODH reactions is how to develop a catalyst that is capable of activating only the C–H bonds of alkanes to alkenes in the presence of oxygen.¹¹

Mizuno et al. examined various transition metals-substituted HPC ($\text{Cs}_{2.5}\text{M}_{0.08}^{\text{III}}\text{H}_{1.5\text{--}0.08n}\text{PVMo}_{11}\text{O}_{40}$ with $\text{M} = \text{Fe}^{3+}$, Cu^{2+} , Co^{2+} , Mn^{2+} , Ni^{2+}) for the oxidation of ethane.^{106–110} Their catalytic performances were assessed under both oxygen-rich and oxygen-poor conditions at $425\text{ }^\circ\text{C}$ (Table 11). These systems are based, as described for methane, on the combination of one high surface area acidic salt of the polyoxometalate and transition metal cations to replace some or all of the protons. HPC with Fe^{3+} and Cu^{2+} counteraction ($\text{Cs}_{2.5}\text{Fe}_{0.08}\text{H}_{1.26}\text{PVMo}_{11}\text{O}_{40}$ and $\text{Cs}_{2.5}\text{Cu}_{0.08}\text{H}_{1.34}\text{PVMo}_{11}\text{O}_{40}$) exhibited the best results. The products were ethylene and CO_x under both conditions. With oxygen-rich feeds, the

addition of iron increased the selectivity to ethylene from 35% to 39%, while leaving the conversion unchanged. By contrast, under oxygen-poor conditions, the addition of iron increased the conversion from 4% to 6% without affecting the selectivity. The copper-substituted heteropoly compound led to different results.^{107–109} Under oxygen-rich conditions, the addition of copper to $\text{Cs}_{2.5}\text{H}_{1.5}\text{PVMo}_{11}\text{O}_{40}$ decreased the conversion of ethane from 9.7% to 6.6%, and the selectivity to ethylene also decreased from 35% to 31%. In contrast, under oxygen-poor conditions, the addition of copper increased the conversion of ethane from 4.0% to 8.6%, while the selectivity to ethylene decreased from 61% to 52%. In conclusion, while iron was an effective additive under both rich and poor oxygen conditions, copper was effective only for oxygen-poor ethane oxidehydrogenation feeds.

Cavani, Trifirò, and co-workers examined the oxidative dehydrogenation of ethane on salts of 12-molybdenophosphoric acid with both potassium and ammonium cations.¹¹¹ The Keggin anion was modified by substitution of one or two atoms of molybdenum by antimony. The addition of antimony led to a remarkable increase in the thermal structural stability of the sample obtained, but also led to a decrease in the catalytic activity as compared to the antimony-free compound. The conversion of ethane ranged from 1% to 7%, while the selectivities to ethylene were 34–56% (see Table 12). No evidence for the formation of acetaldehyde or acetic acid was reported. With samples containing potassium, iron, and antimony, the selectivity toward ethylene reached a value as high as 86% but with a conversion of 2.6%. The highest yield of ethylene (19.6%) was obtained on fresh $\text{K}_3\text{Fe}_1\text{Ce}_{0.25}\text{Cr}_{0.5}\text{Sb}_1$ catalyst with an ethane conversion of 36.2%.¹¹² Monitoring of the time on stream revealed that a steady-state regime was reached after 3 h.

Nowinska et al. also reported the use of phosphotungstic heteropolyoxometalates (as precursors) containing an excess of manganese and observed high activity and selectivity in the oxidative dehydrogenation of ethane¹¹³ at $400\text{--}430\text{ }^\circ\text{C}$. The steady-state ethane conversion over Mn-modified lacunary heteropoly compound ($\text{PW}_{11}\text{O}_{39}^{7-}$) catalyst at $430\text{ }^\circ\text{C}$ was about 40%, and the selectivity to ethylene was about 65% (see Table 13). As the samples were preliminarily calcined at 430 or 500 $^\circ\text{C}$ before use, the polyoxometalate structure was destroyed, and the true catalytic species could be described as that of an ill-defined mixed oxide.

Table 11. Selective Oxidation from Ethane to Ethylene^a

	catalyst	temp (°C)	C_2H_6 conversion (%)	CO_x selectivity ^b (%)	C_2H_4 selectivity ^b (%)	C_2H_4 yield (%)
(A)	$\text{Cs}_{2.5}\text{Cu}_{0.08}\text{H}_{1.34}\text{PVMo}_{11}\text{O}_{40}$	425	6.6	69	31	2.05
	$\text{Cs}_{2.5}\text{H}_{1.5}\text{PVMo}_{11}\text{O}_{40}$	425	9.7	65	35	3.40
	$\text{Cs}_{2.5}\text{Ni}_{0.08}\text{H}_{1.34}\text{PVMo}_{11}\text{O}_{40}$	425	7.5	51	49	3.68
	$\text{Cs}_{2.5}\text{Fe}_{0.08}\text{H}_{1.26}\text{PVMo}_{11}\text{O}_{40}$	425	10	60	39	3.90
	$\text{Cs}_{2.5}\text{Co}_{0.08}\text{H}_{1.34}\text{PVMo}_{11}\text{O}_{40}$	425	9.5	56	44	4.18
	$\text{Cs}_{2.5}\text{Mn}_{0.08}\text{H}_{1.34}\text{PVMo}_{11}\text{O}_{40}$	425	10	57	43	4.30
(B)	$\text{Cs}_{2.5}\text{Cu}_{0.08}\text{H}_{1.34}\text{PVMo}_{11}\text{O}_{40}$	425	8.6	48	52	4.47
	$\text{Cs}_{2.5}\text{Fe}_{0.08}\text{H}_{1.26}\text{PVMo}_{11}\text{O}_{40}$	425	6.4	42	58	3.71
	$\text{Cs}_{2.5}\text{Mn}_{0.08}\text{H}_{1.34}\text{PVMo}_{11}\text{O}_{40}$	425	5.8	41	59	3.42
	$\text{Cs}_{2.5}\text{H}_{1.5}\text{PVMo}_{11}\text{O}_{40}$	425	4.0	39	61	2.44
	$\text{Cs}_{2.5}\text{Ni}_{0.08}\text{H}_{1.34}\text{PVMo}_{11}\text{O}_{40}$	425	3.4	42	58	1.97
	$\text{Cs}_{2.5}\text{Co}_{0.08}\text{H}_{1.34}\text{PVMo}_{11}\text{O}_{40}$	425	5.7	70	30	1.71

^a(A) Ethane, 33 vol %; O_2 , 33 vol %; N_2 , balance; catalyst, 1.0 g; total flow rate, $15\text{ cm}^3\text{ min}^{-1}$. (B) Ethane, 57 vol %; O_2 , 9 vol %; N_2 , balance; catalyst, 1.0 g; total flow rate, $15\text{ cm}^3\text{ min}^{-1}$. ^bCalculated on the C_2 (ethane)-basis.

Table 12. Selective Oxidation from Ethane to Ethylene over Transition Metal-Modified Antimony-Containing Potassium Salts of 12-Molybdophosphate^a

precatalyst ^d	temp (°C)	time-on-stream (h)	C ₂ H ₆ conversion (%)	C ₂ H ₄ selectivity (%)	C ₂ H ₄ yield (%)
K ₃ Fe ₁ Ce _{0.25} Cr _{0.5} Sb ₁ ^c	540		36.2	54	19.55
K ₃ Fe ₁ Ce _{0.25} Cr _{0.5} Sb ₁	540	1	17.2	62	10.66
K ₃ Fe ₁ Ce _{0.25} Sb ₁	540	1	9.6	65	6.24
K ₃ Fe ₁ Sb ₁	540	3	6.8	83	5.64
K ₃ V ₁ Sb ₀	425	1	24	22	5.28
K ₃ Fe ₁ Sb ₀	500	1	9.7	48	4.66
K ₃ Fe ₁ Sb ₀	500	3	7.2	51	3.67
K ₃ V ₁ Sb ₀	425	3	11.2	29	3.25
K ₃ V ₁ Sb ₁	425	3	6.5	49	3.19
K ₃ Fe ₁ Sb ₀	425	1	5.4	59	3.19
K ₃ V ₁ Sb ₁	425	1	6.8	46	3.13
K ₃ Fe ₁ Sb ₀	425	3	4.7	65	3.06
K ₁ Sb ₀	425	1	5.6	48	2.69
K ₃ Sb ₀	425	1	5.6	43	2.41
K ₃ Sb ₁	540	40	5.7	41	2.34
K ₃ Sb ₁	540	10	6.1	38	2.32
K ₃ Sb ₁	540	1	6.7	34	2.28
K ₃ Sb ₁	500	1	5.9	38	2.24
K ₃ Fe ₁ Sb ₁	425	1	2.6	86	2.24
K ₃ Fe ₁ Ce _{0.25} Cr _{0.5} Sb ₁ ^b	500	1	9.2	22	2.02
K ₁ Sb ₁	425	1	3.5	52	1.82
K ₁ Sb ₁	425	3	3.1	56	1.74
K ₃ Sb ₀	425	3	3.8	40	1.52
K ₃ Sb ₁	425	1	2.8	42	1.18
K ₃ Sb ₁	425	3	2.5	44	1.10
K ₁ Sb ₀	425	3	2.5	43	1.08
K ₁ Sb ₀	400	1	2	54	1.08
K ₁ Sb ₀	400	3	1.2	46	0.55
K ₃ Fe ₁ Ce _{0.25} Cr _{0.5} Sb ₁ ^b	500	3	<1	25	<0.25

^aReaction conditions: atmospheric pressure; ethane (3.6%), oxygen (10%), and balanced with inert diluent gas. No other condition was mentioned.

^bThis compound was prepared without phosphorous and did not possess the heteropoly compound structure; residence time, 10 s. ^cFresh catalyst.

^dThe precatalysts' abbreviations denote their K, Sb, Fe, Ce, V, and Cr content; for example, K₁Sb₁ stands for the sample with composition K₁(NH₄)_xPMo₁₁Sb₁O₄₀.

6.2.2. Selective Oxidation of Ethane to Ethylene and Acetaldehyde. Moffat et al. first reported in 1994 the oxidative dehydrogenation of ethane on SiO₂-supported heteropoly acid catalysts (viz., HSiMo₁₂, HPMo₁₂, HM₉V₃, HPW₁₂, HSiW₁₂)^{104,114} in studies similar to that about methane (vide supra). Ethane was converted to both ethylene and acetaldehyde at temperatures between 450 and 570 °C using nitrous oxide and oxygen (Scheme 15 and Table 14).

For both oxidants, molybdenum-based catalysts outperformed their tungsten counterparts in conversion and selectivity toward ethylene. Inclusion of a minor amount of vanadium addenda showed little effect on the conversion but directed the selectivity toward ethylene instead of acetaldehyde. Using oxygen as oxidant increased the conversion of ethane to ethylene yet with more CO_x by products; N₂O reduced the conversion but led to a significant amount of acetaldehyde. Several other variables such as reaction temperature, partial pressure of reactants, residence time, and loading amount of the heteropoly acid influenced the results. For example, for H₃PMo₁₂O₄₀ supported on SiO₂, the conversion and yield of acetaldehyde were the highest for a loading of ca. 20 wt %.

The mechanism proposed for this system involved the formation of a C₂H₅[•] radical by reaction of ethane with one oxygen atom (bridging or terminal) of the polyoxometalate and formation of a Mo(V) species. The reoxidation of the

polyoxometalate was then achieved by the oxidant. In this mechanism, ethanol should be a primary product but was not observed presumably due to its short lifetime under the reaction conditions. It can be formed from the reaction of protons of H₃PMo₁₂O₄₀ with the ethoxy group resulting from the ethylation of the Keggin anion or from the reaction of the ethoxy group with water. Its further oxidation can lead, in parallel to ethylene, to acetaldehyde and then to CO_x (Scheme 16).

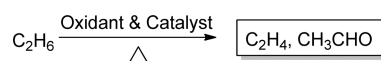
6.2.3. Selective Oxidation of Ethane to Ethylene and Acetic Acid. Subsequent investigations reported the production of ethylene and acetic acid without that of acetaldehyde (Scheme 17). Series of HPC supported on inorganic support or modified by inclusion of transition metal counterion or even organic additive were reported (see Table 15).

Nowinska et al. studied molybdo(vanado) phosphoric heteropoly acids supported on oxide supports (viz., SiO₂, TiO₂, Al₂O₃). Ethane was converted to ethylene and acetic acid at atmospheric pressure of a mixture of O₂ and H₂O in the 250–400 °C temperature range (Table 13).¹¹⁵ The type of inorganic carrier used was non innocent over the performance of the catalyst over SiO₂-supported H_{3+x}PMoV_xO₄₀ (abbreviated by HPMoV_x, x = 0, 1, 2, 3) catalysts; selectivity toward ethylene was about 70% from 300 to 360 °C. TiO₂-supported HPMoV_x catalysts led to a higher acetic acid yield, but carbon

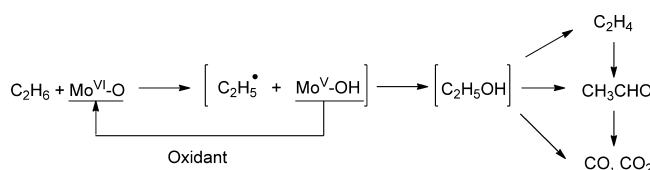
Table 13. Selective Oxidation from Ethane to Ethylene^{113 a}

precatalyst	calcination temp (°C)	temp (°C)	time-on-stream (h)	C ₂ H ₆ conversion (%)	C ₂ H ₄ selectivity (%)	C ₂ H ₄ yield (%)
Mn-modified lacunary HPW	430	400	1	26	18	4.68
Mn-modified lacunary HPW	430	400	2	17	35	5.95
Mn-modified lacunary HPW	430	400	3	15	32	4.80
Mn-modified lacunary HPW	430	400	4	12	26	3.12
Mn-modified lacunary HPW	430	400	5	9	32	2.88
Mn-modified lacunary HPW	430	400	6	11	27	2.97
Mn-modified lacunary HPW	430	430	1	46	47	21.62
Mn-modified lacunary HPW	430	430	2	36	67	24.12
Mn-modified lacunary HPW	430	430	3	37	62	22.94
Mn-modified lacunary HPW	430	430	4	42	66	27.72
Mn-modified lacunary HPW	430	430	5	43	65	27.95
Mn-modified lacunary HPW	430	430	6	44	69	30.36
Mn-modified lacunary HPW	500	430	1	20	63	12.60
Mn-modified lacunary HPW	500	430	2	27	63	17.01
Mn-modified lacunary HPW	500	430	3	29	64	18.56
Mn-modified lacunary HPW	500	430	4	26	60	15.60
Mn-modified lacunary HPW	500	430	5	26	60	15.60
Mn-modified lacunary HPW	500	430	6	26	60	15.60
Mn-P-W-O oxide	430	430	1	64	73	46.72
Mn-P-W-O oxide	430	430	2	56	66	36.96
Mn-P-W-O oxide	430	430	3	49	64	31.36
Mn-P-W-O oxide	430	430	4	35	54	18.90
Mn-P-W-O oxide	430	430	5	30	50	15.00
Mn-P-W-O oxide	430	430	6	20	50	10.00

^aMn-modified lacunary HPW was synthesized under pH = 3.5. Reaction conditions: catalyst, 0.5 g; 400 and 430 °C; WHSV (weight hourly space velocity) = 0.22 or 0.12 g g⁻¹ h⁻¹; feed composition, air:ethane = 25:1.

Scheme 15. General Conditions Employed for the Oxidation of Ethane to Ethylene and Acetaldehyde^a

^aOxidant: N₂O and O₂; P = 20 atm; T = 540 °C.

Scheme 16. Possible Reaction Paths for the Oxidation of Ethane over SiO₂-Supported H₃PMo₁₂O₄₀ Catalyst¹⁰⁵

dioxide was the major product. When Al₂O₃ was employed, the catalysts showed only a very low selectivity that was explained by the possible destruction of the Keggin unit by the basic surface group onto alumina. The influence of the vanadium

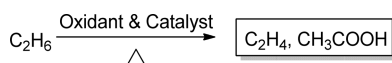
incorporation was assessed by screening HPC with different formulations (Figure 6).

Table 14. Selective Oxidation from Ethane to Ethylene and Acetaldehyde^{114 a}

	precatalyst	oxidant	temp (°C)	C ₂ H ₆ conversion (%)	selectivity (%)			yield (%)	
					CO _x	C ₂ H ₄	CH ₃ CHO	C ₂ H ₄	CH ₃ CHO
(A)	H ₃ PW ₁₂ O ₄₀ /SiO ₂	N ₂ O	540	0.7	8.3	62.5	28.8	0.44	0.20
	H ₄ SiW ₁₂ O ₄₀ /SiO ₂	N ₂ O	540	0.7	7.4	61.8	30.1	0.43	0.21
	H ₃ PMo ₁₂ O ₄₀ /SiO ₂	N ₂ O	540	2.7	19.3	47.7	30.0	1.29	0.81
	H ₄ SiMo ₁₂ O ₄₀ /SiO ₂	N ₂ O	540	3.1	22.7	48.7	26.1	1.51	0.81
	H ₆ PV ₃ Mo ₉ O ₄₀ /SiO ₂	N ₂ O	540	3.2	26.1	69.3	2.7	2.22	0.09
	H ₃ PMo ₁₂ O ₄₀	N ₂ O	540	0.2	18.8	81.2		0.16	0.00
	V/SiO ₂	N ₂ O	540	9.3	23.4	73.6		6.84	0.00
	Mo/SiO ₂	N ₂ O	540	0.5	32.6	51.1	12.7	0.26	0.06
(B)	SiO ₂	N ₂ O	540	0.1	15	72.1		0.07	0.00
	H ₆ PV ₃ Mo ₉ O ₄₀ /SiO ₂	O ₂	540	5.1	65.6	34.5		1.76	0.00
	H ₃ PMo ₁₂ O ₄₀ /SiO ₂	O ₂	540	4.8	67.8	31.1	1.1	1.49	0.05
	V/SiO ₂	O ₂	540	7.9	43.7	55.9		4.42	0.00
	Mo/SiO ₂	O ₂	540	1.4	60.2	37.1	2.7	0.52	0.04
	SiO ₂	O ₂	540	0.3	70.7	26.4		0.08	0.00

^aReaction conditions: catalyst, 0.5 g; total flow rate, 25 mL min⁻¹. (A) C₂H₆ (80%), N₂O (20%); (B) C₂H₆ (80%), O₂ (20%).

Scheme 17. General Conditions Employed for the Oxidation of Ethane to Ethylene and Acetic Acid^a



^aOxidant: O₂; T = 250–400 °C.

Improvement of the catalytic performances was observed when vanadium atoms were introduced into the Keggin structure, while the vanadyl group introduced into the cationic position (H(VO)P–MoV_x) resulted in a decrease in oxidative activity. The presence of water vapor in the reagents mixture was required for both acetic acid desorption and modification of catalyst surface.

Davis et al. modified a series of pyridine-exchanged HPC phosphomolybdic by introducing transition metals, particularly niobium, as either addenda or counteraction. All HPC were screened for the oxidative dehydrogenation of ethane at atmospheric pressure and moderate temperature under oxygen and steam (see Table 16).^{116–119} Conversion as high as 18% was observed with niobium as counteraction and various addenda formulations. In those cases, selectivities for ethylene were comprised between 25% and 42%, while that for acetic acid is between 5% and 10%. The highest selectivities for ethylene were for pyridine-exchanged phosphomolybdic with antimony and zirconium (86% and 63%) at low conversion (0.6% and 0.2%). Total conversion of ethane to acetic acid was observed for (VO)_{0.5}PMo₁₁GaPyr yet at low conversion (0.4%). It is noteworthy that acetic acid (46%) can be produced by Nb_{0.04}PMo₁₂Pyr without vanadium. Overall, niobium and pyridine are essential for efficient catalysis with the best activity being observed under reducing or mild oxidizing conditions.

Extensive structural studies have been undertaken to probe the active species by EXAFS, XANES, XRD, DSC, XPS, and ³¹P NMR. The pyridine is believed to modify the secondary structure by forming pyridinium ion. Under the catalysis condition over the temperature range 380–420 °C, the unit is believed to undergo partial decomposition, and the molybdenum and niobium centers are reduced by removal of the pyridine species.

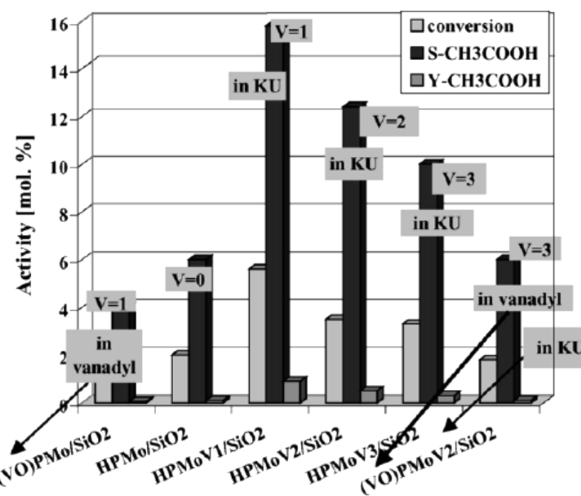


Figure 6. Influence of vanadium localization (in the Keggin structure or in the cationic position) on ethane conversion and selectivity toward acetic acid. Reprinted with permission from ref 115. Copyright 2005 Elsevier B.V.

Over partially reduced niobium-exchanged phosphomolybdic Keggin-type heteropolyanions (NbPMo₁₂Pyr), their results suggested the possible reaction scheme shown in Scheme 18. Ethane could be oxidized directly to ethylene and a small amount of acetic acid with large losses to carbon oxides. Ethylene was collected as a product or further oxidized to acetic acid with a significant degradation to carbon oxides.

Oshihara et al. have prepared mixed oxide catalysts by hydrothermal treatment of heteropolytungstate with Anderson structure incorporating vanadium, gallium, or iron ions; variable amounts of [(CH₃CH₂)₂NH⁺] were added during the crystallization growth step. The catalyst was contacted by ethane, oxygen, and water vapor at 340 °C to yield mostly ethylene (60–85%) and a minor amount of acetic acid.¹²⁰ Best conversion was observed with Mo₆V₂GaO_x but with the lowest yield of CH₃COOH (see Table 17). Using [(CH₃CH₂)₂NH⁺] during the preparation increased the conversion for each HPC, regardless of the formulation of the Anderson structure. The role of [(CH₃CH₂)₂NH⁺] remains unclear.

Table 15. Selective Oxidation from Ethane to Ethylene and Acetic Acid^{115 a}

precatalyst	temp (°C)	C ₂ H ₆ conversion (%)	selectivity (%)			yield (%)	
			CO _x	C ₂ H ₄	CH ₃ COOH	C ₂ H ₄	CH ₃ COOH
H ₅ PMoV ₂ O ₄₀ /SiO ₂	250	0.4	11	67	22	0.27	0.09
H ₅ PMoV ₂ O ₄₀ /SiO ₂	300	1.5	15	70	15	1.05	0.23
H ₅ PMoV ₂ O ₄₀ /SiO ₂	330	3.5	19	69	12	2.42	0.42
H ₅ PMoV ₂ O ₄₀ /SiO ₂	360	5.5	19	70	11	3.85	0.61
H ₅ PMoV ₂ O ₄₀ /SiO ₂	400	12	45	50	5	6.00	0.60
H ₅ PMoV ₂ O ₄₀ /Al ₂ O ₃	250	0.4	n.d.	n.d.	28	0.00	0.11
H ₅ PMoV ₂ O ₄₀ /Al ₂ O ₃	300	3	n.d.	n.d.	7	0.00	0.21
H ₅ PMoV ₂ O ₄₀ /Al ₂ O ₃	330	7.5	n.d.	n.d.	6.2	0.00	0.47
H ₅ PMoV ₂ O ₄₀ /Al ₂ O ₃	360	15	n.d.	n.d.	4.5	0.00	0.68
H ₅ PMoV ₂ O ₄₀ /Al ₂ O ₃	400	22	n.d.	n.d.	2.5	0.00	0.55
H ₅ PMoV ₂ O ₄₀ /TiO ₂	250	3	n.d.	n.d.	25	0.00	0.75
H ₅ PMoV ₂ O ₄₀ /TiO ₂	300	6.5	n.d.	n.d.	12	0.00	0.78
H ₅ PMoV ₂ O ₄₀ /TiO ₂	330	12	n.d.	n.d.	7	0.00	0.84
H ₅ PMoV ₂ O ₄₀ /TiO ₂	360	14	n.d.	n.d.	6	0.00	0.84
H ₅ PMoV ₂ O ₄₀ /TiO ₂	400	18	n.d.	n.d.	3	0.00	0.54

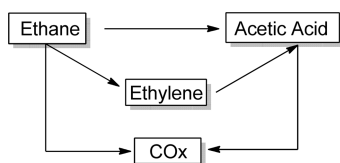
^aReaction conditions: catalyst, 2 g; C₂H₆:O₂:H₂O:N₂ = 2:1:1.8:4; WHSV (weight hourly space velocity) = 0.35 g/g·h.

Table 16. Selective Oxidation from Ethane to Ethylene and Acetic Acid¹¹⁶^a

precatalyst ^c	temp (°C)	C ₂ H ₆ conversion (%)	selectivity (%)			yield (%)	
			CO _x	C ₂ H ₄	CH ₃ COOH	C ₂ H ₄	CH ₃ COOH
Zr _{0.4} PMo ₁₂ Pyr	380	0.2	35	63	1.9	0.13	0.004
Ti _{0.4} PMo ₁₂ Pyr	380	1.3	81	18	0.6	0.23	0.008
Ta _{0.4} PMo ₁₂ Pyr	380	0.1	88	9	3.6	0.01	0.004
Nb _{0.4} PMo ₁₂	380	0.3	39	52.8	8.2	0.16	0.025
Sb ₁ PMo ₁₁ NbPyr	380	3	54	43	3	1.29	0.090
Sb _{0.5} PMo ₁₁ NbPyr	380	7	53	43	5	3.01	0.350
Sb _{0.4} PMo ₁₂ Pyr	380	0.6	11	86	3.2	0.52	0.019
Sb _{0.15} PMo ₁₁ NbPyr	380	7	63	32	5	2.24	0.350
PMo ₁₂ Pyr	380	0.6	70	30	0	0.18	0.000
Nb ₁ PMo ₁₂ Pyr	380	10.6	49	42	9	4.45	0.954
Nb ₁ PMo ₁₁ V ₁ Pyr	380	7	60	31	9	2.17	0.630
Nb ₁ PMo ₁₁ SbPyr	380	3	54	43	3	1.29	0.090
Nb _{0.8} PMo ₁₂ Pyr	380	11.7	54	36	10	4.21	1.170
Nb _{0.85} PMo ₁₁ V ₁ Pyr	380	6.1	54	36	11	2.20	0.671
Nb _{0.6} PMo ₁₂ Pyr	380	15.9	62	29	9	4.61	1.431
Nb _{0.68} PMo ₁₁ V ₁ Pyr	380	7.4	52	36	12	2.66	0.888
Nb _{0.6} PMo ₁₁ SbPyr	380	9	53	40	8	3.60	0.720
Nb _{0.5} PMo ₁₁ GaPyr	380	18	65	30	5	5.40	0.900
Nb _{0.5} PMo ₁₁ FePyr	380	18	69	25	6	4.50	1.080
Nb _{0.4} PMo ₁₂ Pyr ^b	380	4.7	30	62	8	2.91	0.376
Nb _{0.4} PMo ₁₂ Pyr	380	17	66	28	6	4.76	1.020
Nb _{0.4} PMo ₁₁ V ₁ Pyr	380	4.6	48	40	11	1.84	0.506
Nb _{0.2} PMo ₁₂ Pyr	380	5.9	40	49	11	2.89	0.649
Nb _{0.2} PMo ₁₁ V ₁ Pyr	380	5.5	49	41	11	2.26	0.605
Nb ₁ PMo ₁₁ SbPyr	380	2	49	49	2	0.98	0.040
Nb _{0.5} PMo ₁₁ SbPyr	380	9	53	40	8	3.60	0.720
Nb _{0.15} PMo ₁₁ SbPyr	380	5	47	45	8	2.25	0.400
Nb _{0.04} PMo ₁₂ Pyr	380	0.7	12	42	46	0.29	0.322
Nb _{0.04} PMo ₁₁ V ₁ Pyr	380	1.8	40	51	9	0.92	0.162
(VO) _{0.5} PMo ₁₁ GaPyr	380	0.4	0	0	100	0.00	0.400
(VO) _{0.5} PMo ₁₁ FePyr	380	0.9	43	24	33	0.22	0.297
PMo ₁₂	380	0.1	100	0	0	0.00	0.000

^aReaction conditions: catalyst, 0.6 g; flow rates, 16:8:16:20 mL min⁻¹ (ethane:oxygen:helium:steam); GHSV (gas hourly space velocity), 2250 h⁻¹.^bExchanged with pyridinium chloride rather than pyridine. ^cThe precatalysts' abbreviations denote their Zr, Ti, Ta, Nb, Sb, VO, and Mo content.

Scheme 18. Reaction Pathway for the Production of Ethylene and Acetic Acid over Partially Reduced Niobium-Exchanged Phosphomolybdic Keggin-type Heteropolyanions¹¹⁶



6.3. Conclusion

To summarize, the general condition of catalysis from the transformation of ethane was with temperature comprised between 250 and 540 °C under atmospheric pressure.

Conversion of ethane as high as 46% (Mn-modified lacunary heteropoly compound (PW₁₁O₃₉⁷⁻)) was obtained,¹¹³ 18% for Nb_{0.5}PMo₁₁GaPyr,¹¹⁶ and 22% for HPMoV₂/Al₂O₃,^{113,115} which appear to be structurally destroyed.

Maximum selectivities for ethylene production were reported with Mn-modified lacunary heteropoly compound (PW₁₁O₃₉⁷⁻).¹¹³ Acetaldehyde with 30% selectivity was reported only in Moffat's studies (HSiW₁₂ on SiO₂).¹¹⁴

Selectivities to acetic acid were as high as 86% (Nb_{0.4}PMo₁₂Pyr)¹¹⁶ and 100% ((VO)_{0.5}PMo₁₁GaPyr),¹¹⁶ respectively, although at low conversion.

It is worthy of note that temperatures of catalysis reported are significantly lower than previous results on the conversion of methane; yet no catalysis at low to ambient temperature has been reported.

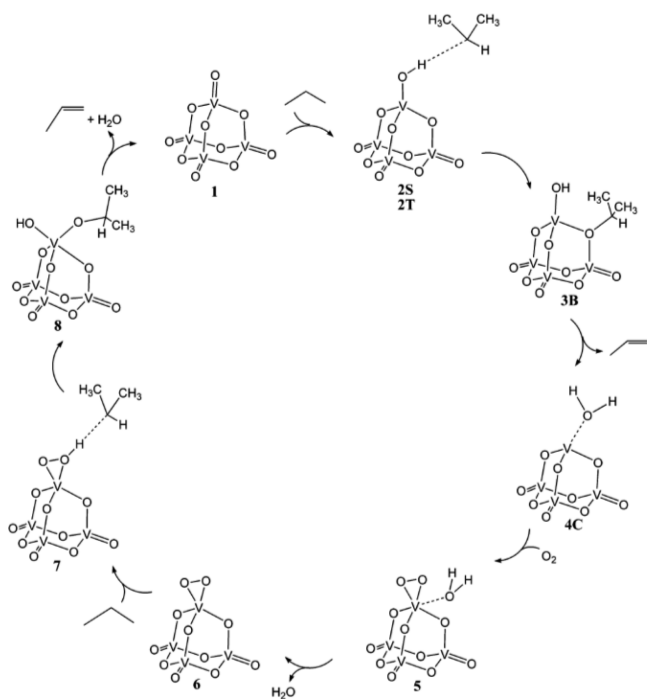
7. SELECTIVE OXIDATION OF PROPANE

Propane can be oxidized to several products such as acetic acid, ethylene, and acrolein, with propylene and acrylic acid being the two major ones. Some catalytic systems have been able to direct the reaction toward propylene or acrylic acid, and they will be examined separately.

7.1. Oxidative Dehydrogenation (ODH) of Propane to Propylene

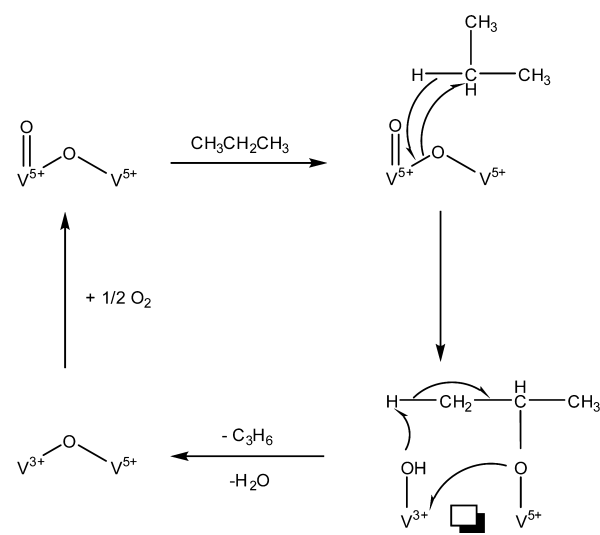
Propylene is a very important chemical feedstock for the productions of polypropylene, acrylonitrile, and propylene oxide, and its worldwide demand keeps on growing. However, in the current chemical industry, propylene is mainly produced together with ethylene via the cracking of naphtha. The development of new routes for propylene production becomes more and more urgent. The ODH of propane is a promising

Scheme 19. The Catalytic Cycle for ODH of Propane on V_4O_{10} , a Prototype of the Single Site Vanadyl Activation, Functionalization, and Reoxidation (SS-VAFR)^a



^aReprinted with permission from ref 131. Copyright 2007 American Chemical Society.

Scheme 20. The Proposed Propane ODH Mechanism through Alkoxy Intermediate¹³⁵



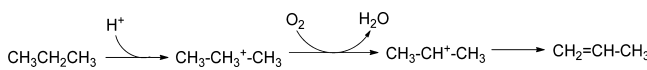
Scheme 21. General Conditions Employed for the Oxidative Dehydrogenation of Propane to Propylene^a



^aOxidant: O_2 ; $T = 305\text{--}450\ ^\circ\text{C}$.

alternative for propylene production by utilizing the abundant inexpensive propane resource. However, because propane is a stable molecule, and the weakest C–H bond in propane is much stronger than that in propylene,¹²¹ the ODH of propane

Scheme 22. Proposed Reaction Scheme for the Conversion of Propane Catalyzed by Brønsted Acid Sites¹³⁷



to propylene is still suffering from low yield. Many supported metal oxides and composite metal oxides have been examined as catalyst for ODH of propane, and most of them contain V or Mo as the active components.^{122–126}

7.1.1. General Mechanisms for Propane ODH to Propylene Reaction. Concerning the reaction mechanism for propane ODH to propylene, the general agreement in literature is that the rate-determining step is the breaking of the first C–H bond, leading to a propyl species. Many mechanism studies have been carried out on V-based catalysts,^{44,127–130} among which H-abstraction via TS6 (Scheme 2) is the most favorable pathway. Goddard¹³¹ and Sauer¹²³ found that the H-abstraction mechanism was dominant for propane ODH reaction over V_2O_5 (001) surface, which involved the single vanadyl oxygen ($V=O$) together with the bridging oxygens ($V-O-V$) serving to stabilize the iso-propyl radical intermediate (Scheme 19).

Another proposed propane ODH mechanism involves an alkoxy species, which comes from the direct insertion of a lattice oxygen atom into a propane C–H bond (Scheme 20). This alkoxy species could further decompose to propylene.^{132,133} However, the ΔE barrier values of this alkoxy path have sparked controversy.^{130,131,133,134} Therefore, the former propyl radical mechanism from hydrogen abstraction is still the most acceptable mechanism to date.

7.1.2. ODH of Propane to Propylene over HPC Catalysts. Mizuno et al. tested the catalytic performances of $Cs_{2.5}Cu_{0.08}H_{1.34}PVMo_{11}O_{40}$ for the oxidative dehydrogenation of propane at $380\ ^\circ\text{C}$ under both oxygen-rich and oxygen-poor conditions.^{107,108,136} A higher selectivity to propylene was observed in the presence of excess oxygen, and the higher was the number of vanadium atoms in the polyoxometalate, the better was the yield of propylene (Scheme 21). For example, under oxygen-rich conditions at $380\ ^\circ\text{C}$ over the $Cs_{2.5}Cu_{0.08}H_{3.34}PV_3Mo_9O_{40}$ catalyst precursor, 35% propane conversion and 27% propylene selectivity (9.5% yield) were observed. Addition of Fe^{3+} to $Cs_{2.5}H_{1.5}PVMo_{11}O_{40}$ ^{108,110} led to increased yield of propylene without influencing that of acrylic acid (see Table 18).

Sun et al. found that the molybdophosphate heteropoly compound, $Cs_xH_{3-x}PMo_{12}O_{40}$ ($x = 2.0\text{--}3.0$), could also catalyze the oxidative dehydrogenation of propane. The best yield of propylene (9.3%) could be achieved over the $Cs_{2.56}H_{0.44}PMo_{12}O_{40}$ catalyst at $380\ ^\circ\text{C}$ (Table 19).¹³⁷ This C_3H_6 yield is comparable to that (9.5%) reported over a heavily substituted polyoxometalate catalyst, that is, $Cs_{2.5}Cu_{0.08}H_{3.34}PV_3Mo_9O_{40}$, under similar reaction conditions (see Table 18).¹³⁶ However, the selectivity to C_3H_6 over $Cs_{2.56}H_{0.44}PMo_{12}O_{40}$ catalyst (58%) is significantly higher than that over the $Cs_{2.5}Cu_{0.08}H_{3.34}PV_3Mo_9O_{40}$ (27%). The substitution of one Mo by one V could not increase the maximum yield of C_3H_6 .

They showed that the conversion was proportional to the number of Brønsted acid sites, while the selectivity to propylene decreased when the surface acidity increased. A proposed reaction scheme for propane conversion catalyzed by Brønsted acid sites is shown in Scheme 22. The main step is the

Table 17. Selective Oxidation from Ethane to Ethylene and Acetic Acid^{120 a}

precatalyst ^b	(C ₂ H ₅) ₃ NHCl (mol L ⁻¹)	C ₂ H ₆ conversion (%)	selectivity (%)			yield (%)	
			CO _x	C ₂ H ₄	CH ₃ COOH	C ₂ H ₄	CH ₃ COOH
Mo ₆ V ₁ Al ₁ O _x	0.00	2.4	16.3	78.4	5.3	1.88	0.13
Mo ₆ V ₁ Al ₁ O _x	0.16	3.9	16.7	73.1	10.2	2.85	0.40
Mo ₆ V ₃ Fe ₁ O _x	0.00	1.8	25.8	68.2	6	1.23	0.11
Mo ₆ V ₃ Fe ₁ O _x	0.52	2.4	27.7	62.8	9.5	1.51	0.23
Mo ₆ V ₃ Ga ₁ O _x	0.00	5.6	25.2	72.1	2.8	4.04	0.16
Mo ₆ V ₃ Ga ₁ O _x	0.16	12.6	11.4	84.5	4.2	10.65	0.53

^aReaction conditions: catalyst, 1.0 g; C₂H₆:O₂:N₂:H₂O (vapor) = 15:5:20:10 mL min⁻¹; temperature, 340 °C. ^bThe precatalysts' abbreviations denote their Mo, V, Al, Fe, and Ga content.

Table 18. Selective Oxidation from Propane to Propylene, Acrylic Acid, Acetic Acid, Ethylene, and Acrolein

catalyst	C ₃ H ₈ conversion (%)	selectivity ^d (%)						ref
		CO _x	C ₃ H ₆	CH ₂ CHCHO	CH ₂ CHCOOH	C ₂ H ₄	CH ₃ COOH	
Cs _{2.5} H _{1.5} PVMo ₁₁ O ₄₀ ^a	15.1	8.4	3.4	0.7	0.5	0.5	1.6	0.51
Cs _{2.5} Cu _{0.08} H _{1.34} PVMo ₁₁ O ₄₀ ^a	17.9	9.4	4.1	0.9	0.6	1.0	1.9	0.73
Cs _{2.5} Cu _{0.08} H _{0.34} PMo ₁₂ O ₄₀ ^b	35	59	21	3	2	6	6	7.35
Cs _{2.5} Cu _{0.08} H _{1.34} PVMo ₁₁ O ₄₀ ^b	36	55	20	3	6	6	8	7.20
Cs _{2.5} Cu _{0.08} H _{2.34} PV ₂ Mo ₁₀ O ₄₀ ^b	35	52	25	4	1	7	7	8.75
Cs _{2.5} Cu _{0.08} H _{3.34} PV ₃ Mo ₉ O ₄₀ ^b	35	53	27	2	2	6	7	9.45
Cs _{2.5} H _{0.5} PMo ₁₂ O ₄₀ ^c	12	77	6	1	8	0	8	0.72
Cs _{2.5} Fe _{0.08} H _{0.26} PMo ₁₂ O ₄₀ ^c	13	60	9	2	18	0	11	1.17

^aPropane, 33 vol %; O₂, 17 vol %; N₂, balance; catalyst, 1.0 g; total flow rate, 30 cm³ min⁻¹; temperature, 380 °C. ^bPropane, 33 vol %; O₂, 33 vol %; N₂, balance; catalyst, 1.0 g; total flow rate, 30 cm³ min⁻¹; temperature, 380 °C. ^cPropane, 30 vol %; O₂, 40 vol %; N₂, balance; catalyst, 1.0 g; total flow rate, 30 cm³ min⁻¹; temperature, 360 °C. ^dSelectivity calculation based on C₃ (propane).

Table 19. Selective Oxidation from Propane to Propylene^{137 a}

catalyst	temp (°C)	C ₃ H ₈ conversion (%)	selectivity (%)			yield (%)
			CO _x	C ₃ H ₆	others ^b	
H _{3.0} PMo ₁₂ O ₄₀	380	3.6	51	45	4	1.62
Cs _{2.0} H _{1.0} PMo ₁₂ O ₄₀	380	30	96	3	1	0.90
Cs _{2.2} H _{0.8} PMo ₁₂ O ₄₀	380	25	96	4	0	1.00
Cs _{2.4} H _{0.6} PMo ₁₂ O ₄₀	380	21	84	15	1	3.15
Cs _{2.48} H _{0.52} PMo ₁₂ O ₄₀	380	18	60	37	3	6.66
Cs _{2.56} H _{0.44} PMo ₁₂ O ₄₀	380	16	39	58	3	9.28
Cs _{2.6} H _{0.4} PMo ₁₂ O ₄₀	380	12	36	61	3	7.32
Cs _{2.8} H _{0.2} PMo ₁₂ O ₄₀	380	0.8	13	87	0	0.70
Cs _{3.0} PMo ₁₂ O ₄₀	380	0.2	9	91	0	0.18
H _{4.0} PVMo ₁₁ O ₄₀	380	26	91	8	1	2.08
Cs _{2.0} H _{2.0} PVMo ₁₁ O ₄₀	380	30	76	19	5	5.70
Cs _{2.5} H _{1.5} PVMo ₁₁ O ₄₀	380	25	77	23	0	5.75
Cs _{2.75} H _{1.25} PVMo ₁₁ O ₄₀	380	24	68	32	0	7.68
Cs _{3.0} H _{1.0} PVMo ₁₁ O ₄₀	380	20	52	41	7	8.20
Cs _{3.25} H _{0.75} PVMo ₁₁ O ₄₀	380	2.4	26	71	3	1.70
Cs _{3.5} H _{0.5} PVMo ₁₁ O ₄₀	380	0.8	19	75	6	0.60
Cs _{4.0} PVMo ₁₁ O ₄₀	380	0.03	14	86	0	0.03

^aReaction conditions: catalyst, 1.8 g; total flow rate, 32 mL min⁻¹; P(C₃H₈) = 4.8 kPa, P(O₂) = 96.5 kPa; time on stream, 1 h. ^bOthers: CH₃CHO, CH₂CHCHO.

reaction of the acidic proton with propane, leading to the evolution of hydrogen and the formation of a propyl cation. The characterizations of the catalyst after ~120 h of reaction revealed that there were no significant changes in catalyst structures as reflected by XRD and FT-IR.

Later, they successfully synthesized a series of Cs salts of 12-tungstophosphoric acid (Cs_xH_{3-x}PW₁₂O₄₀, x = 0–3.0) samples with systematically varied surface areas, acidities, and microstructures, and used them as catalysts in oxidative dehydrogenation of propane reaction.¹³⁸ Their studies demonstrated that,

except the acidity, the porous structure of the Cs_xH_{3-x}PW₁₂O₄₀ catalysts also plays a key role in this reaction. The mesopore structure could improve C₃H₈ conversion significantly. The best yield of propylene (11%) was achieved over the Cs_{1.5}H_{1.5}PW₁₂O₄₀ catalyst (Table 20), which possessed a high concentration of acid sites and nonporous structure. The catalyst remained stable even after 10 h of reaction.

Nowinska et al.¹³⁹ used Keggin-type lacunary tungstophosphoric HPC (HPW₁₁) modified with transition metal ions (Fe²⁺, Fe³⁺, and Mn²⁺) as precursors of catalysts for the

Table 20. Selective Oxidation from Propane to Propylene^{138 a}

catalyst	temp (°C)	C ₃ H ₈ conversion (%)	selectivity (%)			yield (%)
			CO _x	C ₃ H ₆	others ^b	
H _{3.0} PW ₁₂ O ₄₀	380	22	67	21	12	4.62
Cs _{0.9} H _{2.1} PW ₁₂ O ₄₀	380	19	49.6	38	12.4	7.22
Cs _{1.5} H _{1.5} PW ₁₂ O ₄₀	380	18	51.6	38	10.4	6.84
Cs _{1.5} H _{1.5} PW ₁₂ O ₄₀	400	17	49.6	39	11	6.63
Cs _{1.5} H _{1.5} PW ₁₂ O ₄₀	420	20	49	39	12	7.80
Cs _{1.5} H _{1.5} PW ₁₂ O ₄₀	440	25	49.1	38	13	9.50
Cs _{1.5} H _{1.5} PW ₁₂ O ₄₀	460	36	58	30	12	10.80
Cs _{1.5} H _{1.5} PW ₁₂ O ₄₀	480	55	89	8.5	2.1	4.68
Cs _{2.0} H _{1.0} PW ₁₂ O ₄₀	380	16	52	36	12	5.76
Cs _{2.1} H _{0.9} PW ₁₂ O ₄₀	380	18	69	19	12	3.42
Cs _{2.2} H _{0.8} PW ₁₂ O ₄₀	380	28	99	0.9	0.1	0.25
Cs _{2.4} H _{0.6} PW ₁₂ O ₄₀	380	27	99	0.8	0.2	0.22
Cs _{2.7} H _{0.3} PW ₁₂ O ₄₀	380	26	99	0.9	0.1	0.23
Cs _{3.0} PW ₁₂ O ₄₀	380	0				0.00

^aReaction conditions: catalyst, 1.8 g; total flow rate, 31 mL min⁻¹; feed gas, C₃H₈:O₂ = 5:95. ^bOthers: CH₃CHO, CH₂CHCHO, CH₂CHCOOH, CH₃COOH, CH₃COCH₃.

oxidative dehydrogenation of propane. Iron did not lead to highly active systems, but the systems prepared with an excess of manganese showed good conversion (41%; Mn(12)/Al₂O₃) and selectivity (71%; MnPWMn) (Table 21).

Table 21. Selective Oxidation from Propane to Propylene^{139 a}

precatalyst	temp (°C)	C ₃ H ₈ conversion (%)	selectivity (%)		yield (%)
			CO _x	C ₃ H ₆	
Mn(12)/Al ₂ O ₃	400	41	82	12	4.92
Mn(12)/SiO ₂	400	29	80	16	4.64
Mn(12)/MgO	400	19	72	25	4.75
Mn(12)/CsPW	400	10	32	42	4.20
MnPWMn ^b	400	15	23	71	10.65

^aReaction conditions: catalyst, 0.5 g; WHSV (weight hourly space velocity) = 0.22 or 0.12 g g⁻¹ h⁻¹; feed composition, air:ethane = 25:1.

^bManganese modified lacunary heteropoly compound prepared at pH = 4.2.

Védrine et al. synthesized a series of heteropolyoxometalates (Cs_{2.5}H_{6x-y}M_{1-x}PVM_xMo_{11-x}O₄₀) in which a transition metal M (M = Co²⁺, Fe³⁺, Ga³⁺, Ni²⁺, Sb³⁺, or Zn²⁺) is incorporated in the Keggin anion by substitution of Mo.^{140,141} Figure 7 shows the selectivities of the different systems at iso-conversion (5%). Clearly the introduction of a metal such as iron, cobalt, and even zinc (which does not display redox properties) increased drastically the selectivity toward propylene up to ca. 80%.

The reaction pathways they suggested are shown in Scheme 23, with the blue arrows corresponding to the major route of propane conversion.¹⁴²

Zhang et al. and co-workers synthesized a novel nanocomposite of NiO and polyoxometalate (Cs_{2.5}H_{0.5}PMo₁₂O₄₀), NiO–Cs_{2.5}H_{0.5}PMo₁₂O₄₀, with particle sizes in the 5–10 nm range, which were very different from the simple mixtures of NiO and polyoxometalate.^{143,144} These “nanocomposites” exhibited unique capabilities for the adsorption of oxygen and ammonia and superior catalytic behaviors in the ODH of propane. A stable propylene yield of 19.8% was obtained at 450

Table 22. Catalytic Performances of NiO–Cs_{2.5}H_{0.5}PMo₁₂O₄₀ Nanocomposites for the Oxidative Dehydrogenation of Propane^{144 a}

catalyst	temp (°C)	C ₃ H ₈ conversion (%)	selectivity (%)		yield (%)
			CO _x	C ₃ H ₆	
NiO	450	100	72	0	0.00
Cs _{2.5} H _{0.5} PMo ₁₂ O ₄₀	450	1.5	4.9	95	1.43
85% NiO–Cs _{2.5} H _{0.5} PMo ₁₂ O ₄₀	450	72	80	20	14.40
80% NiO–Cs _{2.5} H _{0.5} PMo ₁₂ O ₄₀	450	44	54.6	45	19.80
75% NiO–Cs _{2.5} H _{0.5} PMo ₁₂ O ₄₀	450	23	33.4	65	14.95
70% NiO–Cs _{2.5} H _{0.5} PMo ₁₂ O ₄₀	450	11	21.9	75	8.25
50% NiO–Cs _{2.5} H _{0.5} PMo ₁₂ O ₄₀	450	3	19.2	81	2.43
80% NiO–Cs _{2.5} H _{0.5} PMo ₁₂ O ₄₀ ^b	450	55	86	14	7.70

^aReaction conditions: catalyst, 0.5 g; total flow rate, 50 mL min⁻¹; P(C₃H₈) = 4.1 kPa, P(O₂) = 16.2 kPa, P(N₂) = 81.1 kPa; other products mainly include CH₄, C₂H₆, and C₂H₄. ^bPrepared by physical mixing.

°C over 80% NiO–Cs_{2.5}H_{0.5}PMo₁₂O₄₀ catalyst (Table 22). This result is regarded as the highest one reported to date at such a mild temperature.

7.2. Selective Oxidation of Propane to Acrolein and Acrylic Acid

7.2.1. General Mechanisms for Selective Oxidation of Propane to Acrolein and Acrylic Acid. The reaction mechanism and intermediates have been well established for the selective oxidation of propylene but not for propane.^{145,146} Few details are known about the involved adsorbed intermediate species in propane selective oxidation. The most acceptable route involves the isopropyl radical, and propylene is proposed to be formed first as intermediate. Propylene production may occur either on catalysts surface^{147–149} or in the gas phase (Scheme 24).^{150–152} It is implicitly believed that π - and σ -allyl species are formed following propyl species, and

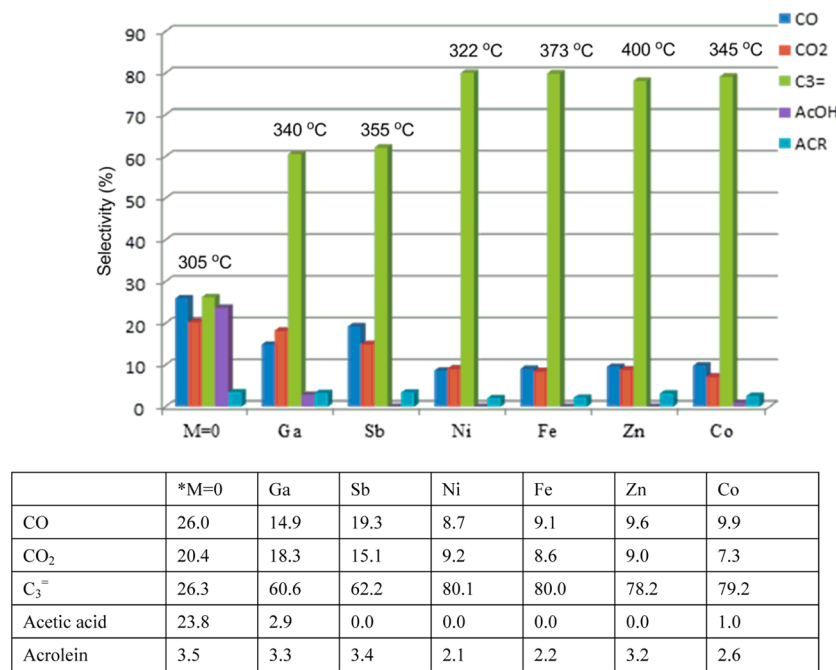
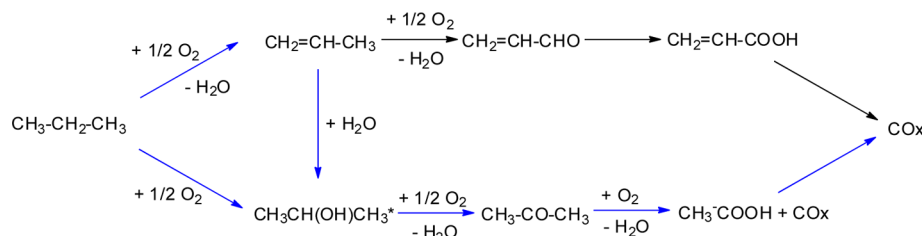


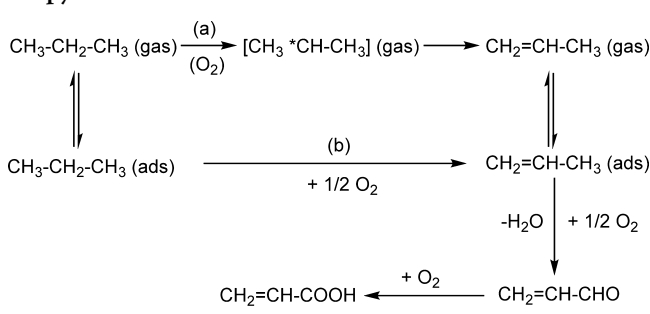
Figure 7. Selectivities of $\text{Cs}_{2.5}\text{H}_y\text{PVM}_x\text{Mo}_{11-x}\text{O}_{40}$ samples at 5% propane conversion as a function of the metal cation M. The reaction temperature necessary to reach 5% conversion is indicated on the top of each bar diagram. Reaction conditions: $\text{C}_3\text{H}_8/\text{O}_2/\text{He} = 40/20/40$.¹⁴⁰ * $\text{Cs}_{2.5}\text{H}_{1.5}\text{PVMo}_{11}\text{O}_{40}$ sample.

Scheme 23. Proposed Pathways for the Propane Oxidation over Keggin-type Compounds ($\text{Cs}_{2.5}\text{H}_{6x-y}\text{M}_{1-x}\text{PVMo}_{11-x}\text{O}_{40}$)^a



^aThe star indicates that the product has not yet been detected.¹⁴²

Scheme 24. Proposed Mechanism of Propane Selective Oxidation to Acrolein and Acrylic Acid through the Propylene Intermediate¹³⁵



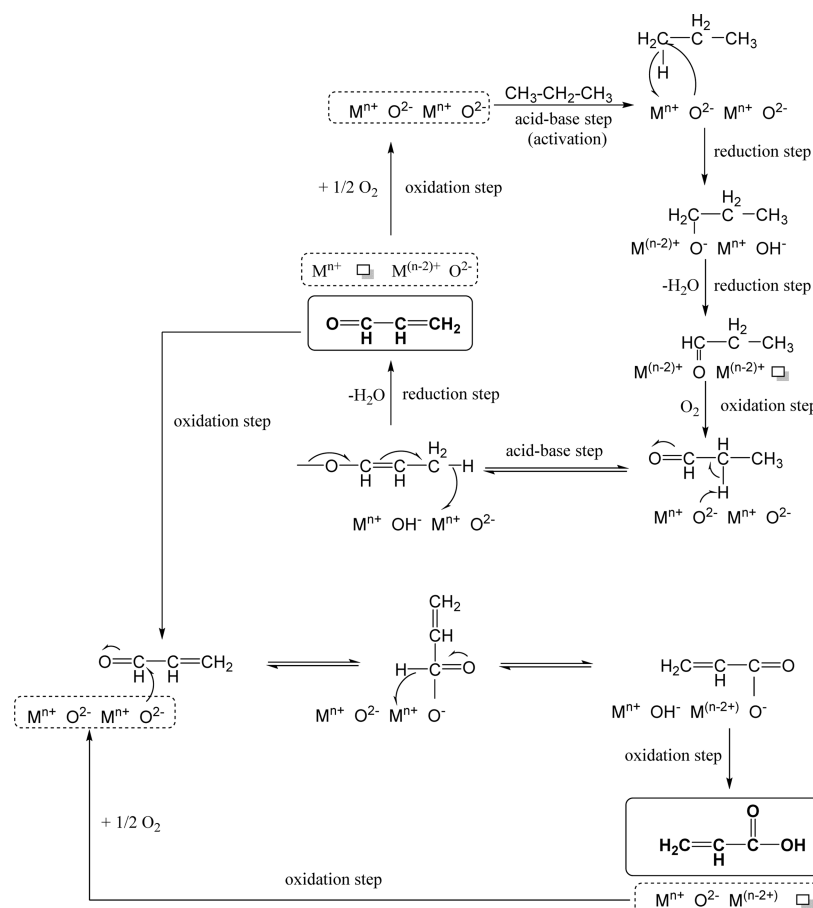
then further abide by the mechanism proposed for propylene selective oxidation to oxygenates.

On the other hand, oxygenate products may also be formed directly from propane without going through propylene intermediate. It has been inferred that a direct insertion of lattice oxygen occurs in propane C–H bond leading to 1-propyloxy or 2-propyloxy species, which are further transformed to organic oxygenates (Scheme 25).

However, with the lack of experimental results, the nature and the number of steps to organic oxygenate products cannot be further approved.

7.2.2. Selective Oxidation of Propane to Acrolein and Acrylic Acid over HPC Catalysts. Rabia et al. investigated the ammonium salts $(\text{NH}_4)_6\text{HPMo}_{11}\text{MO}_{40}$ (M = Ni, Co, Fe) in the oxidation of propane with molecular oxygen at temperatures between 380 and 420 °C (Scheme 26).¹⁵³ The catalysts were found active in propane oxidation and selective to propylene or acrolein, in particular, the samples that were pretreated in situ at the given reaction temperature (380–420 °C) for 1 h under an oxygen stream (40 mL min⁻¹) with a heating rate of 9 °C min⁻¹ during the temperature rising step. Table 23 gives the catalytic performances of the different catalysts tested after different pretreatments (heating rates of 5 and 9 °C min⁻¹). When the reaction was performed at 380 °C, the catalysts were only partially reduced, and this point was proposed as the key for the formation of valuable products (propylene and acrolein). At 400 °C, the catalysts were partially decomposed, which led the propane conversion and selectivities to valuable products to decrease and the selectivity to CO_x to increase. At 420 °C, the salts were totally decomposed to a mixture of metal oxides that became more active in propane oxidation, favoring especially the formation of deep oxidation products.

Scheme 25. Proposed Mechanism of the Direct Propane Oxidation to Acrolein and Acrylic Acid through the 1-Propyloxy Adsorbed Species¹³⁵



Scheme 26. General Conditions Employed for the Oxidation of Propane to Acrolein and Acrylic Acid^a



^aOxidant: O₂; T = 300–430 °C.

Ueda et al.^{154–157} reported that propane could be catalytically oxidized to acrylic acid with molecular oxygen over heteropoly molybdophosphoric acids (as precursors) that were pretreated with pyridine in the catalyst preparation. A selectivity of 24% to acrylic acid at 12% propane conversion could be achieved at 360 °C over this HPMo(Pyr) catalyst (see Table 24). They also examined the catalytic performance of H₃PW₁₂O₄₀ pretreated with pyridine. In contrast to its molybdc analogue, this system was totally inactive. A reaction mechanism was proposed, where protons and electrons in the reduced HPMo(Pyr) catalyst cooperate to activate molecular oxygen (Scheme 27).

The oxygen molecule reacts first with two protons and reduced Mo to form one molecule of water. The remaining oxygen atom remains coordinated on the Mo site and is the active oxygen species for propane activation. This reaction leads to adsorbed propylene-like species, which rapidly evolve by allylic oxidation to acrylic acid, or to adsorbed alcoholic species, followed by oxidative dehydrogenation.

Mizuno et al. tested the effects of addition of various transition metals to Cs_{2.5}H_{0.5}PMo₁₂O₄₀ on its catalytic perform-

ances for selective propane oxidation.^{106,107,110,158} Their results are summarized in Table 25. The substitution of H⁺ by Fe³⁺ or Ni²⁺ enhanced the acrylic acid production, and the maximum yield was observed on Cs_{2.5}Fe_{0.08}H_{0.26}PMo₁₂O₄₀ (2.4%) at 360 °C. Further replacement of one molybdenum atom by vanadium in the above catalyst increased the yield of acrylic acid to 4.5%.¹⁰⁶

Besides the introduction of Ga³⁺ in the Keggin anion,¹⁴⁰ Védrine et al. also exchanged protons with Ga³⁺ and prepared Ga_x–Cs_{2.5}H_{1.5}PVMo₁₁O₄₀ catalysts with different Ga contents.¹⁵⁹ Their work showed that Ga could be used as an effective counterion for promoting the selective oxidation of propane to acrylic acid. There was an optimum value of the Ga content of 0.16 per Keggin unit in the Keggin structure. Furthermore, a preheating temperature of 300 °C maximized the propane conversion (18.1%) and the acrylic acid selectivity (20%) at 340 °C (Table 26).

Later, they synthesized Cs_{2.5}H_{1.5}PVMo_{11-x}W_xO₄₀ compounds and studied their catalytic performance for selective propane oxidation in the 300–400 °C temperature range.¹⁶⁰ Pretreatment temperature played an important role in influencing the distribution of products in propane oxidation; that is, pretreatment temperature at 400 °C favors the formation of propylene, while pretreatment temperature at 300 °C favors the formation of oxygenates (Table 27). The substitution of W⁶⁺ for Mo⁶⁺ in Keggin anion enhances Brønsted acid strength and leads propane oxidation reaction to

Table 23. Catalytic Performances of Different Heteropoly Salts Tested in Propane Oxidation at Different Temperatures with Different Pretreatments¹⁵³

	precatalyst	temp (°C)	C ₃ H ₈ conversion (%)	selectivity (%)				yield (%)	
				CO _x	C ₃ H ₆	C ₂ ^b	ARO	C ₃ H ₆	ARO
(A)	PMo ₁₁ Fe	380	14	30	36	0	34	5.04	4.76
		400	9	48	24	1	27	2.16	2.43
		420	20	54	22	1	23	4.40	4.60
	PMo ₁₁ Co	380	11	18	33	1	48	3.63	5.28
		400	9	31	28	2	39	2.52	3.51
		420	17	62	24	2	12	4.08	2.04
	PMo ₁₁ Ni	380	16	27	31	tr	42	4.96	6.72
		400	10	43	12	1	44	1.20	4.40
		420	21	67	21	1	11	4.41	2.31
(B)	PMo ₁₁ Fe	380	10	32	30	tr	29	3.00	2.90
		400	5	61	18	tr	21	0.90	1.05
		420	16	66	16	tr	18	2.56	2.88
	PMo ₁₁ Co	380	6	34	24	tr	42	1.44	2.52
		400	5	52	20	tr	28	1.00	1.40
		420	10	74	18	1	7	1.80	0.70
	PMo ₁₁ Ni	380	7	40	22	tr	37	1.54	2.59
		400	4	53	8	tr	36	0.32	1.44
		420	13	83	10	tr	4	1.30	0.52

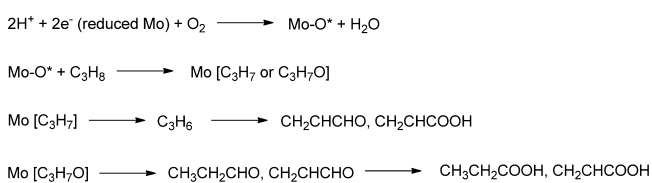
^aReaction conditions: C₃H₈/O₂/N₂ = 20/20/60; flow rate = 40 mL min⁻¹; catalyst weight 0.2 g; pretreatment: O₂ for 1 h. (A) Pretreatment heating rate: 9 °C min⁻¹. (B) Pretreatment heating rate: 5 °C min⁻¹. tr: trace. ARO: acrolein. ^bC₂ = ethane + ethylene.

Table 24. Comparison of the Catalytic Performance of Various HPC in Propane Oxidation^a

precatalyst	C ₃ H ₈ conversion (%)	selectivity (%)				yield (%)		
		CO _x	C ₃ H ₆	AA	AcOH	C ₃ H ₆	AA	AcOH
H ₃ PW ₁₂ O ₄₀ ^b	0					0.98	0.02	0.07
H ₃ PW ₁₂ O ₄₀ Pyr ^c	0					0.66	0.01	0.10
H ₃ PMo ₁₂ O ₄₀ ^b	1.6	33.3	61.1	1.3	4.1	0.00	1.79	0.76
H ₃ PMo ₁₂ O ₄₀ * ^b	0.9	11.8	73.0	1.3	10.6	0.00	2.14	1.15
H ₃ PMo ₁₂ O ₄₀ Pyr ^c	8.5	69.5	tr	21.1	8.9	0.00	0.28	0.12
H ₃ PMo ₁₂ O ₄₀ Pyr* ^{c,d}	7.5	55.0	tr	28.5	15.3	0.00	2.66	1.37
H ₃ PMo ₁₂ O ₄₀ Pyr* ^{c,e} ¹⁵⁸	0.8	38.7	tr	35.0	14.4	0.00	0.00	0.00
H ₃ PMo ₁₂ O ₄₀ Pyr* ^e ¹⁵⁸	8.7	43.7	tr	30.6	15.7	0.71	0.25	1.18
K ₃ PMo ₁₂ O ₄₀ ^b	0					0.82	0.02	0.03
(NH ₄) ₃ PMo ₁₂ O ₄₀ * ^c	4.5	49.2	15.8	5.6	26.2	1.07	0.16	0.22
H ₄ PVMo ₁₁ O ₄₀ ^b	0.9	3.7	90.6	2.2	3.3	0.98	0.02	0.07
H ₄ PVMo ₁₁ O ₄₀ Pyr ^f	2.1	30.3	50.8	7.4	10.7	0.66	0.01	0.10

^aReaction conditions: catalyst, 3 g; total flow rate, 50 mL min⁻¹; feed composition, C₃H₈/O₂/N₂ = 20/10/70 (mol %) [^{*}C₃H₈/O₂/H₂O/N₂ = 20/10/20/50 (mol %)]; time on stream, 7 h; reaction temperature, 340 °C. tr: trace. AA: acrylic acid. ARO: acrolein. AcOH: acetic acid. ^bPretreatment conditions: 380 °C, 2 h under 20% O₂/N₂ flow. ^cPretreatment conditions: 420 °C, 2 h under N₂ flow, followed by 380 °C, 2 h under 20% O₂/N₂ flow. ^dPrecatalyst, 0.5 g. ^ePretreatment conditions: 430 °C, 2 h under N₂ flow. ^fPretreatment conditions: 430 °C, 2 h under N₂ flow, followed by 380 °C, 2 h under 20% O₂/N₂ flow.

Scheme 27. Proposed Reaction Path for Propane Oxidation over Reduced HPMo(Pyr) Catalyst¹⁵⁵



forming more acetic acid (via isopropanol route) and CO_x at the expense of forming acrylic acid via propylene.

Li et al. systematically studied the catalytic behavior of Cs salts of heteropoly acids with vanadium species substituted at the primary and/or secondary structure of Keggin anions for the selective oxidation of propane.¹⁶¹ The highest acrylic acid

yield (8.2%) was observed over the H_{0.1}Cs_{2.5}(VO)_{0.2}PMo₁₂O₄₀ catalyst at 420 °C (see Table 28).

Similar acrylic acid yield was achieved on Cs₃PMo₁₂O₄₀-supported two vanadium-substituted 12-molybdochosphate catalyst reported by Volpe, Lyons et al. in their patents.^{162–166} The catalytic performance comparison results of different kinds of Cs₃PMo₁₂O₄₀-supported heteropoly acid catalysts in their patents are listed in Table 29.

Zhong et al. prepared partially reduced multicomponent heteropoly compound catalysts with the Keggin structure and studied their catalytic performance in the selective oxidation of propane.¹⁶⁷ Results showed that the partially reduced heteropoly acid catalyst (H_xCu_{0.6}Cr_{0.6}As_{0.6}PMo₁₀V₂O₄₀) exhibited the highest activity for the selective oxidation of propane. At 390 °C, the maximum conversion of propane and

Table 25. Selective Oxidation of Propane over $M_{0.08}^{N+}Cs_{2.5}H_{0.5-0.08N}PMo_{12}O_{40}^{106}$ ^a

catalyst	temp (°C)	C_3H_8 conversion (%)	selectivity (%)				yield (%)
			AA	ARO	AcOH	CO_x	
$Cs_{2.5}Rh_{0.08}H_{0.26}PMo_{12}O_{40}^b$	360	17	8	1	7	78	1.36
$Cs_{2.5}Fe_{0.08}H_{0.26}PMo_{12}O_{40}^b$	360	13	18	2	11	60	2.34
$Cs_{2.5}Fe_{0.08}H_{1.26}PVMo_{11}O_{40}^b$	360	17	27	2	9	51	4.59
$Cs_{2.5}Fe_{0.08}H_{1.26}PVMo_{11}O_{40}^c$	300	8	33	0	12	52	2.64
$Cs_{2.5}Fe_{0.08}H_{1.26}PVMo_{11}O_{40}^c$	320	12	30	0	12	53	3.60
$Cs_{2.5}Fe_{0.08}H_{1.26}PVMo_{11}O_{40}^c$	340	17	28	0	11	57	4.76
$Cs_{2.5}Fe_{0.08}H_{1.26}PVMo_{11}O_{40}^c$	360	29	24	0	12	59	6.96
$Cs_{2.5}Fe_{0.08}H_{1.26}PVMo_{11}O_{40}^c$	380	47	28	0	10	60	13.16
$Cs_{2.5}Fe_{0.08}H_{1.26}PVMo_{11}O_{40}^c$	400	48	25	0	7	66	12.00
$Cs_{2.5}Fe_{0.08}H_{2.26}PV_2Mo_{10}O_{40}^b$	360	10	16	1	10	50	1.60
$Cs_{2.5}Fe_{0.08}H_{3.26}PV_3Mo_9O_{40}^b$	360	11	8	1	5	30	0.88
$Cs_{2.5}Ni_{0.08}H_{0.34}PMo_{12}O_{40}^b$	360	12	17	2	10	64	2.04
$Cs_{2.5}H_{0.8}PMo_{12}O_{40}^b$	360	12	8	1	8	77	0.96
$Cs_{2.5}Co_{0.08}H_{0.34}PMo_{12}O_{40}^b$	360	8	16	3	11	59	1.28
$Cs_{2.5}Cu_{0.08}H_{0.34}PMo_{12}O_{40}^b$	360	8	9	3	4	74	0.72
$Cs_{2.5}Mn_{0.08}H_{0.34}PMo_{12}O_{40}^b$	360	6	19	3	10	53	1.14

^aCatalyst, 1.0 g. Selectivity was calculated on the C_3 (propane)-basis. AA: acrylic acid. ARO: acrolein. AcOH: acetic acid. ^bTotal flow rate, 30 mL min⁻¹; $C_3H_8/O_2/N_2 = 30/40/30$. ^cTotal flow rate, 15 mL min⁻¹; $C_3H_8/O_2/N_2 = 30/50/20$.

Table 26. Catalytic Performances of $Ga_x-Cs_{2.5}H_{1.5}PMo_{11}O_{40}$ Catalysts in Propane Oxidation at Different Temperatures¹⁵⁹^a

precatalyst	temp (°C)	C_3H_8 conversion (%)	selectivity (%)					yield (%)			
			CO_x	C_3H_6	AA	AcOH	ARO	C_3H_6	AA	AcOH	ARO
$Ga_0-Cs_{2.5}H_{1.5}PVMo_{11}O_{40}$	300	3.4	22.1	52.8	0	22.4	2.7	1.8	0.0	0.8	0.1
	320	6.0	28.3	43.1	3.2	23.7	1.7	2.6	0.2	1.4	0.1
	340	9.9	26.5	38.5	2.4	28.2	3.5	3.8	0.2	2.8	0.3
$Ga_{0.08}-Cs_{2.5}H_{1.5}PVMo_{11}O_{40}$	300	2.1	29.2	25.5	15.8	26.7	2.8	0.5	0.3	0.6	0.1
	320	7.9	40.9	14.7	13.9	27.7	2.8	1.2	1.1	2.2	0.2
	340	12.8	47.0	17.3	11.1	21.7	2.9	2.2	1.4	2.8	0.4
$Ga_{0.16}-Cs_{2.5}H_{1.5}PVMo_{11}O_{40}$	300	8.7	33.6	21.7	13.6	28.7	2.4	1.9	1.2	2.5	0.2
	320	12.7	37.8	16.4	18.0	25.3	2.5	2.1	2.3	3.2	0.3
	340	18.1	38.9	16.3	20.0	22.4	2.4	3.0	3.6	4.1	0.4
$Ga_{0.32}-Cs_{2.5}H_{1.5}PVMo_{11}O_{40}$	300	7.1	46.1	29.5	0	24.4	0	2.1	0.0	1.7	0.0
	320	11.2	47.1	20.5	4.9	25.5	2.0	2.3	0.5	2.9	0.2
	340	16.6	52.2	15.9	6.3	23.5	2.1	2.6	1.0	3.9	0.3

^aReaction condition: preheating temperature, 300 °C; total flow rate, 15 mL min⁻¹; $C_3H_8/O_2/He = 40:20:40$; time on stream, 4 h. AA: acrylic acid. ARO: acrolein. AcOH: acetic acid.

Table 27. Catalytic Performances of $Cs_{2.5}H_{1.5}PVMo_{11-x}W_xO_{40}$ Catalysts Pretreated at Different Temperatures in Propane Oxidation¹⁶⁰^a

catalyst	temp (°C)	C_3H_8 conversion (%)	selectivity (%)					yield (%)			
			CO_x	C_3H_6	AA	AcOH	ARO	C_3H_6	AA	AcOH	ARO
(A)	$Cs_{2.5}H_{1.5}PVMo_{11}O_{40}$	305	5	46	26	0	24	4	1.30	0.00	1.20
	$Cs_{2.5}H_{1.5}PVMo_{10}W_1O_{40}$	345	5	32	57	0	7	4	2.85	0.00	0.35
	$Cs_{2.5}H_{1.5}PVMo_9W_2O_{40}$	349	5	38	24	13	17	8	1.20	0.65	0.85
	$Cs_{2.5}H_{1.5}PVMo_7W_4O_{40}$	342	5	44	21	18	15	2	1.05	0.90	0.75
	$Cs_{2.5}H_{1.5}PVMo_5W_6O_{40}$	323	5	62	25	0	12	1	1.25	0.00	0.60
(B)	$Cs_{2.5}H_{1.5}PVMo_{11}O_{40}$	292	5	3	97	0	0	0	4.85	0.00	0.00
	$Cs_{2.5}H_{1.5}PVMo_{10}W_1O_{40}$	343	5	31	66	0	2	1	3.30	0.00	0.10
	$Cs_{2.5}H_{1.5}PVMo_9W_2O_{40}$	347	5	43	35	4	13	5	1.75	0.20	0.65
	$Cs_{2.5}H_{1.5}PVMo_7W_4O_{40}$	333	5	60	24	0	13	3	1.20	0.00	0.65
	$Cs_{2.5}H_{1.5}PVMo_5W_6O_{40}$	328	5	28	55	0	14	3	2.75	0.00	0.70

^aReaction conditions: catalyst, 0.6 g; total flow rate, 7.5–30 mL min⁻¹; $C_3H_8/O_2/He = 40:20:40$; time on stream, 2 h. Catalyst pretreatment: under dry O_2 flow (30 mL min⁻¹) at (A) 300 °C or (B) 400 °C for 1 h. AA: acrylic acid. ARO: acrolein. AcOH: acetic acid.

the maximum yield of acrylic acid reached 38% and 14.8%, respectively (see Table 30).

Partial reduced niobium- and pyridine-exchanged salts of phosphomolybdic ($NbPMo_{12}Pyr$) and phosphovanadomolybdic acids ($NbPMo_{11}VPyr$) were also used as catalysts for the

Table 28. Selective Oxidation of Propane over Heteropoly Acids with Different Vanadium Locations^{161 a}

precatalyst	temp (°C)	gas composition C ₃ H ₈ /O ₂ /He/H ₂ O	C ₃ H ₈ conversion (%)	selectivity (%)				yield (%)	
				C ₃ H ₆	AA	AcOH	ARO	AA	ARO
H ₃ PMo ₁₂ O ₄₀	400	13/30/53/0	2.0	6.3	0.6	0.6	0.4	0.01	0.33
Cs ₁ H ₂ PMo ₁₂ O ₄₀	400	13/30/53/0	7.2	32.4	7.2	6.6	4.6	0.52	0.25
Cs ₂ H ₁ PMo ₁₂ O ₄₀	400	13/30/53/0	10.1	15.5	9.6	7.4	2.5	0.97	0.42
Cs _{2.5} H _{0.5} PMo ₁₂ O ₄₀	400	13/30/53/0	32.5	28.5	7.3	8.5	1.3	2.37	0.00
Cs ₃ PMo ₁₂ O ₄₀	400	13/30/53/0	0	0	0	0	0	0.00	0.01
H ₃ PMo ₁₂ O ₄₀	400	17/30/53/0	2.0	6.3	0.6	0.6	0.4	0.01	0.11
H(VO)PMo ₁₂ O ₄₀	400	17/30/53/0	52.7	1.9	4.9	7.9	0.2	2.58	0.29
H ₄ PMo ₁₁ VO ₄₀	400	17/30/53/0	13.3	58.9	2.9	3.7	2.2	0.39	0.44
Cs _{2.5} H _{0.5} PMo ₁₂ O ₄₀	420	10/20/70/0	24.2	11.6	7.8	4.2	1.8	1.89	0.36
H _{0.3} Cs _{2.5} (VO) _{0.1} PMo ₁₂ O ₄₀	420	10/20/70/0	36.1	3.5	19.5	4.5	1.0	7.04	0.37
H _{0.2} Cs _{2.5} (VO) _{0.15} PMo ₁₂ O ₄₀	420	10/20/70/0	36.6	3.6	21.9	4.7	1.0	8.02	0.31
H _{0.1} Cs _{2.5} (VO) _{0.2} PMo ₁₂ O ₄₀	400	10/20/70/0	38.6	3.0	18.6	6.7	0.8	7.18	0.37
H _{0.1} Cs _{2.5} (VO) _{0.2} PMo ₁₂ O ₄₀	420	10/20/70/0	40.6	3.6	20.3	4.5	0.9	8.24	0.43
H _{0.1} Cs _{2.5} (VO) _{0.2} PMo ₁₂ O ₄₀	400	20/10/70/0	24.1	16.2	21.8	11.3	1.8	5.25	0.51
H _{0.1} Cs _{2.5} (VO) _{0.2} PMo ₁₂ O ₄₀	420	20/10/70/0	26.7	12.2	26.0	9.8	1.9	6.94	0.36
Cs _{2.5} (VO) _{0.25} PMo ₁₂ O ₄₀	420	10/20/70/0	39.5	3.4	17.4	4.4	0.9	6.87	0.23
H _{1.5} Cs _{2.5} PMo ₁₁ VO ₄₀	420	10/20/70/0	46.2	2.8	2.0	1.8	0.5	0.92	0.26
H _{1.1} Cs _{2.5} (VO) _{0.2} PMo ₁₁ VO ₄₀	420	10/20/70/0	43.6	4.2	5.3	3.1	0.6	2.31	0.38
H _{0.1} Cs _{2.5} (VO) _{0.2} PMo ₁₂ O ₄₀	420	7/14/49/30	26.9	5.7	24.3	12.6	1.4	6.54	0.50
H _{0.1} Cs _{2.5} (VO) _{0.2} PMo ₁₂ O ₄₀	430	7/14/49/30	29.7	7.8	20.1	10.8	1.7	5.97	0.85
H _{0.1} Cs _{2.5} (VO) _{0.2} PMo ₁₂ O ₄₀	420	14/7/49/30	20.3	12.3	31.5	12.8	4.2	6.39	0.63
H _{0.1} Cs _{2.5} (VO) _{0.2} PMo ₁₂ O ₄₀	430	14/7/49/30	22.5	12.5	31.4	12.9	2.8	7.07	0.33

^aReaction conditions: catalyst, 1.0 g; total flow rate, 15 mL min⁻¹. AA: acrylic acid. ARO: acrolein. AcOH: acetic acid.

Table 29. Selective Oxidation of Propane over Cs₃PMo₁₂O₄₀-Supported Heteropoly Acid Catalysts

catalyst	temp (°C)	gas composition C ₃ H ₈ /O ₂ /H ₂ O/N ₂	HPA cover on Cs ₃ PMo ₁₂ O ₄₀ surface (%)	C ₃ H ₈ conversion (%)	AA		
					selectivity (%)	yield (%)	AA
H ₃ PMo ₁₂ O ₄₀ /Cs ₃ PMo ₁₂ O ₄₀	372	1:5:1.5:6	10	16	3.8	0.61	
(VO) _{1.5} PMo ₁₂ O ₄₀ /Cs ₃ PMo ₁₂ O ₄₀	365	1:11:2.7:0	10	20	3.0	0.60	
H ₅ PMo ₁₀ VO ₄₀ /Cs ₃ PMo ₁₂ O ₄₀	371	1:11:4.5:0	10	18	7.2	1.30	
H ₃ PMo ₁₂ O ₄₀ /Cs ₃ PMo ₁₂ O ₄₀	391	1:11:4.5:0	10	23	0.4	0.09	
H ₃ PMo ₁₂ O ₄₀ /Cs ₃ PMo ₁₂ O ₄₀	370	1:11:5:0	5	23	5.2	1.20	
H ₃ PMo ₁₂ O ₄₀ /Cs ₃ PMo ₁₂ O ₄₀	378	1:11:5:0	50	15	8	1.20	
H ₃ PMo ₁₂ O ₄₀ /Cs ₃ PMo ₁₂ O ₄₀	387	1:11:5.2:0	100	18	11	1.98	
(VO) _{1.5} PMo ₁₂ O ₄₀ /Cs ₃ PMo ₁₂ O ₄₀	396	1:11:5.5:0	100	29	26	7.54	
H ₅ PMo ₁₀ VO ₄₀ /Cs ₃ PMo ₁₂ O ₄₀	394	1:11:5.4:0	100	66	13	8.58	
H ₂ (VO) _{0.5} PMo ₁₂ /Cs ₃ PMo ₁₂ O ₄₀	440	1.76:15.8:0:9.6	n.d.	45	23	10.35	
H ₂ (VO) _{0.5} PMo ₁₂ /Cs ₃ PMo ₁₂ O ₄₀ ^a	420	1.76:15.8:0:9.6	n.d.	50	22	11.00	
H _x Cu _{0.1} As _{0.1} PMo ₁₁ VO ₄₀ /Cs ₃ PMo ₁₂ O ₄₀	420	n.d.	n.d.	26.7	18.7	4.99	
H _x Cu _{0.1} As _{0.1} PMo ₁₁ VO ₄₀ /Cs ₃ PMo ₁₂ O ₄₀	420	n.d.	n.d.	27.9	15.1	4.21	
H _x Cu _{0.1} As _{0.1} PMo ₁₁ VO ₄₀ /Cs ₃ PMo ₁₂ O ₄₀	420	n.d.	n.d.	30.3	24.3	7.36	
H _x Cu _{0.1} Sb _{0.1} (VO)PMo ₁₂ O ₄₀ /Cs ₃ PMo ₁₂ O ₄₀	420	n.d.	n.d.	27.1	20.4	5.53	
H _x Cu _{0.1} Sb _{0.1} (VO)PMo ₁₂ O ₄₀ /Cs ₃ PMo ₁₂ O ₄₀	420	n.d.	n.d.	31.9	26.9	8.58	
H ₂ (VO) ₂ [P ₂ Mo ₁₈ O ₆₂] ^c /Cs ₃ PMo ₁₂ O ₄₀	350	b	n.d.	33	28.4	9.37	

^aCatalyst was pretreated with bipyridine in amount of 0.25. ^bC₃H₈, 55 mL min⁻¹; air, 28 mL min⁻¹; time on stream, 24 h. ^cThe molecular formula as determined prior to drying at elevated temperatures, impregnation on the support, and calcination. AA: acrylic acid.

selective oxidation of propane by Davis and co-workers.^{117–119} Under their reaction conditions (C₃H₈/O₂/He/H₂O = 4:2:4:5; total flow rate, 120 mL/min; 380 °C), a 10.5% yield of acrylic acid could be achieved when the propane conversion was 21% over NbPMo₁₁VPyr catalyst, and this activity could be kept after 72 h reaction. Catalytic performance comparison results of

niobium- and pyridine-exchanged HPC (as precursors) catalysts are listed in Table 31.

7.3. Conclusion

When considering the transformation of propane catalyzed by HPC catalysts, the best yield of propylene (19.8%) was

Table 30. Selective Oxidation of Propane over Three Different Catalysts over Multicomponent Heteropoly Compound Catalysts^{167 a}

precatalyst	C ₃ H ₈ conversion (%)	selectivity (%)				yield (%)
		CH ₂ CHCHO	CH ₃ COOH	CH ₂ CHCOOH	CH ₂ CHCOOH	
H _x Cu _{0.6} Cr _{0.6} PMo ₁₀ V ₂ As _{0.6} O ₄₀	9	3.3	12.2	2		0.18
H _x Cu _{1.2} PMo ₁₀ V ₂ As _{0.6} O ₄₀ ^b	30	3.0	8.3	31		9.30
H _x Cu _{0.6} Cr _{0.6} PMo ₁₀ V ₂ As _{0.6} O ₄₀ ^b	38	2.0	18.7	39		14.82

^aReaction conditions: C₃H₈:O₂:N₂:H₂O = 1:2:5:2; space velocity = 1500 h⁻¹; reaction temperature, 390 °C. ^bPartially reduced.

Table 31. Selective Oxidation of Propane over Niobium- and Pyridine-Exchanged HPC Catalysts^a

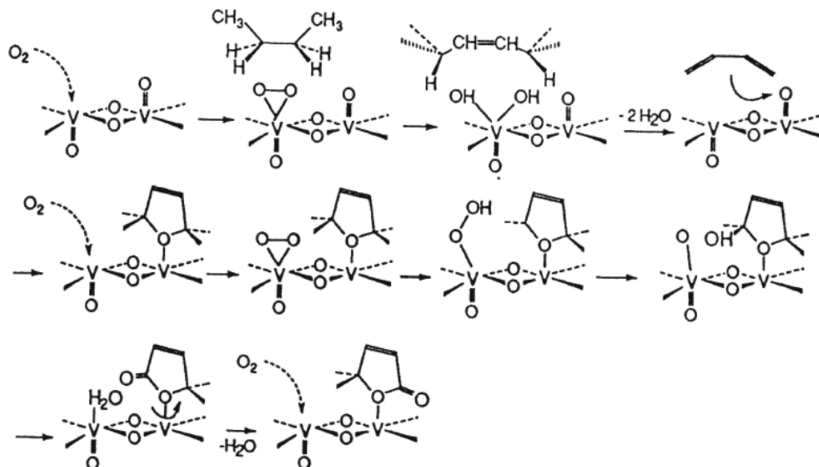
precatalyst	flow (mL min ⁻¹) C ₃ H ₈ :O ₂ :He:H ₂ O	C ₃ H ₈ conversion (%)	selectivity (%)						AA yield (%)	ref
			CO _x	C ₃ H ₆	AcOH	AA	MA	C ₂ H ₄		
PMo ₁₁ V ^{b,d}	8:4:8:10	0.4	30	54	4	0	0	12	0.00	118
NbPMo ₁₁ V ^{b,d}	8:4:8:10	1.4	22	44	16	10	0	6	0.14	118
PMo ₁₁ VPyr ^{b,d}	8:4:8:10	3.4	10	37	30	17	0	4	0.58	118
NbPMo ₁₂ Pyr ^{b,d}	8:4:8:10	25	79	1	2	2	14	0	0.50	118
NbPMo ₁₂ Pyr ^{b,d}	32:16:32:40	18	65	1	3	6	21	0	1.08	118
NbPMo ₁₁ VPyr ^{b,d}	32:16:32:40	21	11	0	23	49	15	0	10.29	118
NbPMo ₁₁ VPyr ^{b,d}	8:4:8:10	25	15		19	21	43	n.d.	5.25	118
PMo ₁₁ NbPyr ^{b,d}	8:4:8:10	25	65	0	3	3	29	0	0.75	118
PMo ₁₁ NbPyr ^{b,d}	32:16:32:40	8	45	0	8	17	23	0	1.36	118
(VO)PMo ₁₁ NbPyr ^{b,d}	32:16:32:40	18	25	0	10	28	22	0	5.04	118
NbPMo ₁₁ VPyr ^{b,e}	32:16:32:40	11	24	n.d.	28	17	28	n.d.	1.87	118
NbPMo ₁₁ VPyr ^{b,e}	16:8:16:20	15	18	n.d.	32	16	22	n.d.	2.40	118
PMo ₁₂ Pyr ^{c,e}	10:5:25:10	7.5	55	tr	15.3	28.5	n.d.	n.d.	2.14	154
Cs _{2.5} Fe _{0.08} H _{1.26} PVMo ₁₁ O ₄₀ ^d	4.5:7.5:3:0	47	60	2	10	28	n.d.	n.d.	13.16	106
NbPMo ₁₁ VPyr ^{b,d}	3:8.6:18:21	10	n.d.	n.d.	n.d.	29	n.d.	n.d.	2.90	118
MoSbVNbO _x ^f	2:3.2:11.8:28	31	n.d.	n.d.	n.d.	30	n.d.	n.d.	9.30	168
MoVNbTeO _x ^d	0.6:2.7:4.8:8	80	n.d.	n.d.	n.d.	61	n.d.	n.d.	48.80	169

^aReaction conditions: catalyst, 0.2 g; time on stream, 2 h. AA: acrylic acid. MA: maleic acid. AcOH: acetic acid. ^bTo remove all organic components from the catalyst precursors, catalysts were pretreated by heating to 420 °C for 5 h and kept at this temperature for 6 h before cooling to 380 °C in flowing He before reaction. ^cReaction conditions: catalyst, 3 g; time on stream, 7 h. Precatalyst pretreatment condition: 420 °C for 2 h in N₂, followed by 380 °C for 2 h in 20% O₂/N₂ flow. ^dReaction temperature, 380 °C. ^eReaction temperature, 340 °C. ^fReaction temperature, 400 °C.

Table 32. Selective Oxidation of n-Butane to Maleic Acid

precatalyst	temp (°C)	flow (mL min ⁻¹) C ₄ H ₁₀ :O ₂ :He:H ₂ O	C ₄ H ₁₀ conversion (%)	selectivity (%)					ref
				CO _x	AcOH	AA	MA	MA yield (%)	
MoO ₃	380	4:2:4:5	0.7	95	2.4	n.d.	n.d.	0.00	119
PMo ₁₂	380	4:2:4:5	0.2	64	34	2	n.d.	0.00	119
NbPMo ₁₂	380	4:2:4:5	3	13	7	2	70	2.10	119
PMo ₁₂ Pyr	380	4:2:4:5	13.5	14	3	1	82	11.07	119
PMo ₁₂ Pyr	340	4:2:4:5	7	10	4	1	83	5.81	119
NbPMo ₁₂ Pyr	380	4:2:4:5	15 ^a	25	3	1	71	10.65	119
NbPMo ₁₂ Pyr	380	32:16:32:40	15 ^a	5	3	1	90	13.50	119
NbPMo ₁₂ Pyr	340	32:16:32:40	14	6	4	1	89	12.46	119
PMo ₁₁ V	380	4:2:4:5	0.5	31	17	n.d.	50	0.25	119
NbPMo ₁₁ V	380	4:2:4:5	0.4	42	19	4	25	0.10	119
PMo ₁₁ VPyr	380	4:2:4:5	13.5	5	3	1	90	12.15	119
PMo ₁₁ VPyr	340	4:2:4:5	2	16	4	1	78	1.56	119
NbPMo ₁₁ VPyr	380	4:2:4:5	15 a	16	5	2	76	11.40	119
NbPMo ₁₁ VPyr	300	4:2:4:5	9	26	12	2	60	5.40	119
NbPMo ₁₁ VPyr	380	32:16:32:40	14	9	5	3	80	11.20	119
NbPMo ₁₁ VPyr	340	32:16:32:40	13	26	10	4	59	7.67	119
NbPMo ₁₁ VPyr	340	1:10:35:5	62	50	3.8	0.8	46	28.52	119
VPO	380	4:6:26:0	30	8	n.d.	n.d.	80	24.00	185
H ₅ PMo ₁₀ V ₂ O ₄₀	340	0.6:5.4:24:0	90	n.d.	n.d.	n.d.	38	34.20	186
BiPMo ₁₂ O ₄₀ +2VO ²⁺	360	6.3:58:218:34	31.8	37	17	14	32	10.18	187

^aTheoretical maximum conversion. AA: acrylic acid. MA: maleic acid. AcOH: acetic acid.

Scheme 28. Possible Mechanism of *n*-Butane Selective Transformation on VPO Catalyst^a

^aReprinted with permission from ref 41. Copyright 1993 Kluwer Academic Publishers.

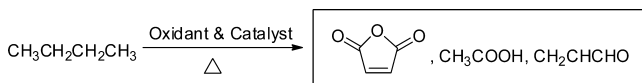
obtained on 80% NiO–Cs_{2.5}H_{0.5}PMo₁₂O₄₀ catalyst with a 45% selectivity. The highest selectivity was 95% (1.5% propane conversion) obtained on Cs_{2.5}H_{0.5}PMo₁₂O₄₀.

8. SELECTIVE OXIDATION OF BUTANE

8.1. Selective Oxidation of *n*-Butane to Maleic Acid or Maleic Anhydride

8.1.1. General Mechanisms for Selective Oxidation of *n*-Butane to Maleic Anhydride or Maleic Acid. The

Scheme 29. General Conditions Employed for the Oxidation of *n*-Butane to Maleic Acid or Maleic Anhydride^a



^aOxidant: O₂; T = 300–380 °C.

Scheme 30. General Conditions Employed for the Oxidative Dehydrogenation of Iso-butane to Iso-butene^a



^aOxidant: O₂; T = 382–427 °C.

selective oxidation of *n*-butane to maleic anhydride is one of the most complex selective oxidation reactions used in industry today.^{170–180} Among different approaches toward selectively oxidizing *n*-butane, the 1,4-electron activation to maleic acid on vanadium–phosphorus–oxide (VPO) catalysts is one of the most fascinating processes, which is the only industrial process of a selective vapor-phase oxidation of an alkane that uses dioxygen.^{15,181,40}

VPO catalysts have been mostly used as model catalysts in understanding the mechanisms of *n*-butane selective oxidation to maleic anhydride (or acid). The most agreed mechanism involves the intermediate formation of adsorbed butenes and butadiene (Scheme 28). According to refs 41,182,183, after a series of hydrogen abstraction reactions, *n*-butane is converted to the adsorbed butadiene intermediate, which can further react with a vanadyl (V=O) surface group to give a [2 + 4] cycloaddition forming a surface-bound 2,5-dihydrofuran,

followed by an interaction between the surface-bound 2,5-dihydrofuran and an adsorbed peroxy species. This peroxy species activates a carbon–hydrogen bond in the 2-position of 2,5-dihydrofuran leading to a transfer of a hydrogen to the dioxygen fragment. A surface-bound hydroperoxide species then transfers an hydroxyl group back to the radical-like 2,5-dihydrofuran derivative forming the 2-hydroxy derivative. The remaining adsorbed oxygen atom abstracts the two remaining hydrogens and is eliminated as water, with contemporaneous formation of the asymmetric lactone, which is then further converted to maleic anhydride with a similar mechanism.⁴¹

8.1.2. Selective Oxidation of *n*-Butane to Maleic Acid or Maleic Anhydride over HPC Catalysts. In 1993, Casarini et al. reported the catalytic behavior of molybdoavanadophosphoric acids with vanadium localized inside the primary (oxoanion) and/or the secondary structure in the oxidation of *n*-butane.¹⁸⁴ In this reaction, the main oxygenate product was maleic anhydride. They found that the substituent positions of vanadium ions apparently affected the maximum selectivity and yield to maleic anhydride from *n*-butane. Vanadium ions in the secondary structure (VO²⁺/H₃PMo₁₂O₄₀) were more selective at low conversion, while vanadium ions inside the oxoanion (H_{3+x}PV_xMo_{12-x}O₄₀) were more selective at higher conversions and thus led to higher yields to maleic anhydride. Besides oxidation of ethane and propane, the partially reduced niobium- and pyridine-exchanged salts of phosphomolybdic (NbPMo₁₂Pyr) and phosphovanadomolybdic acids (NbPMo₁₁V⁵⁺Pyr) showed excellent catalytic performances for the oxidation of *n*-butane to maleic acid (Scheme 29).^{117,119} The reaction was carried out under hydrocarbon-rich conditions (C₄/O₂ = 2/1) to restrain the formation of CO_x. Table 32 summarizes the obtained data. The NbPMo₁₂Pyr and NbPMo₁₁V⁵⁺Pyr catalysts exhibit substantially higher productivities and at least comparable selectivities, as well as the ability to operate at lower temperatures (300 °C, entry 14).

8.2. Oxidative Dehydrogenation of Iso-butane to Iso-butene

The most acceptable reaction mechanism for iso-butane ODH to iso-butene is similar to that for ethane and propane through the H-abstraction pathway (Scheme 5), which is abiding by the most common Mars–van Krevelen mechanism for selective oxidation reaction,^{188,189} so here we will not discuss this in

Table 33. Selective Oxidation of Iso-butane to Iso-butene^a

catalyst	temp (°C)	residence (s)	time	flow (mol %) C ₄ H ₁₀ :O ₂ :He:H ₂ O	iso-C ₄ H ₁₀ conversion (%)	selectivity (%)				ref	
						CO _x	iso-C ₄ H ₈	C ₃ H ₆	others ^b		
K ₆ P ₂ W ₁₈ O ₆₂	383	3.6		26:13:49:12	3.3	22	64	3	11	2.1	190
K ₆ P ₂ W ₁₈ O ₆₂	427	3.6		26:13:49:12	15.4	29	55	7	9	8.5	190
K ₁₀ P ₂ W ₁₇ O ₆₁	387	3.6		26:13:49:12	2.8	16	77	3	4	2.2	190
K ₁₀ P ₂ W ₁₇ O ₆₁	431	3.6		26:13:49:12	16.3	22	62	8	7	10.1	190
K ₇ P ₂ W ₁₇ FeO ₆₁	383	3.6		26:13:49:12	4.1	14	76	3	7	3.1	190
K ₇ P ₂ W ₁₇ FeO ₆₁	427	3.6		26:13:49:12	17.4	20	61	7	12	10.6	190
K ₇ P ₂ W ₁₇ MnO ₆₁	383	3.6		26:13:49:12	2.1	18	79	3	n.d.	1.7	190
K ₇ P ₂ W ₁₇ MnO ₆₁	426	3.6		26:13:49:12	10.9	25	65	6	4	7.1	190
K ₈ P ₂ W ₁₇ CoO ₆₁	382	3.6		26:13:49:12	1.9	22	77	1	n.d.	1.5	190
K ₈ P ₂ W ₁₇ CoO ₆₁	424	3.6		26:13:49:12	14.3	23	66	7	4	9.4	190
K ₈ P ₂ W ₁₇ CuO ₆₁	382	3.6		26:13:49:12	2.9	19	78	3	n.d.	2.3	190
K ₈ P ₂ W ₁₇ CuO ₆₁	426	3.6		26:13:49:12	17.2	26	61	8	5	10.5	190
NiP ₂ O ₇	550	11		75:5:20:0	10.8	n.d.	83	n.d.	n.d.	9.0	192
Zn ₂ P ₂ O ₇	550	11		75:5:20:0	8.1	n.d.	70	n.d.	n.d.	5.7	192
Mn ₂ P ₂ O ₇	550	11		75:5:20:0	6.4	n.d.	60	n.d.	n.d.	3.8	192
Mg ₃ V ₂ O ₈ /MgO	500	0.045 ^c		4:8:88:0	8	n.d.	64	n.d.	n.d.	5.1	193
ferrisilicate	450	0.06 ^c		4.3:4.3:91:3:0	1.6	n.d.	40	n.d.	n.d.	0.6	194
Y ₂ O ₃ /CeF ₃	480	0.6		50:50:0:0	12.0	n.d.	75	n.d.	n.d.	9.0	195

^aReaction conditions: residence time, 3.6 s; feed composition, iso-C₄H₁₀:O₂:H₂O:He = 26:13:12:49; time on stream, 10 h. ^bOthers: methacrylic acid, methacrolein, acetic acid. ^cW/F (weight catalyst/total flow rate), in g s mL⁻¹.

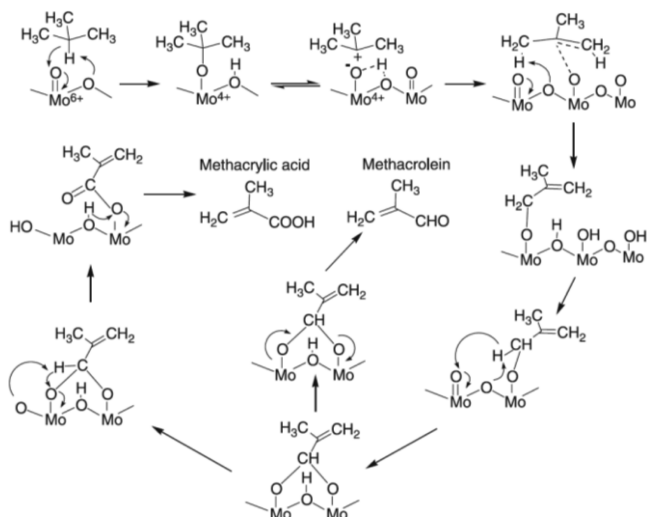
Table 34. Catalytic Performances of NiO–Cs_{2.5}H_{0.5}PMo₁₂O₄₀ Nanocomposites for the Selective Oxidation of Iso-butane^a

catalyst	temp (°C)	iso-C ₄ H ₁₀ conversion (%)	selectivity (%)			ref
			iso-C ₄ H ₈	MA	CO ₂	
NiO	400	43	11	0	67	4.7
	450	50	0	0	69	0.0
80% NiO–Cs _{2.5} H _{0.5} PMo ₁₂ O ₄₀	400	16	63	0	38	10.1
	450	48	20	0	80	9.6
70% NiO–Cs _{2.5} H _{0.5} PMo ₁₂ O ₄₀	400	15	79	11	10	11.9
	450	21	71	11	18	14.9
50% NiO–Cs _{2.5} H _{0.5} PMo ₁₂ O ₄₀	400	4.7	93	0	7	4.4
	450	8.4	87	0	13	7.3
Cs _{2.5} H _{0.5} PMo ₁₂ O ₄₀	400	<0.1				0.00

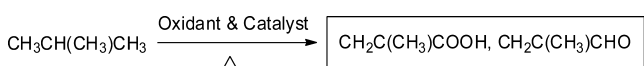
^aReaction conditions: catalyst, 0.5 g; P(iso-C₄H₁₀) = 5.6 kPa, P(O₂) = 11.2 kPa, P(N₂) = 84.2 kPa; total flow rate, 90 mL min⁻¹. Other products are mainly CH₄.

detail. A side cracking reaction to propylene may accompany the main iso-butane ODH to iso-butene process.¹⁸⁹ A few HPC catalysts employed for iso-butane ODH to iso-butene reactions will be discussed and compared in detail below (Scheme 30).

Cavani et al. reported that the Wells–Dawson-type HPC K_xP₂W₁₇MO_{62-y}·nH₂O ($y = 0$ for M = W and $y = 1$ for M = Fe, Mn, Co, Cu) were stable and efficient catalysts for the oxidative dehydrogenation of iso-butane.^{190,191} In all cases, isobutene was formed with a good selectivity. The results clearly evidenced that the greater activity for oxidative dehydrogenation of iso-butane was obtained over K₇P₂W₁₇FeO₆₁ catalyst. Under their reaction conditions (residence time 3.6 s; temperature 380–430 °C; i-C₄/O₂/H₂O/He = 26:13:12:49), the selectivity to isobutene could reach 61% with an iso-butane conversion of

Scheme 31. Mechanism of the Oxidation of Iso-butane to Methacrolein and Methacrylic Acid Catalyzed by HPC Catalysts^a

^aReprinted with permission from ref 4. Copyright 2007 John Wiley & Sons, Inc.

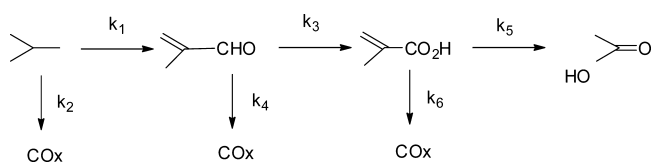
Scheme 32. General Conditions Employed for the Oxidation of Iso-butane to Methacrolein and Methacrylic Acid^a

^aOxidant: O₂; T = 300–400 °C.

17.4% at 427 °C (see Table 33). These values remained stable after at least 300 h.

The NiO–Cs_{2.5}H_{0.5}PMo₁₂O₄₀ nanocomposites reported by Zhang et al.^{144,196} also showed superior catalytic performance for the oxidative dehydrogenation of iso-butane. Over 70%

Scheme 33. Proposed Reaction Pathway for the Oxidation of Iso-butane over $\text{Cs}_{2.5}\text{H}_{1.34}\text{Ni}_{0.08}\text{PMo}_{11}\text{O}_{40}$ Catalyst²⁰⁰



$\text{NiO}-\text{Cs}_{2.5}\text{H}_{0.5}\text{PMo}_{12}\text{O}_{40}$ nanocomposites, the selectivities to isobutene were 79% and 71% at iso-butane conversions of 15% and 21%, at 450 and 500 °C, respectively. The total selectivity to isobutene and methacrolein could reach up to 90% and 82% at the same time (see Table 34). To our knowledge, these performances are significantly better than those reported for other catalysts.^{188,190,191,197}

8.3. Selective Oxidation of Iso-butane to Methacrolein and Methacrylic Acid

8.3.1. General Mechanisms for Selective Oxidation of Iso-butane to Methacrolein and Methacrylic Acid. Because of continued increasing demand of polymethylmethacrylate, an alternative green and more economic pathway other than traditional acetone-cyanohydrin (ACH) process is eagerly needed. The method that can directly oxidize iso-butane to methacrylic acid in one single step has potential advantages in terms of environment and economics. During the past few decades, special attention has been paid to HPC catalysts in selective oxidation of iso-butane to methacrylic acid, because HPC catalysts have strong acidity to activate the C–H bond of saturated iso-butane, oxidehydrogenation properties, and oxygen insertion properties.¹⁹⁸ The reaction mechanism of this reaction has been specially proposed for HPC catalysts system.^{4,198} As shown in Scheme 31 with molybdenum as the model metal, the oxidative breaking of C–H bond at the tertiary carbon is the first step in activating iso-butane and produces an alkoxide group together with a hydroxyl group, which is also the rate-limiting step of the reaction. After that, the same primary carbon atom is further connected to the

catalyst surface via two C–O–Mo bridges and then forms a dioxyalkylidene species. This dioxyalkylidene intermediate can be transferred through the dissociation of a C–O bond either to methacrolein or to a carboxylate species via oxidation on a Mo–O bond. The carboxylate species is the precursor of methacrylic acid. Because methacrolein and methacrylic acid develop from the same dioxyalkylidene intermediate, two reactions exist in parallel. However, a certain amount of C2 compounds including acetic acid and acrolein can also be observed during the reaction, which still cannot be satisfactorily explained by the reaction mechanism proposed in the literature.

8.3.2. Selective Oxidation of Iso-butane to Methacrolein and Methacrylic Acid over HPC Catalysts. Mizuno et al. also studied the oxidation of iso-butane over $\text{Cs}_x\text{H}_{3-x}\text{PMo}_{12}\text{O}_{40}$ -based HPC (Scheme 32).¹⁹⁹ The results showed that the substitution of Cs^+ for H^+ in $\text{H}_3\text{PMo}_{12}\text{O}_{40}$ greatly enhanced the yield of methacrylic acid, which reached a maximum value around a Cs^+ content of 2.5. Further modification of $\text{Cs}_{2.5}\text{H}_{0.5}\text{PMo}_{12}\text{O}_{40}$ by substitution of Mo^{6+} addenda by V^{5+} and H^+ counteraction by Ni^{2+} has also been made. The best yield of methacrylic acid was 9.0%, which was obtained at 340 °C by using the heteropoly catalyst with one vanadium atom in the Keggin unit ($\text{Cs}_{2.5}\text{H}_{1.34}\text{Ni}_{0.08}\text{PMo}_{11}\text{VO}_{40}$).²⁰⁰ In their proposed mechanism (Scheme 33), iso-butane is converted into various oxygenated compounds, each step being potentially the subject of a complete oxidation.

Iron- and copper-substituted HPC $\text{Cs}_{2.5}\text{M}_{0.08}^{n+}\text{H}_{0.5-0.08}\text{P-Mo}_{12}\text{O}_{40}$, whose catalytic activity had been studied in the oxidation of ethane and propane (see sections 6 and 7),^{106–108,110} were also investigated in catalyzing the selective oxidation of iso-butane at 340 °C under both oxygen-rich and oxygen-poor conditions (Table 35). Under oxygen-rich conditions, the main products were methacrylic acid (MAA), methacrolein (MAL), acetic acid (AcOH), and CO_x . The addition of iron increased the selectivity to MAA from 24% to 35% without any change in the iso-butane conversion. Under oxygen-poor conditions, the products were MAL, iso-butene,

Table 35. Effect of Addition of Iron or Copper to $\text{Cs}_{2.5}\text{H}_{0.5}\text{PMo}_{12}\text{O}_{40}$ on Oxidation of Iso-butane at 340 °C under Both Oxygen-Rich^a and Oxygen-Poor^b Conditions^{107,110}

catalyst	iso-C ₄ H ₈ conversion (%)	selectivity ^c (%)					yield (%)	
		CO _x	MAA	MAL	CH ₃ COOH	CH ₃ COCH ₃	MAA	MAL
$\text{H}_3\text{PMo}_{12}\text{O}_{40}^a$	7	70	4	18	8	n.d.	0.3	1.3
$\text{Cs}_{1.0}\text{H}_{2.0}\text{PMo}_{12}\text{O}_{40}^a$	6	50	23	17	10	n.d.	1.4	1.0
$\text{Cs}_{2.0}\text{H}_{1.0}\text{PMo}_{12}\text{O}_{40}^a$	11	50	34	10	7	n.d.	3.7	1.1
$\text{Cs}_{2.5}\text{H}_{0.5}\text{PMo}_{12}\text{O}_{40}^a$	16	62	24	7	7	n.d.	3.8	1.1
$\text{Cs}_{2.85}\text{H}_{0.15}\text{PMo}_{12}\text{O}_{40}^a$	17	81	5	10	5	n.d.	0.9	1.7
$\text{Cs}_{3.0}\text{PMo}_{12}\text{O}_{40}^a$	18	67	5	10	6	n.d.	0.9	1.8
$\text{Cs}_{2.5}\text{Fe}_{0.08}\text{H}_{0.26}\text{PMo}_{11}\text{O}_{40}^a$	14	53	35	11	7	n.d.	4.9	1.5
$\text{Cs}_{2.5}\text{Cu}_{0.08}\text{H}_{0.34}\text{PMo}_{11}\text{O}_{40}^a$	12	71	12	10	7	n.d.	1.4	1.2
$\text{Cs}_{2.5}\text{Ni}_{0.08}\text{H}_{0.34}\text{PMo}_{11}\text{O}_{40}^a$	24	59	27	6	7	n.d.	6.5	1.4
$\text{Cs}_{2.5}\text{Mn}_{0.08}\text{H}_{0.34}\text{PMo}_{11}\text{O}_{40}^a$	21	60	20	11	9	n.d.	4.2	2.3
$\text{Cs}_{2.5}\text{Co}_{0.08}\text{H}_{0.34}\text{PMo}_{11}\text{O}_{40}^a$	7	68	11	15	6	n.d.	0.8	1.1
$\text{Cs}_{2.5}\text{H}_{0.5}\text{PMo}_{12}\text{O}_{40}^b$	10	42	n.d.	15	1	30	0.0	1.5
$\text{Cs}_{2.5}\text{Fe}_{0.08}\text{H}_{0.26}\text{PMo}_{11}\text{O}_{40}^b$	15	40	n.d.	30	2	26	0.0	4.5
$\text{Cs}_{2.5}\text{Fe}_{0.16}\text{H}_{0.02}\text{PMo}_{11}\text{O}_{40}^b$	13	74	n.d.	7	4	15	0.0	0.9
$\text{Cs}_{2.5}\text{Cu}_{0.08}\text{H}_{0.34}\text{PMo}_{11}\text{O}_{40}^b$	14	42	n.d.	35	2	24	0.0	4.9

^aIso-butane, 17 vol %; O_2 , 33 vol %; N_2 , balance; catalyst, 1.0 g; total flow rate, $30 \text{ cm}^3 \text{ min}^{-1}$; reaction temperature, 340 °C. ^bIso-butane, 33 vol %; O_2 , 13 vol %; N_2 , balance; catalyst, 1.0 g; total flow rate, $15 \text{ cm}^3 \text{ min}^{-1}$; reaction temperature, 340 °C. ^cCalculated on the C₄ (iso-butane)-basis. MAA: methacrylic acid. MAL: methacrolein.

Table 36. Selective Oxidation of Iso-butane to Methacrylic Acid^{a,203}

catalyst	temp (°C)	iso-C ₄ H ₈ conversion (%)	selectivity (%)					yield (%)	
			CO _x	MAA	MAL	AcOH	AA	MAA	MAL
H _x PVAs _{0.3} Mo ₁₁ O _y	370	17	65	22	9	5	0	3.7	1.5
H _x Fe _{0.08} PVAs _{0.3} Mo ₁₁ O _y	370	21	37	43	6	10	3	9.0	1.3
H _x Fe _{0.12} PVAs _{0.3} Mo ₁₁ O _y ^b	370	20	23	57	4	14	1	11.4	0.8
H _x Fe _{0.12} PVAs _{0.3} Mo ₁₁ O _y ^c	370	24	10	70	4	12	4	16.8	1.0
H _x Fe _{0.12} PVAs _{0.3} Mo ₁₁ O _y ^d	370	5	100	0	0	0	0	0.0	0.0
H _x Fe _{0.16} PVAs _{0.3} Mo ₁₁ O _y	370	20	35	48	6	10	2	9.6	1.2
H _x KFe _{0.12} PVAs _{0.3} Mo ₁₁ O _y	360	26	74	16	2	6	2	4.2	0.5
H _x KFe _{0.12} PVAs _{0.3} Mo ₁₁ O _y	370	28	78	12	1	7	2	3.4	0.3
H _x CsFe _{0.12} PVAs _{0.3} Mo ₁₁ O _y	350	18	22	58	5	12	2	10.4	0.9
H _x CsFe _{0.12} PVAs _{0.3} Mo ₁₁ O _y	370	22	44	36	4	14	3	7.9	0.9
H _x Fe _{0.12} PVMo ₁₁ O _y	370	31	58	21	2	16	3	6.5	0.6
H _x Fe _{0.12} PVAs _{0.2} Mo ₁₁ O _y	370	24	28	50	5	13	4	12.0	1.2
H _x Fe _{0.12} PVAs _{0.4} Mo ₁₁ O _y	370	23	41	42	6	8	3	9.7	1.4

^aReaction conditions: catalyst, 1.2 g; feed, iso-C₄H₁₀:O₂:N₂ = 2:2:3 mL min⁻¹; time on stream, 4 h. MAA: methacrylic acid. MAL: methacrolein. AA, acrylic acid. AcOH, acetic acid. ^bPretreatment: calcined under air atmosphere at 350 °C for 2.5 h. ^cPretreatment: calcined under air atmosphere at 400 °C for 2.5 h. ^dPretreatment: calcined under air atmosphere at 450 °C for 2.5 h.

Table 37. Selective Oxidation of Iso-butane to Methacrylic Acid Catalyzed by Cesium and Copper- or Iron-Substituted Keggin-type Phosphomolybdic HPC

precatalyst	temp (°C)	iso-C ₄ H ₈ conversion (%)	selectivity (%)				yield (%)		ref
			CO _x	MAA	MAL	AcOH	MAA	MAL	
H ₃ PMo ₁₂ O ₄₀ ^a	340	5	82	3	7	7	0.2	0.4	203
Cs ₂ HPMo ₁₂ O ₄₀ ^b	340	7.2	61	12	14	11	0.9	1.0	203
Cs ₂ Cu _{0.05} H _{0.9} PMo ₁₂ O ₄₀ ^b	340	7.0	64	7	16	13	0.5	1.1	203
Cs ₂ Cu _{0.20} H _{0.6} PMo ₁₂ O ₄₀ ^b	340	7.5	72	6	15	7	0.5	1.1	203
Cs ₂ Cu _{0.30} H _{0.4} PMo ₁₂ O ₄₀ ^b	340	6.6	72	6	16	5	0.4	1.1	203
Cs ₂ Cu _{0.43} H _{0.14} PMo ₁₂ O ₄₀ ^b	340	5.9	76	5	15	4	0.3	0.9	203
Fe _{0.85} H _{0.45} PMo ₁₂ O ₄₀ ^a	340	4	53	9	27	9	0.4	1.1	203
Cs ₂ Fe _{0.05} H _{0.85} PMo ₁₂ O ₄₀ ^b	340	6.7	53	21	15	11	1.4	1.0	203
Cs ₂ Fe _{0.1} H _{0.7} PMo ₁₂ O ₄₀ ^b	340	6.8	51	21	16	10	1.4	1.1	203
Cs ₂ Fe _{0.2} H _{0.4} PMo ₁₂ O ₄₀ ^b	340	6.8	50	24	17	9	1.6	1.2	203
Cs ₂ Fe _{0.25} H _{0.25} PMo ₁₂ O ₄₀ ^b	340	6.0	52	17	18	7	1.0	1.1	203
Cs ₂ Fe _{0.3} H _{0.1} PMo ₁₂ O ₄₀ ^b	340	6.3	52	18	17	7	1.1	1.1	203
Cs _{2.5} H _{0.5} PMo ₁₂ O ₄₀ ^b	340	10.3	68	12	10	9	1.2	1.0	203
Cs _{2.5} Fe _{0.05} H _{0.35} PMo ₁₂ O ₄₀ ^b	340	10.4	73	5	10	10	0.5	1.0	203
Cs _{2.5} Fe _{0.1} H _{0.2} PMo ₁₂ O ₄₀ ^b	340	10.3	58	19	10	11	2.0	1.0	203
H _{1.8} Te _{0.6} PMo ₁₂ O ₄₀ ^c	330	3.9	30	25	36	10	1.0	1.4	206
H ₁ Te ₁ PMo ₁₂ O ₄₀ ^c	360	4.8	23	33	39	5	1.6	1.9	206
Te _{1.8} PMo ₁₂ O ₄₀ ^c	355	4	26	37	30	7	1.5	1.2	206
Cs ₂ Te _{0.05} H _x PMo ₁₂ O ₄₀ ^c	369	14.4	50	25	13	11	3.6	1.9	206
Cs ₂ Te _{0.2} H _x PMo ₁₂ O ₄₀ ^c	367	12	28	50	12	10	6.0	1.4	206
Cs ₂ Te _{0.3} V _{0.1} ^{c,d}	350	16.1	26	54	11	9	8.7	1.8	206
Cs ₂ Te _{0.3} V _{0.1} /LMV ^{d,e}	360	21	30	57	2	11	12.0	0.4	205

^aReaction conditions: catalyst, 0.15–0.3 g; feed composition, i-C₄H₁₀:O₂:He:N₂ = 17.2:33.4:10.1:40.5 kPa; time on stream, 48 h. ^bReaction conditions: catalyst, 0.15–0.3 g; feed composition, i-C₄H₁₀:O₂:He:N₂ = 17.2:33.4:10.1:40.5 kPa; time on stream, 8 h. ^cReaction conditions: catalyst, 2 g; total flow rate, 6 mL min⁻¹; feed composition, i-C₄H₁₀:O₂:H₂O:N₂ = 27:13.5:10:49.5 kPa. ^xdepends on the reduction level of molybdenum cations. ^dPrecatalyst. ^eReaction conditions: catalyst, 2 g; GHSV (gas hourly space velocity), 2500 mL g⁻¹ h⁻¹; feed composition, i-C₄H₁₀:O₂:H₂O:N₂ = 10:10:10:70. MAA: methacrylic acid. MAL: methacrolein. AcOH: acetic acid.

Table 38. Selective Oxidation of Iso-butane to Methacrylic Acid^{207,a}

precatalyst	temp (°C)	iso-C ₄ H ₈ conversion (%)	selectivity (%)				yield (%)	
			CO _x	MAA	MAL	AcOH	MAA	MAL
(NH ₄) ₃ PMo ₁₂ O ₄₀ ^b	352	5	33	42	12	13	2.1	0.6
(NH ₄) ₃ PMo ₁₂ O ₄₀ ^c	350	6	73	4	15	8	0.2	0.9

^aMAA: methacrylic acid. MAL: methacrolein. AcOH, acetic acid. Reaction conditions: catalyst, 1.5 g. Residence time, 3.6 s. ^bFeed composition, iso-C₄H₁₀:O₂:N₂:H₂O = 26:13:49:12. ^cFeed composition, iso-C₄H₁₀:O₂:N₂:H₂O = 1:13:74:12.

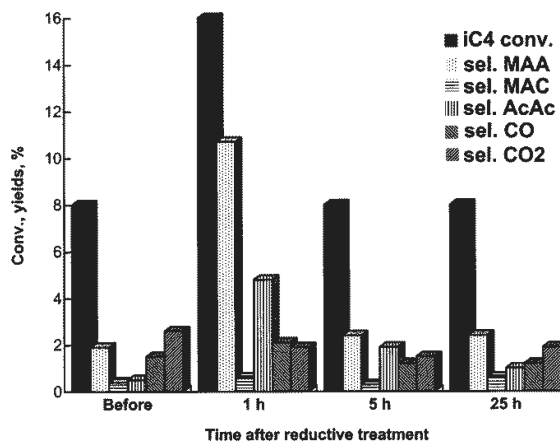


Figure 8. Catalytic performance of the equilibrated catalyst under isobutane-poor conditions ($\text{iso-C}_4\text{H}_{10}\text{:O}_2\text{:N}_2\text{:H}_2\text{O} = 1:13:74:12$) for different times elapsed after further reducing treatment ($\text{iso-C}_4\text{H}_{10}\text{:O}_2\text{:N}_2\text{:H}_2\text{O} = 26:13:49:12$). MAA, methacrylic acid; MAC, methacrolein; AcAc, acetic acid. Reprinted with permission from ref 207. Copyright 2000 Académie des sciences.

AcOH , acetone, and CO_2 , while MAA was not observed under these conditions. The addition of iron increased both the selectivity toward MAL, from 15% to 30%, and the conversion of iso-butane, from 10% to 15%.

Under oxygen-rich conditions, the addition of copper to $\text{Cs}_{2.5}\text{H}_{0.5}\text{PMo}_{12}\text{O}_{40}$ decreased the conversion of iso-butane from 16% to 12%, and the selectivity to methacrylic acid was also decreased from 24% to 12%, while only a small increase (from 7% to 10%) in the MAL selectivity was observed. Under oxygen-poor conditions, the main selective oxidation product was MAL, while no MAA was observed. The addition of copper also increased the conversion of iso-butane from 10% to 14%, together with the selectivity to MAL from 15% to 35%.

The iso-butane oxidation activity and the stability of catalysts with Fe have been studied by Mizuno and co-workers.²⁰¹ Catalytic performances were screened with different initial iron positions (inside or outside the Keggin anions). Addition of Cs was shown to raise Fe, releasing temperature and enhancing the stability. Similar iso-butane conversions (about 8%) were reported when using both $\text{Cs}_{1.5}\text{Fe}_{0.5}(\text{NH}_4)_2\text{PMo}_{12}\text{O}_{40}$ and $\text{Cs}_{1.5}(\text{NH}_4)_2\text{PMo}_{11.5}\text{Fe}_{0.5}\text{O}_{39.5}$ precatalysts, while the selectivities to MAA were slightly different (21% and 15%, respectively).

Deng et al.²⁰² synthesized molybdophosphoric heteropoly acid catalysts modified by incorporation of iron counteraction and substitution of phosphorus by arsenic. The iso-butane conversion was significantly improved by adding iron, and the selectivity to MAA could be enhanced by partially adding ether or arsenic. A 17% yield of MAA was obtained over $\text{H}_x\text{Fe}_{0.12}\text{PVAs}_{0.3}\text{Mo}_{11}\text{O}_y$ catalyst at 370 °C after 4 h reaction, and the iso-butane conversion (24%) also reached the best value at this point (see Table 36). This catalyst was still stable after 24 h of reaction.

Cesium and copper-, iron-, tellurium-, or vanadium-substituted phosphomolybdc HPC ($\text{Cs}_2\text{M}_x^{y+}\text{H}_{1-y}\text{PMo}_{12}\text{O}_{40}$, $\text{M} = \text{Fe}^{3+}$ and Cu^{2+} , $0 \leq x \leq 0.43$) were also studied by Millet et al. in selective oxidation of iso-butane to MAA.^{203–206} Different amounts of cesium and copper or iron were introduced as counter-cations, and their activities are shown in Table 37. The addition of copper appears to help increase the activity but decreases the selectivity to MAA; the addition of iron and tellurium seems to have no significant effect on the activity but helps increase the selectivity to MAA. The cosubstitution of protons by vanadyl cations had a slight effect on the selectivity but increased the activity especially at low level of substitution, which led to a very efficient catalyst. $\alpha\text{-La}_2\text{Mo}_2\text{O}_9$ (LM) or $\beta\text{-La}_2\text{Mo}_{1.9}\text{V}_{0.1}\text{O}_{8.95}$ (LMV) was later added into the system as promoter. When using 50 wt % of LMV, a total selectivity of 59% from MAA and MAL was obtained at 360 °C. The origin of such an effect could be related to the synergistic effect taking place between the phases and results primarily from a support effect of the lanthanum molybdate, stabilizing the phosphomolybdc salt and preventing its sintering.

Cavani, Trifirò, and co-workers^{2,207} reported that a higher selectivity to MAA (40–43% after preliminary activation at 380 °C) was obtained over a ammonium salt of 12-molybdophosphoric acid (i.e., $(\text{NH}_4)_3\text{PMo}_{12}\text{O}_{40}$) catalyst under isobutane-rich condition (26% iso-butane, 13% oxygen). This value is much higher than the one (about 4%) obtained on the same catalyst under isobutane-poor condition (see Table 38). The activation period for this selective oxidation was unusually long, which needed more than 80 h, and the initial conversion and selectivity to methacrylic acid were very low. A further reduction of the polyoxometalate catalyst led to an improvement of the selectivity to MAA (Figure 8). The activity of $(\text{NH}_4)_3\text{PMo}_{12}\text{O}_{40}$ catalyst was also affected by the pH value during preparation steps (see Figure 9).

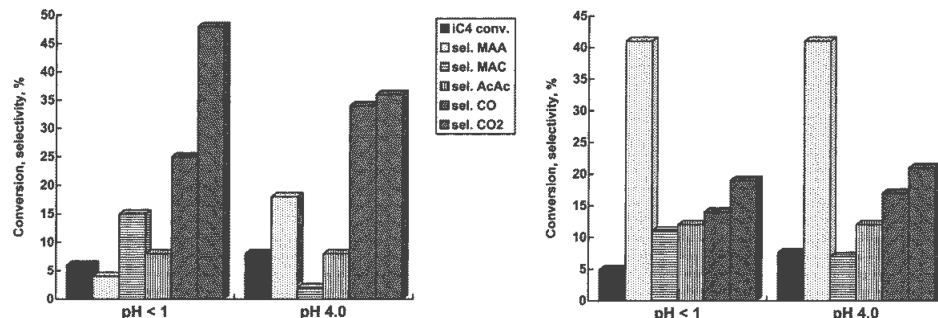


Figure 9. Comparison of the catalytic performance of $(\text{NH}_4)_3\text{PMo}_{12}\text{O}_{40}$ prepared by precipitation at pH < 1 and pH 4.0 and calcination under isobutane-poor (left) conditions and isobutane-rich (right) conditions. Reaction conditions: 1% iso-butane or 26% iso-butane, 13% oxygen, 12% steam, remainder helium. Residence time 3.6 s, temperature 350 °C. MAA, methacrylic acid; MAC, methacrolein; AcAc, acetic acid. Reprinted with permission from ref 2. Copyright 2001 Elsevier Science B.V.

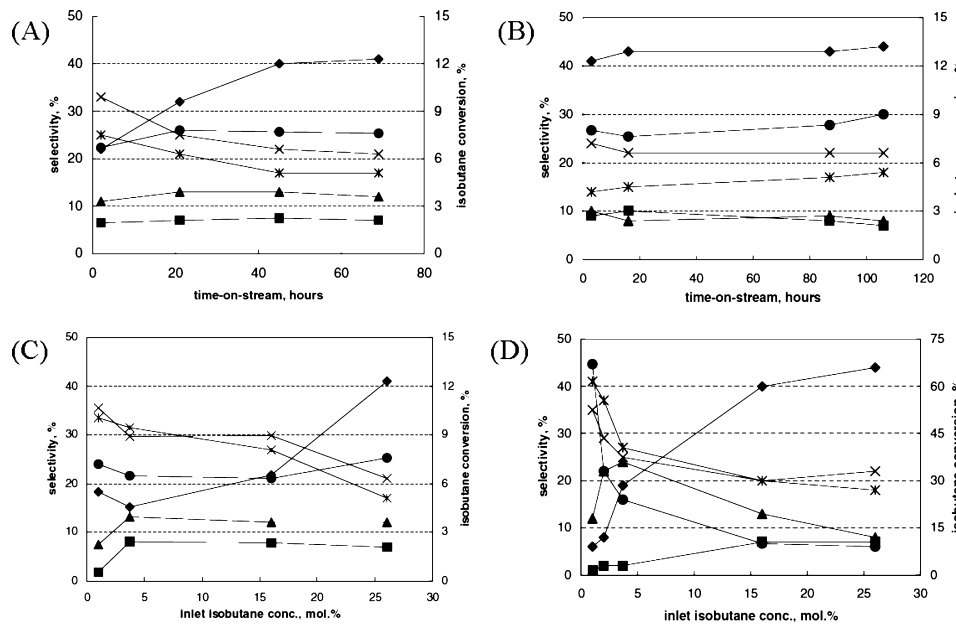


Figure 10. Comparison results of catalytic performance of POM4.0 and POMSB4.0 catalysts. Catalytic performance of (A) POM4.0 catalyst and (B) POMSB4.0 catalyst as functions of time-on-stream at 350 °C with a residence time of 3.6 s; feed composition: 26% iso-C₄H₁₀, 13% O₂, 12% H₂O, and He balance. Catalytic performance of (C) POM4.0 catalyst and (D) POMSB4.0 catalyst as functions of the iso-C₄H₁₀ concentration in the feed at 350 °C with a residence time of 3.6 s; feed composition: 13% O₂, 12% H₂O, and He balance. Iso-C₄H₁₀ conversion (●), selectivity to methacrylic acid (◆), methacrolein (■), acetic acid (▲), CO (*) and CO₂ (×). Adapted with permission from ref 209. Copyright 2003 Plenum Publishing Corp.

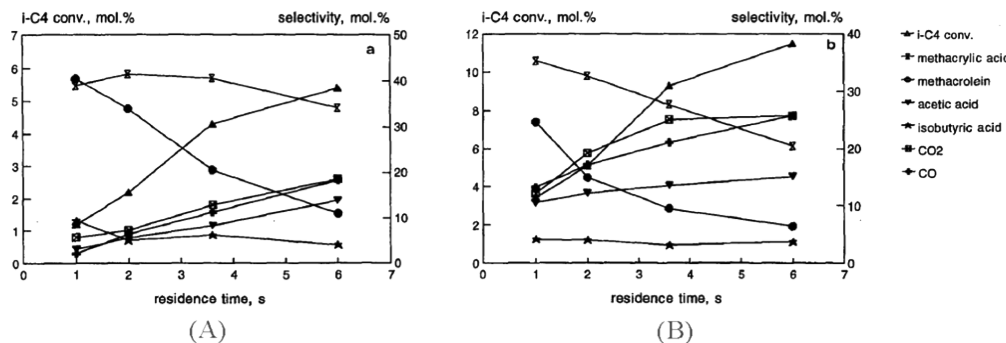


Figure 11. Iso-butane conversion and the yield of the products as functions of the residence time: (A) catalyst K₁Fe₀; (B) catalyst K₁Fe_{1.0}. Other reaction conditions: catalyst, 3.0 g; feed composition, 26% iso-C₄H₁₀, 13% O₂, 12% H₂O, and He balance; reaction temperature, 350 °C. Reprinted with permission from ref 210. Copyright 1995 J. C. Baltzer AG, Science Publishers.

Table 39. Catalytic Performance of Catalyst K₁Fe_x Calcined at 350 and 400 °C in Selective Oxidation of Iso-butane to Methacrylic Acid²¹¹

precatalyst ^b	calcination temp (°C)	iso-C ₄ H ₈ conversion (%)	selectivity (%)				yield (%)	
			CO _x	MAA	MAL	AcOH	MAA	MAL
K ₁ Fe ₀	350	4.2	26	40	20	9	1.7	0.8
K ₁ Fe _{0.5}	350	6.1	37	32	14	15	2.0	0.9
K ₁ Fe _{1.0}	350	10.8	44	29	9	15	3.1	1.0
K ₁ Fe _{1.5}	350	11.4	52	22	8	17	2.5	0.9
K ₁ Fe ₀	400	2.6	24	39	30	5	1.0	0.8
K ₁ Fe _{0.5}	400	4.1	38	30	19	10	1.2	0.8
K ₁ Fe _{1.0}	400	7.2	55	18	8	16	1.3	0.6
K ₁ Fe _{1.5}	400	11.1	50	15	6	20	1.7	0.7

^aReaction conditions: catalyst, 1.5 g; feed composition, 26% iso-C₄H₁₀, 13% O₂, 12% H₂O, and He balance; reaction temperature, 350 °C; residence time, equal to 3.6 s. MAA: methacrylic acid. MAL: methacrolein. AcOH, acetic acid.

^bThe precatalysts' abbreviations denote their K and Fe content.

Partially reduced catalysts^{208,209} were prepared by preparing a Sb³⁺-doped (NH₄)₃PMo₁₂O₄₀ HPC and screened for iso-butane oxidation (Figure 10). POM4.0 refers to the catalyst

obtained by calcination of the precursor precipitated at pH 4.0 (in this case, a lacunary polyoxometalate (POM) of composition (NH₄)₇PMo₁₁O₃₉). Catalysts containing Sb

Table 40. Catalytic Performance of Different Keggin-type Heteropoly Compound-Based Catalysts with Various Compositions in the Selective Oxidation of Iso-butane

catalyst	temp (°C)	residence time (s)	iso-C ₄ /O ₂ /H ₂ O/N ₂ molar ratios	iso-C ₄ H ₈ conv. (%)	selectivity (%)		yield (%)	
					MAA	MAL	MAA	MAL
H _x PM ₁₂ SbO _y ²¹²	340	6.1	10/13/30/47	10	50	20	5.0	2.0
H _x P _{1.1} Mo ₁₂ V _{1.1} Cu _{0.1} Cs _{1.1} O _y ²¹³	320	3.6	30/15/20/35	10.3	55.7	16.3	5.7	1.7
H _x P _{1.5} Mo ₁₂ V ₁ Cu _{0.2} Nd _{0.5} Cs ₁ O _y ²¹⁴	320	3.6	30/15/20/35	12.8	53.8	15.9	6.9	2.0
H _x P _{1.5} Mo ₁₂ VO _{0.04} Cu _{0.2} Ba _{0.2} K _{0.5} Cs _{0.5} O _y ³	320	2.4	10/16.8/10/63.2	16.3	50.1	10.0	8.2	1.6
H ₄ PMo ₁₁ VO ₄₀ /Ta ₂ O ₅ ²¹⁵	350	2	4/8/0/88	28.5	13.3	41	3.8	11.7
H _x P _{1.5} Mo ₁₂ V _{0.5} As _{0.4} Cs _{1.8} Cu _{0.3} O _y ²¹⁶	320	3.6	26/13/12/49	11.2	53.6	11.5	6.0	1.3
H _x P _{1.5} Mo ₁₂ V _{0.5} As _{0.4} Cs _{1.4} Cu _{0.3} O _y ²¹⁷	330	5.4	6.5/15.5/15/63	25	2.5	42.6	0.6	10.7
H _{3.6} Cu _{2.0} PMo ₁₁ VO ₄₀ /SiO ₂ ^{a218}	348	b	15.1/29.6/19.7/35.5	13.0	11.5	55.6	1.5	7.2
H _{1.34} Cs _{2.5} Ni _{0.08} PMo ₁₁ VO ₄₀ ²¹⁹	340	2	17/33/0/50	31	8	29	2.5	9.0
(Pyr) ₃ PMo ₁₂ O ₄₀ ²²⁰	300	c	2.2/13.7/33.5/50.6	22.2	tr	51.1	0.0	11.3
H _{2.4} Cs _{1.6} P _{1.7} Mo ₁₁ V _{1.1} O ₄₀ ²²¹	349	3.6	26/12/12/50	10.6	7.9	37.6	0.8	4.0
H _x Fe _{0.12} PVAs _{0.3} Mo ₁₁ O _y ²⁰²	370	8.6	29/29/0/42	23.9	70	4	16.7	1.0
H _x Mo _{1.2} V _{0.3} P _{1.5} As _{0.4} Cu _{0.3} Cs _{1.4} O _y ²²²	366	5.4	25/25/15/35 ^d	21.8	total 44.9	total 9.8		
H ₄ PVMo ₁₁ O ₄₀ /HCs ₃ PVMo ₁₁ O ₄₀ ²²³	340	e	26/13/12/49	11.4	24	6.7	2.7	0.8

^a40% of active phase. ^bW/F = 2.1 g h mL⁻¹. ^cW/F = 0.1 g min mL⁻¹. ^dP_{tot} = 1.5 atm. ^eGHSV (gas hourly spave velocity), 2500 mL g⁻¹ h⁻¹. MAA: methacrylic acid. MAL: methacrolein.

(POMsB4.0) obtained by calcination of the precursor precipitated at pH = 4.0 were surprisingly very active (as high as 70% iso-butane conversion) from the beginning of its reaction time even under isobutane-poor conditions, but the selectivity to MAA was low in this case (about 7%). During the calcination of the polyoxometalate precursor (at 350 °C for 6 h), a solid-state redox reaction between Sb³⁺ and Mo⁶⁺ occurred in the Keggin framework. The corresponding catalyst was significantly more stable and efficient selectively to MAA.

The selective oxidation of iso-butane was also carried out over Fe-doped Keggin-type P/Mo polyoxometalate catalysts with different Fe contents^{210,211} at 350 °C, with a total selectivity to oxygenate products higher than 50%. The reaction products were methacrylic acid, methacrolein, isobutyric acid, acetic acid, and CO_x. The replacement of ammonium cation by Fe in the K₁(NH₄)₂PMo₁₂O₄₀ polyoxometalate precursor led to an increase of activity proportional to the amount of Fe introduced, but also led to a decrease in the selectivity to methacrylic acid. The iso-butane conversion increased almost linearly under elevated flow velocities, while the selectivities to methacrolein and methacrylic acid decreased in varying degrees (Figure 11). A maximum yield (3.1%) of methacrylic acid was obtained over the catalyst calcined at 350 °C with one atom of Fe per Keggin unit (i.e., K₁Fe_{1.0} catalyst), while the iso-butane conversion was 10.8% (see Table 39).

A selection of the other good results obtained over various HPC-based catalysts for the selective oxidation of iso-butane is also summarized in Table 40.

9. CONCLUSION

Heteropoly compounds (HPC) have revealed their potential to generate catalyst for selectively converting light alkanes to oxygenated products. It should be noted that understanding the mechanism and the essential steps occurring between the HPC and the alkane remains extremely limited at the molecular level for the HPC can undergo structural reorganization at the temperature or under the conditions employed. Indeed, the same limitation applies for most heterogeneous catalytic systems.

This Review indicates the variety of activities of HPA that can be obtained in solution or in solid phase or on supports. For this variety, there are several reasons. (i) There are various structures in which they are active: the primary structure being that of the heteropolyanion itself, the secondary structure is the three-dimensional arrangements of polyanions, and the tertiary structure representing the manner in which the secondary structure assembles into solid particles. (ii) There are also a huge variety of elements inside the HPA (the variety of cations make the comparison between each of them extremely difficult). (iii) The heteropoly acids can have acidity, which varies dramatically depending on composition (this acidity can go up to superacidity!). (iv) The HPA have also varying degrees of oxidizing properties depending on transition elements. This complexity of situation makes it very difficult to really have a predictive vision of their ability to activate and functionalize alkanes. However, a large amount of data reported suggests that the initial formula of the precatalyst is pivotal to direct the selectivity of the reaction toward different oxygenates. Independently from the substrates treated, a few trends in catalytic conditions may emerge under the scrutiny of the multiple parameters pertaining to the HPC: the overall formulation, the modification of the addenda and that of the counteractions, and the addition of organic additive. Molybdenum-based HPC surpass in most cases their tungsten counterpart in conversion and selectivity. Inclusion of alternative transition metal atoms as addenda is highly influential with iron, vanadium, and antimony being particularly outstanding. The counteraction using Cs⁺, NH⁴⁺ can be highly effective.

To fully make a deep structure activity relationship in this kind of catalysis, it is necessary to decompose elementary steps and study them in a systematic way.

AUTHOR INFORMATION

Corresponding Authors

*E-mail: jeanmarie.basset@kaust.edu.sa.

*E-mail: miao.sun@aramco.com.

Notes

The authors declare no competing financial interest.

Biographies

Dr. Miao Sun was born in Fushun, China in 1981. She obtained her doctoral degree in 2009 under the supervision of Prof. Huilin Wan from Xiamen University. After that, she joined Prof. Jean-Marie Basset's group and worked as a Post-Doctoral Fellow for King Abdullah University of Science and Technology (KAUST, Saudi Arabia) from 2009 to 2012 on low temperature direct transformation of methane and ethane by using heterogeneous catalysts including heteropoly compounds. During her Post-Doctoral Fellow period, Dr. Miao Sun also worked at Organometallic Catalysis Lab (CNRS) in Université Claude Bernard Lyon 1 (France) for nearly 1 year. Dr. Miao Sun has been working on synthesizing and utilizing heteropolyacids-based catalysts in both homogeneous and heterogeneous catalytic reactions since 2004. She has 8 journal papers and 3 patents on heteropolyacid-based catalysts' synthesis, natural gas transformation, and extensive characterizations. Her research interests are in the area of crude oil and nature gas direct catalytic transformation. Currently, she is working as an Engineer at Research and Development Center of Saudi Aramco Oil Co. in Saudi Arabia.



Jizhe Zhang is a Ph.D. student in Prof. Yu Han's group at King Abdullah University of Science and Technology. He obtained his M.Sc. degree in the Chinese key laboratory, the group of Prof. Huilin Wan (member of CAS) from Xiamen University. He currently is visiting Lawrence Berkeley National Laboratory in the U.S. He is strongly interested in catalysis and has comprehensive experience on catalytic performance research in various catalytic reactions. Heteropolyacid catalysts were applied by him into alkane conversion, biomass conversion, energy generation, and other catalytic fields. So far, he has published 12 papers and 3 patents, in which 2 papers were selected as hot papers by the journal publisher.



Dr. Piotr Putaj received his Ph.D. degree in Chemistry from Lyon I (Claude Bernard) University in 2012 under the supervision of Dr. F. Lefebvre. He then moved to Charles University in Prague to work as a postdoctoral research fellow in the Asymmetric Synthesis group of Dr. J. Vesely. His current research interests focus on highly selective approaches in organic synthesis via combined organo- and organometallic catalysis.



Dr. Valérie Caps obtained her Ph.D. degree in Inorganic Chemistry in 2001 from the University of Reading (United Kingdom) under the mentorship of Prof. S. C. E. Tsang. Her postdoctoral experiences at Johnson-Matthey (Dr. D. Thompsett, Sonning Common, UK) and Max Planck Institut für Kohlenforschung (Prof. H. Bönnemann, Mülheim an der Ruhr, Germany) involved the design of magnetic catalytic supports, ferro-fluids, and low density alloys. In 2003, she received a Full Tenured Research position from the French National Center for Scientific Research to develop the potentials of gold nanoparticles in oxidation catalysis at the Institute of Catalysis in Lyon (IRCELYON, France). She was awarded the CNRS Bronze Medal for this work in 2008. After becoming a Founding Member of King Abdullah University of Science and Technology (Saudi Arabia) in 2009, she contributed to the installation of KAUST Catalysis Center and managed several projects dealing with catalysis by metal, alloy, and composite nanostructures for petrochemical valorization. She is currently leading research within the IDEX framework of the University of Strasbourg at ICPEES (France).



Dr. Frédéric Lefebvre came to Centre National de la Recherche Scientifique (CNRS) at Villeurbanne in 1981 after a 2 year period at the Laboratoire de Chimie des Métaux de Transition in Paris where he worked on the synthesis and characterization of polyoxometalates under the direction of Professor G. Hervé. He received his doctoral degree in 1985 for a work on the synthesis of carbonyl compounds inside zeolites. After a postdoctoral stay at Namur under the direction of Professor Derouane, he returned to Villeurbanne where he was in charge of solid-state NMR. He joined the group of Professor Basset in 1993 where he worked on surface organometallic chemistry on zeolites and on metathesis. He also developed a new approach of grafting of polyoxometalates on surfaces and studied their reactivity with various molecules. He has published more than 260 papers and 9 patents.



Prof. J. M. Basset received his doctoral degree in 1969 from the University of Lyon, France. He came to Centre National de la Recherche Scientifique (CNRS) in 1971 and has occupied several positions, including vice director of the Institute of Catalysis (Lyon). He was appointed research Director at the CNRS in 1987, and funded his laboratory of Surface Organometallic Chemistry that became later the laboratory of Chemistry, Catalysis, Polymer, Process (C2P2) that he has held from 1994 to 2007. Prof. Basset also founded the consortium, "Actane", on alkane activation with 11 university laboratories and five companies. Since 1992, he also has served as Scientific Director of L'École Supérieure de Chimie Physique Electronique de Lyon (CPE Lyon), which has trained 450 chemists and 350 physicists in a 3-year scholarship program. Prof. Basset founded and serves as President of the network: Integrated Design of Catalytic Nanomaterials for a Sustainable Production (IDECAT). IDECAT is the only European Network of Excellence in Catalysis, which includes 40 laboratories and 20 companies. Professor Basset holds various professional memberships: Member of the European Academy of Sciences and Arts, Member of the European Academy of Sciences, Member of the French Academy of Technologies, and Member of the French Academy of Sciences. He is a distinguished author of over 450 scientific papers and reports. His main research interests are the relations between homogeneous and heterogeneous catalysis, and the metathesis of olefins and alkanes. He developed "surface organometallic chemistry". His research also includes the synthesis of single site catalysts in various fields of chemistry, petroleum, and polymers. Prof. Basset holds various professional memberships, is the recipient of several international and national awards, and is Doctor Honoris Causa of several universities. Currently, he is the Director of the KAUST Catalysis Center (KCC) in Saudi Arabia.



Dr. Jérémie Pelletier graduated from Université de Nice Sophia Antipolis (France) before receiving in 2006 a Ph.D. degree in homogeneous catalysis from the University of Leicester (UK). After pursuing related research interests as a postdoctoral fellow at SASOL technology (St Andrews, UK) and research associate at University of Liverpool, he moved back to France as a postdoctoral fellow at LCOMS (Université de Lyon 2 - C2P2) to practice surface organometallic chemistry. He was appointed research engineer in 2010 of the Catalysis Center in King Abdullah University of Science and Technology (Saudi Arabia) where he has been the current Lab Manager since 2011.

ABBREVIATIONS

HPC	heteropoly compounds
HPA	heteropoly acid
DFT	density functional theory
EXAFS	X-ray absorption fine structure spectroscopy
XANES	X-ray absorption near edge structure spectroscopy
XRD	X-ray diffraction
DSC	differential scanning calorimetry
XPS	X-ray photoelectron spectroscopy
NMR	nuclear magnetic resonance spectroscopy
ODH	oxidative dehydrogenation
FT-IR	Fourier transform infrared spectroscopy
POM	polyoxometalate
MAL/MAC	methacrolein
MAA	methacrylic acid

CO_x	carbon monoxide and carbon dioxide
VPO	vanadium–phosphorus–oxides
AA	acrylic acid
AcOH/AcAc	acetic acid
ARO	acrolein
MA	maleic acid

REFERENCES

- (1) Baca, M.; Aouine, M.; Dubois, J. L.; Millet, J. M. M. *J. Catal.* **2005**, *233*, 234.
- (2) Cavani, F.; Mezzogori, R.; Pigamo, A.; Trifirò, F.; Etienne, E. *Catal. Today* **2001**, *71*, 97.
- (3) Kuroda, T.; Okita, M. Japan Patent 04128247; Mitsubishi Rayon Co., Ltd.: Japan, 1991.
- (4) Ballarini, N.; Cavani, F.; Degrand, H.; Etienne, E.; Pigamo, A.; Trifirò, F.; Dubois, J. L. The Oxidation of Isobutane to Methacrylic Acid: An Alternative Technology for MMA Production. In *Methods and Reagents for Green Chemistry: An Introduction*; Tundo, P., Perosa, A., Zecchini, F., Eds.; John Wiley & Sons, Inc.: Hoboken, NJ, 2007; p 265.
- (5) Korovchenko, P.; Shiju, N. R.; Dozier, A. K.; Graham, U. M.; Guerrero-Perez, M. O.; Gulants, V. V. *Top. Catal.* **2008**, *50*, 43.
- (6) Okuhara, T.; Mizuno, N.; Misono, M. *Adv. Catal.* **1996**, *41*, 113.
- (7) Schlägl, R. In *Modern Heterogeneous Oxidation Catalysis: Design, Reactions and Characterization*; Mizuno, N., Ed.; Wiley-VCH Verlag GmbH & Co. KGaA: Weinheim, Germany, 2009; Chapter 1. Concepts in selective oxidation of small alkane molecules.
- (8) Cavani, F.; Ballarini, N.; Cericola, A. *Catal. Today* **2007**, *127*, 113.
- (9) López Nieto, J. M. *Top. Catal.* **2006**, *41*, 3.
- (10) Grabowski, R. *Catal. Rev.: Sci. Eng.* **2006**, *48*, 199.
- (11) Punniyamurthy, T.; Velusamy, S.; Iqbal, J. *Chem. Rev.* **2005**, *105*, 2329.
- (12) Overview of Natural Gas; <http://www.naturalgas.org/overview/background.asp>; retrieved 06 Aug 2013.
- (13) EIA. *Oil Gas J.* **2007**, *105*, 24.
- (14) Lunsford, J. H. *Catal. Today* **2000**, *63*, 165.
- (15) Centi, G.; Cavani, F.; Trifirò, F. *Selective Oxidation by Heterogeneous Catalysis*; Kluwer Academic/Plenum Publishers: New York, 2001.
- (16) Madeira, L. M.; Portela, M. F. *Catal. Rev.: Sci. Eng.* **2002**, *44*, 247.
- (17) Nexant. Maleic Anhydride (MAN), PERP Program Report, ChemSystems, 2009.
- (18) Arakawa, H.; Aresta, M.; Armor, J. N.; Barteau, M. A.; Beckman, E. J.; Bell, A. T.; Bercaw, J. E.; Creutz, C.; Dinjus, E.; Dixon, D. A.; Domen, K.; DuBois, D. L.; Eckert, J.; Fujita, E.; Gibson, D. H.; Goddard, W. A.; Goodman, D. W.; Keller, J.; Kubas, G. J.; Kung, H. H.; Lyons, J. E.; Manzer, L. E.; Marks, T. J.; Morokuma, K.; Nicholas, K. M.; Periana, R.; Que, L.; Rostrup-Nielson, J.; Sachtler, W. M. H.; Schmidt, L. D.; Sen, A.; Somorjai, G. A.; Stair, P. C.; Stults, B. R.; Tumas, W. *Chem. Rev.* **2001**, *101*, 953.
- (19) Brazdil, J. F. *Top. Catal.* **2006**, *38*, 289.
- (20) Misono, M.; Nojiri, N. *Appl. Catal.* **1990**, *64*, 1.
- (21) Izumi, Y. S.; Urabe, K.; Onaka, M. *Zeolite, Clay, and Heteropoly Acid in Organic Reactions*; Wiley-VCH: Tokyo; Weinheim; New York, 1992.
- (22) Izumi, Y. *Catal. Today* **1997**, *33*, 371.
- (23) Katsoulis, D. E. *Chem. Rev.* **1998**, *98*, 359.
- (24) Armor, J. N. *Appl. Catal., A* **2001**, *222*, 407.
- (25) Kozhevnikov, I. V. *Catalysts for Fine Chemical Synthesis: Catalysis by Polyoxometalates*; John Wiley & Sons Ltd.: The Atrium, Southern, Chichester, England, 2002; Vol. 2.
- (26) Weisselmel, K.; Arpe, H.-J. R. *Industrial Organic Chemistry*, 3rd ed.; VCH: Weinheim; New York, 1997.
- (27) Aoshima, A.; Tonomura, S.; Yamamoto, S. *Polym. Adv. Technol.* **1990**, *1*, 127.
- (28) Sano, K.; Uchida, H.; Wakabayashi, S. *Catal. Surv. Jpn.* **1999**, *3*, 55.
- (29) Howard, M. J.; Sunley, G. J.; Poole, A. D.; Watt, R. J.; Sharma, B. K. *Sci. Technol. Catal.* **1999**, *121*, 61.
- (30) Burch, R.; Crittle, D. J.; Hayes, M. J. *Catal. Today* **1999**, *47*, 229.
- (31) Labinger, J. A. *J. Mol. Catal. A: Chem.* **2004**, *220*, 27.
- (32) Hu, J.; Chen, L.; Richards, R. *Properties, Synthesis and Applications of Highly Dispersed Metal Oxide Catalysts*; Wiley-VCH Verlag GmbH & Co. KGaA: Weinheim, Germany, 2009; Vol. 2, Chapter 16.
- (33) Mizuno, N.; Kamata, K.; Uchida, S.; Yamaguchi, K. *Modern Heterogeneous Oxidation Catalysis: Liquid-Phase Oxidation with Hydrogen Peroxide and Molecular Oxygen Catalyzed by Polyoxometalate-Based Compounds*; Wiley-VCH: Weinheim, 2009.
- (34) Kozhevnikov, I. V. *J. Mol. Catal. A: Chem.* **2007**, *262*, 86.
- (35) Proust, A.; Thouvenot, R.; Gouzerh, P. *Chem. Commun.* **2008**, *1837*.
- (36) Long, D. L.; Tsunashima, R.; Cronin, L. *Angew. Chem., Int. Ed.* **2010**, *49*, 1736.
- (37) Védrine, J. C.; Millet, J.-M. M. *Heteropolyoxometallate Catalysts for Partial Oxidation*; Wiley-VCH Verlag GmbH & Co. KGaA: Weinheim, Germany, 2009; Vol. 2, Chapter 14.
- (38) Witko, M.; Tokarz-Sobieraj, R.; Grybos, R. *Nato. Sci. Ser., II* **2005**, *191*, 85.
- (39) Schwarz, H. *Angew. Chem., Int. Ed.* **2011**, *50*, 10096.
- (40) Gulants, V. V.; Carreon, M. A. *Catalysis* **2005**, *18*, 1.
- (41) Centi, G. Selective oxidation pathways at oxide surfaces: the transformation of alkanes on vanadyl pyrophosphate. In *Elementary Reaction Steps in Heterogeneous Catalysis*; Joyner, R. W., van Santen, R. A., Eds.; Springer Science+Business Media Dordrecht; Kluwer Academic Publishers: Vaucluse, France, 1993.
- (42) Fu, G.; Xu, X.; Wan, H. *Catal. Today* **2006**, *117*, 133.
- (43) Agaskar, P. A.; DeCaul, L.; Grasselli, R. K. *Catal. Lett.* **1994**, *23*, 339.
- (44) Fu, G.; Xu, X. Mechanistic Insights into Selective Oxidation of Light Alkanes by Transition Metal Compounds/Complexes. In *Computational Organometallic Chemistry*; Wiest, O., Wu, Y., Eds.; Springer-Verlag: Berlin Heidelberg, Germany, 2012.
- (45) Coperet, C. *Chem. Rev.* **2010**, *110*, 656.
- (46) Thomas, J. M.; Raja, R. *Chem. Commun.* **2001**, 675.
- (47) Sheldon, R. A.; Kochi, J. K. *Metal-Catalyzed Oxidations of Organic Compounds: Mechanistic Principles and Synthetic Methodology Including Biochemical Processes*; Academic Press: New York, 1981.
- (48) Hill, C. L. In *Advances in Oxygenated Processes*; Baumstark, A. L., Ed.; JAI Press: Greenwich, CT, 1988; Vol. 1, Chapter I.
- (49) Hudlicky, M. *Oxidations in Organic Chemistry*; American Chemical Society: Washington, DC, 1990.
- (50) Romao, C. C.; Kuhn, F. E.; Herrmann, W. A. *Chem. Rev.* **1997**, *97*, 3197.
- (51) Ishii, Y.; Sakaguchi, S.; Iwahama, T. *Adv. Synth. Catal.* **2001**, *343*, 393.
- (52) Chen, K.; Costas, M.; Que, L. *J. Chem. Soc., Dalton Trans.* **2002**, *672*.
- (53) Corma, A.; Garcia, H. *Chem. Rev.* **2002**, *102*, 3837.
- (54) De Vos, D. E.; Sels, B. F.; Jacobs, P. A. *Adv. Catal.* **2002**, *46*, 1.
- (55) Bregeault, J. M. *Dalton Trans.* **2003**, 3289.
- (56) Böckvall, J.-E. *Modern Oxidation Methods*; Wiley-VCH: Weinheim, 2004.
- (57) de Bruin, B.; Budzelaar, P. H. M.; Gal, A. W. *Angew. Chem., Int. Ed.* **2004**, *43*, 4142.
- (58) Sibbons, K. F.; Shastri, K.; Watkinson, M. *Dalton Trans.* **2006**, *645*.
- (59) Shilov, A. E.; Shul'pin, G. B. *Chem. Rev.* **1997**, *97*, 2879.
- (60) Hashiguchi, B. G.; Bischof, S. M.; Konnick, M. M.; Periana, R. A. *Acc. Chem. Res.* **2012**, *45*, 885.
- (61) Periana, R. A.; Taube, D. J.; Evitt, E. R.; Loffler, D. G.; Wentzcek, P. R.; Voss, G.; Masuda, T. *Science* **1993**, *259*, 340.
- (62) Catlow, C. R. A.; French, S. A.; Sokol, A. A.; Thomas, J. M. *Philos. Trans. R. Soc., A* **2005**, *363*, 913.
- (63) Kasztelan, S.; Moffat, J. B. *J. Catal.* **1987**, *106*, 512.
- (64) Moffat, J. B. *Stud. Surf. Sci. Catal.* **1988**, *35*, 139.

- (65) Moffat, J. B. *Proceedings of a Symposium on the Production of Fuels and Chemicals from Natural Gas*; Elsevier: Amsterdam, 1988.
- (66) Ahmed, S.; Moffat, J. B. *Appl. Catal.* **1988**, *40*, 101.
- (67) Moffat, J. B.; Kasztelan, S. *J. Catal.* **1988**, *109*, 206.
- (68) Kasztelan, S.; Moffat, J. B. *J. Catal.* **1988**, *112*, 54.
- (69) Payen, E.; Moffat, J. B. *J. Catal.* **1988**, *112*, 320.
- (70) Kasztelan, S.; Moffat, J. B. *Partial Oxidation of Methane by Nitrous Oxide or Oxygen over Silica-Supported 12-Molybdochosphoric Acid*; Chemical Institute of Canada: Ottawa, 1988.
- (71) Kasztelan, S.; Moffat, J. B. *J. Catal.* **1989**, *116*, 82.
- (72) Kasztelan, S.; Payen, E.; Moffat, J. B. *J. Catal.* **1991**, *128*, 479.
- (73) Kasztelan, S.; Payen, E.; Moffat, J. B. *J. Catal.* **1990**, *125*, 45.
- (74) Ahmed, S.; Kasztelan, S.; Moffat, J. B. *Faraday Discuss.* **1989**, *87*, 23.
- (75) Ahmed, S.; Moffat, J. B. *J. Phys. Chem.* **1989**, *93*, 2542.
- (76) Ahmed, S.; Moffat, J. B. *J. Catal.* **1989**, *118*, 281.
- (77) Ahmed, S.; Moffat, J. B. *Appl. Catal.* **1989**, *54*, 241.
- (78) Ahmed, S.; Moffat, J. B. *Catal. Lett.* **1988**, *1*, 141.
- (79) Pei, S. P.; Yue, B.; Qian, L. P.; Yan, S. R.; Cheng, J. F.; Zhou, Y.; Xie, S. H.; He, H. Y. *Appl. Catal., A* **2007**, *329*, 148.
- (80) Parmaliana, A.; Arena, F. *J. Catal.* **1997**, *167*, 57.
- (81) Spencer, N. D.; Pereira, C. J. *J. Catal.* **1989**, *116*, 399.
- (82) Benlounes, O.; Mansouri, S.; Rabia, C.; Hocine, S. *J. Nat. Gas Chem.* **2008**, *17*, 309.
- (83) Min, J. S.; Ishige, H.; Misono, M.; Mizuno, N. *J. Catal.* **2001**, *198*, 116.
- (84) Mizuno, N.; Ishige, H.; Seki, Y.; Misono, M.; Suh, D. J.; Han, W.; Kudo, T. *Chem. Commun.* **1997**, 1295.
- (85) Sun, M.; Zhang, J. Z.; Zhang, Q. H.; Wang, Y.; Wan, H. L. *Chem. Commun.* **2009**, 5174.
- (86) Park, S.; Baeck, S. H.; Kim, T. J.; Chung, Y. M.; Oh, S. H.; Song, I. K. *J. Mol. Catal. A: Chem.* **2010**, *319*, 98.
- (87) Park, S.; Park, D. R.; Choi, J. H.; Kim, T. J.; Chung, Y. M.; Oh, S. H.; Song, I. K. *J. Mol. Catal. A: Chem.* **2010**, *332*, 76.
- (88) Park, S.; Park, D. R.; Choi, J. H.; Kim, T. J.; Chung, Y. M.; Oh, S. H.; Song, I. K. *J. Mol. Catal. A: Chem.* **2011**, *336*, 78.
- (89) Mizuno, N.; Misono, M.; Nishiyama, Y.; Seki, Y.; Kiyoto, I.; Nozaki, C. *Res. Chem. Intermed.* **2000**, *26*, 193.
- (90) Seki, Y.; Mizuno, N.; Misono, M. *Appl. Catal., A* **2000**, *194*, 13.
- (91) Seki, Y.; Min, J. S.; Misono, M.; Mizuno, N. *J. Phys. Chem. B* **2000**, *104*, 5940.
- (92) Seki, Y.; Mizuno, N.; Misono, M. *Chem. Lett.* **1998**, 1195.
- (93) Seki, Y.; Mizuno, N.; Misono, M. *Appl. Catal., A* **1997**, *158*, L47.
- (94) Mizuno, N.; Seki, Y.; Nishiyama, Y.; Kiyoto, I.; Misono, M. *J. Catal.* **1999**, *184*, 550.
- (95) Shu, L. J.; Nesheim, J. C.; Kauffmann, K.; Munck, E.; Lipscomb, J. D.; Que, L. *Science* **1997**, *275*, 515.
- (96) Wallar, B. J.; Lipscomb, J. D. *Chem. Rev.* **1996**, *96*, 2625.
- (97) Piao, D.; Inoue, K.; Shibasaki, H.; Taniguchi, Y.; Kitamura, T.; Fujiwara, Y. *J. Organomet. Chem.* **1999**, *574*, 116.
- (98) Kitamura, T.; Piao, D. G.; Taniguchi, Y.; Fujiwara, Y. *Stud. Surf. Sci. Catal.* **1998**, *119*, 301.
- (99) Rosenzweig, A. C.; Frederick, C. A.; Lippard, S. J.; Nordlund, P. *Nature* **1993**, *366*, 537.
- (100) Mizuno, N.; Kiyoto, I.; Nozaki, C.; Misono, M. *J. Catal.* **1999**, *181*, 171.
- (101) Bar-Nahum, I.; Khenkin, A. M.; Neumann, R. *J. Am. Chem. Soc.* **2004**, *126*, 10236.
- (102) Neumann, R.; Khenkin, A. M. *Chem. Commun.* **2006**, 2529.
- (103) Bañares, M. A. *Catal. Today* **1999**, *51*, 319.
- (104) Li, X.; Iglesia, E. *J. Phys. Chem. C* **2008**, *112*, 15001.
- (105) Moffat, J. B. *Appl. Catal., A* **1996**, *146*, 65.
- (106) Mizuno, N.; Suh, D. J.; Han, W.; Kudo, T. *J. Mol. Catal. A: Chem.* **1996**, *114*, 309.
- (107) Mizuno, N.; Han, W. C.; Kudo, T. *J. Catal.* **1998**, *178*, 391.
- (108) Min, J. S.; Mizuno, N. *Catal. Today* **2001**, *66*, 47.
- (109) Mizuno, N.; Han, W.; Kudo, T. *Chem. Lett.* **1996**, 1121.
- (110) Min, J. S.; Mizuno, N. *Catal. Today* **2001**, *71*, 89.
- (111) Albonetti, S.; Cavani, F.; Trifirò, F.; Koutyrev, M. *Catal. Lett.* **1995**, *30*, 253.
- (112) Koutyrev, M.; Cavani, F.; Trifirò, F. European Patent EP 0544372; Eniricerche S.P.A.: Italy, 1993.
- (113) Nowinska, K.; Waclaw, A.; Sopa, M.; Klak, M. *Catal. Lett.* **2002**, *78*, 347.
- (114) Hong, S. S.; Moffat, J. B. *Appl. Catal., A* **1994**, *109*, 117.
- (115) Sopa, A.; Waclaw-Held, A.; Grossy, M.; Pijanka, J.; Nowinska, K. *Appl. Catal., A* **2005**, *285*, 119.
- (116) Galownia, J. M.; Wight, A. P.; Blanc, A.; Labinger, J. A.; Davis, M. E. *J. Catal.* **2005**, *236*, 356.
- (117) Dillon, C. J.; Holles, J. H.; Davis, R. J.; Labinger, J. A.; Davis, M. E. *J. Catal.* **2003**, *218*, 54.
- (118) Holles, J. H.; Dillon, C. J.; Labinger, J. A.; Davis, M. E. *J. Catal.* **2003**, *218*, 42.
- (119) Davis, M. E.; Dillon, C. J.; Holles, J. H.; Labinger, J. *Angew. Chem., Int. Ed.* **2002**, *41*, 858.
- (120) Oshihara, K.; Nakamura, Y.; Sakuma, M.; Ueda, W. *Catal. Today* **2001**, *71*, 153.
- (121) Cassidy, F. E.; Hodnett, B. K. *CATTECH* **1998**, *2*, 173.
- (122) Kung, H. H. *Adv. Catal.* **1994**, *40*, 1.
- (123) Cavani, F.; Trifirò, F. *Catal. Today* **1995**, *24*, 307.
- (124) Albonetti, S.; Cavani, F.; Trifirò, F. *Catal. Rev.: Sci. Eng.* **1996**, *38*, 413.
- (125) Chen, K. D.; Bell, A. T.; Iglesia, E. *J. Phys. Chem. B* **2000**, *104*, 1292.
- (126) Chen, K. D.; Iglesia, E.; Bell, A. T. *J. Phys. Chem. B* **2001**, *105*, 646.
- (127) Wachs, I. E.; Wechuysen, B. M. *Appl. Catal., A* **1997**, *157*, 67.
- (128) Eon, J. G.; Olier, R.; Volta, J. C. *J. Catal.* **1994**, *145*, 318.
- (129) Balsko, T.; Lopez Nieto, J. M. *Appl. Catal., A* **1997**, *157*, 117.
- (130) Fu, H.; Liu, Z. P.; Li, Z. H.; Wang, W. N.; Fan, K. N. *J. Am. Chem. Soc.* **2006**, *128*, 11114.
- (131) Cheng, M. J.; Chenoweth, K.; Osgaard, J.; van Duin, A.; Goddard, W. A. *J. Phys. Chem. C* **2007**, *111*, 5115.
- (132) Yoon, Y. S.; Ueda, W.; Moro-oka, Y. *Catal. Lett.* **1995**, *35*, 57.
- (133) Gilardoni, F.; Bell, A. T.; Chakraborty, A.; Boulet, P. *J. Phys. Chem. B* **2000**, *104*, 12250.
- (134) Redfern, P. C.; Zapol, P.; Sternberg, M.; Adiga, S. P.; Zygmunt, S. A.; Curtiss, L. A. *J. Phys. Chem. B* **2006**, *110*, 8363.
- (135) Bettahar, M. M.; Costentin, G.; Savary, L.; Lavalle, J. C. *Appl. Catal., A* **1996**, *145*, 1.
- (136) Mizuno, N.; Suh, D. J. *Appl. Catal., A* **1996**, *146*, L249.
- (137) Sun, M.; Zhang, J. Z.; Cao, C. J.; Zhang, Q. H.; Wang, Y.; Wan, H. L. *Appl. Catal., A* **2008**, *349*, 212.
- (138) Zhang, J. Z.; Sun, M. A.; Cao, C. J.; Zhang, Q. H.; Wang, Y.; Wan, H. L. *Appl. Catal., A* **2010**, *380*, 87.
- (139) Nowinska, K.; Sopa, M.; Waclaw, A.; Szuba, D. *Appl. Catal., A* **2002**, *225*, 141.
- (140) Dimitratos, N.; Védrine, J. C. *Appl. Catal., A* **2003**, *256*, 251.
- (141) Dimitratos, N.; Védrine, J. C. *Catal. Today* **2003**, *81*, 561.
- (142) Nikos, N.; Védrine, J. C. *Applied Catalysis*; Royal Society Chemistry of Great Britain: London, 2003.
- (143) Zhang, Q.; Cao, C.; Sun, M.; Zhang, J.; Wang, Y.; Wan, H. China Patent CN101219389 B, 2008.
- (144) Zhang, Q. H.; Cao, C. J.; Xu, T.; Sun, M.; Zhang, J. H.; Wang, Y.; Wan, H. L. *Chem. Commun.* **2009**, 2376.
- (145) Burrington, J. D.; Kartisek, C. T.; Grasselli, R. K. *J. Catal.* **1980**, *63*, 235.
- (146) Grasselli, R. K.; Burrington, J. D.; Brazdil, J. F. *Faraday Discuss. Chem. Soc.* **1981**, *72*, 203.
- (147) Kim, Y. C.; Ueda, W.; Moro-oka, Y. *Appl. Catal.* **1991**, *70*, 175.
- (148) Kim, Y. C.; Ueda, W.; Moro-oka, Y. *Stud. Surf. Sci. Catal.* **1990**, *55*, 491.
- (149) Kim, Y. C.; Ueda, W.; Moro-oka, Y. *Catal. Today* **1992**, *13*, 673.
- (150) Conner, W. C., Jr.; Soled, S.; Signorelli, A. *Stud. Surf. Sci. Catal.* **1991**, *7*, 1224.
- (151) Komatsu, T.; Uragami, Y.; Otsuka, K. *Chem. Lett.* **1988**, 1903.

- (152) Takita, Y.; Yamashita, H.; Moritaka, K. *Chem. Lett.* **1989**, 1733.
- (153) Mazari, T.; Marchal, C. R.; Hocine, S.; Salhi, N.; Rabia, C. J. *Nat. Gas Chem.* **2009**, 18, 319.
- (154) Ueda, W.; Suzuki, Y. *Chem. Lett.* **1995**, 541.
- (155) Li, W.; Oshihara, K.; Ueda, W. *Appl. Catal., A* **1999**, 182, 357.
- (156) Vitry, D.; Dubois, J. L.; Ueda, W. *J. Mol. Catal. A: Chem.* **2004**, 220, 67.
- (157) Ueda, W.; Suzuki, Y.; Lee, W.; Imaoka, S. *Stud. Surf. Sci. Catal.* **1996**, 101, 1065.
- (158) Mizuno, N.; Tateishi, M.; Iwamoto, M. *Appl. Catal., A* **1995**, 128, L165.
- (159) Dimitratos, N.; Védrine, J. C. *J. Mol. Catal. A: Chem.* **2006**, 255, 184.
- (160) Dimitratos, N.; Védrine, J. C. *Catal. Commun.* **2006**, 7, 811.
- (161) Li, X. K.; Zhao, J.; Ji, W. J.; Zhang, Z. B.; Chen, Y.; Au, C. T.; Han, S.; Hibst, H. *J. Catal.* **2006**, 237, 58.
- (162) Eldredge, J. L.; Link, R. D., III; Volpe, A. F., Jr. European Patent EP 1059276; Rohm and Haas Co.; Sunoco, Inc. R and M: U.S., 2000.
- (163) Lyons, J. E.; Volpe, A. F.; Ellis, P. E., Jr.; Karmakar, S. U.S. Patent US5990348; Sunoco, Inc.; Rohm and Haas Co.: U.S., 1999.
- (164) Ellis, P. E.; Karmakar, S.; Link, R. D., III; Lyons, J. E.; McNeal, N. N.; Volpe, A. F., Jr. European Patent EP 1077082; Rohm and Haas Co.; Sunoco, Inc. R & M: U.S., 2001.
- (165) Karmakar, S.; Volpe, A. F., Jr.; Ellis, P. E., Jr.; Lyons, J. E. U.S. Patent US 6043184; Sunoco, Inc. R&M; Rohm and Haas Co.: U.S., 2000.
- (166) Wijesekera, T. P.; Lyons, J. E.; Ellis, P. E., Jr. U.S. Patent US 6060419; Rohm and Haas Co.; Sunoco, Inc. R&M: U.S., 2000.
- (167) Jiang, H. S.; Mao, X.; Xie, S. J.; Zhong, B. K. *J. Mol. Catal. A: Chem.* **2002**, 185, 143.
- (168) Takahashi, M.; To, S.; Hirose, T. U.S. Patent 6,060,422; Toa Gosei Chemical Industry Co., Ltd.: Japan, 1998.
- (169) Ushikubo, T.; Nakamura, H.; Koyasu, Y.; Wajiki, S. U.S. Patent 5,380,933; Mitsubishi Kasei Corp.: Japan, 1994.
- (170) Birkeland, K. E.; Babitz, S. M.; Bethke, G. K.; Kung, H. H. *J. Phys. Chem. B* **1997**, 101, 6895.
- (171) Centi, G. *Catal. Today* **1993**, 16, 5.
- (172) Cavani, F.; Trifirò, F. *Catalysis* **1994**, 11, 246.
- (173) Abon, M.; Volta, J.-C. *Appl. Catal.* **1997**, 157, 173.
- (174) Hutchings, G. J.; Kiely, C. J.; Sananes-Schulz, M. T.; Burrows, A.; Volta, J. C. *Catal. Today* **1998**, 40, 273.
- (175) Herrmann, J. M.; Vernoux, P.; Bére, K. E.; Abon, M. *J. Catal.* **1997**, 167, 106.
- (176) Hutchings, G. J.; Sananes, M. T.; Sajip, S.; Kiely, C. J.; Burrows, A.; Ellison, I. J.; Volta, J. C. *Catal. Today* **1997**, 33, 161.
- (177) Ait-Lachgar, K.; Tuel, A.; Brun, M.; Herrmann, J. M.; Krafft, J. M.; Martin, J. R.; Volta, J. C.; Abon, M. *J. Catal.* **1998**, 177, 224.
- (178) Hutchings, G. J.; Desmarth-Chomel, A.; Oller, R.; Volta, J. C. *Nature* **1994**, 368, 41.
- (179) Gai, P. L.; Kourtakis, K. *Science* **1995**, 267, 661.
- (180) Coulston, G. W.; Bare, S. R.; Kung, H. H.; Birkeland, K. E.; Bethke, G. K.; Harlow, R.; Herron, N.; Lee, P. L. *Science* **1997**, 275, 191.
- (181) Cavani, F.; Trifirò, F. *Appl. Catal.* **1992**, 88, 115.
- (182) Centi, G.; Trifirò, F. *J. Mol. Catal.* **1986**, 35, 255.
- (183) Schiøtt, B.; Jørgensen, A.; Hoffmann, R. *J. Phys. Chem.* **1991**, 95, 2297.
- (184) Casarini, D.; Centi, G.; Jiru, P.; Lena, V.; Tvaruzkova, Z. *J. Catal.* **1993**, 143, 325.
- (185) Ledoux, M. *J. Catal.* **2001**, 203, 495.
- (186) Centi, G.; Lena, V.; Trifirò, F.; Ghoussoub, D.; Aissi, C. F.; Guelton, M.; Bonnelle, J. P. *J. Chem. Soc., Faraday Trans.* **1990**, 86, 2775.
- (187) Ai, M. *Congress on Catalysis*, 8th ed.; DECHEMA Monogr.: Berlin, 1984; Vol. 5, p 475.
- (188) Takita, Y.; Qing, X.; Takami, A.; Nishiguchi, H.; Nagaoka, K. *Appl. Catal., A* **2005**, 296, 63.
- (189) Słoczyński, J.; Grzybowska, B.; Grabowski, R.; Kozłowska, A.; Wcisło, K. *Phys. Chem. Chem. Phys.* **1999**, 1, 333.
- (190) Cavani, F.; Comuzzi, C.; Dolcetti, G.; Etienne, E.; Finke, R. G.; Selleri, G.; Trifirò, F.; Trovarelli, A. *J. Catal.* **1996**, 160, 317.
- (191) Cavani, F.; Mezzogori, R.; Trovarelli, A. *J. Mol. Catal. A: Chem.* **2003**, 204, 599.
- (192) Takita, Y.; Kuroski, K.; Mizuhara, Y.; Ishihara, T. *Chem. Lett.* **1993**, 335.
- (193) Michalakos, P. M.; Kung, M. C.; Jahan, I.; Kung, H. *J. Catal.* **1993**, 140, 226.
- (194) Uddin, M. A.; Komatsu, T.; Yashima, T. *J. Catal.* **1994**, 150, 439.
- (195) Zhang, W. D.; Tang, D. L.; Zhou, X. P.; Wan, H. L.; Tsai, K. R. *J. Chem. Soc., Chem. Commun.* **1994**, 771.
- (196) Zhang, Q.; Xu, T.; Cao, C.; Sun, M.; Zhang, J.; Wang, Y.; Wan, H. China Patent CN101439292 B, 2009.
- (197) Huerta, L. J.; Amoros, P.; Beltran-Porter, D.; Corberan, V. C. *Catal. Today* **2006**, 117, 180.
- (198) Busca, G.; Cavani, F.; Etienne, E.; Finocchio, E.; Galli, A.; Selleri, G.; Trifirò, F. *J. Mol. Catal. A: Chem.* **1996**, 114, 343.
- (199) Mizuno, N.; Tateishi, M.; Iwamoto, M. *J. Catal.* **1996**, 163, 87.
- (200) Mizuno, N.; Yahiro, H. *J. Phys. Chem. B* **1998**, 102, 437.
- (201) Knapp, C.; Ui, T.; Nagai, K.; Mizuno, N. *Catal. Today* **2001**, 71, 111.
- (202) Deng, Q.; Jiang, S. L.; Cai, T. J.; Peng, Z. S.; Fang, Z. *J. Mol. Catal. A: Chem.* **2005**, 229, 165.
- (203) Langpape, M.; Millet, J. M. M.; Ozkan, U. S.; Delichere, P. *J. Catal.* **1999**, 182, 148.
- (204) Langpape, M.; Millet, J. M. M. *Appl. Catal., A* **2000**, 200, 89.
- (205) Huynh, Q.; Selmi, A.; Corbel, G.; Lacorre, P.; Millet, J. M. M. *J. Catal.* **2009**, 266, 64.
- (206) Huynh, Q.; Schuurman, Y.; Delichere, R.; Lordinat, S.; Millet, J. M. M. *J. Catal.* **2009**, 261, 166.
- (207) Cavani, F.; Mezzogori, R.; Pigamo, A.; Trifirò, F. *C. R. Acad. Sci., Ser. IIc: Chim.* **2000**, 3, 523.
- (208) Cavani, F.; Mezzogori, R.; Pigamo, A.; Trifirò, F. *Stud. Surf. Sci. Catal.* **2001**, 140, 141.
- (209) Cavani, F.; Mezzogori, R.; Pigamo, A.; Trifirò, F. *Top. Catal.* **2003**, 23, 119.
- (210) Cavani, F.; Etienne, E.; Favaro, M.; Galli, A.; Trifirò, F.; Hecquet, G. *Catal. Lett.* **1995**, 32, 215.
- (211) Etienne, E.; Cavani, F.; Mezzogori, R.; Trifirò, F.; Calestani, G.; Gengembre, L.; Guelton, M. *Appl. Catal., A* **2003**, 256, 275.
- (212) Krieger, H.; Kirch, L. S. U.S. Patent 4,260,822; Rohm and Haas Co.: U.S., 1980.
- (213) Yamamatsu, S.; Yamaguchi, T. European Patent EP 0425666; Asahi Chemical Industry Co., Ltd.: Japan, 1990.
- (214) Yamamatsu, S.; Yamaguchi, T. U.S. Patent 5,191,116; Asahi Chemical Industry Co., Ltd.: Japan, 1993.
- (215) Kawakami, K.; Yamamatsu, S.; Yamaguchi, T. Japan Patent 03176438; Asahi Chemical Industry Co., Ltd.: Japan, 1991.
- (216) Nagai, K.; Nagaoka, Y.; Sato, H.; Ohsu, M. European Patent 418657; Sumitomo Chemical Co., Ltd.: Japan, 1991.
- (217) Imai, H.; Nakatsuka, M.; Aoshima, A. European Patent 62132832; Asahi Chemical Industry Co., Ltd.: Japan, 1987.
- (218) Bielmeier, E.; Haeberle, T.; Siegert, H.-J.; Gruber, W. German Patent 4240085; Rohm GmbH: Germany, 1994.
- (219) Mizuno, N.; Tateishi, M.; Iwamoto, M. *Appl. Catal., A* **1994**, 118, L1.
- (220) Li, W.; Ueda, W. *Catal. Lett.* **1997**, 46, 261.
- (221) Jalowiecki-Duhamel, L.; Monnier, A.; Barbaux, Y.; Hecquet, G. *Catal. Today* **1996**, 32, 237.
- (222) Schindler, G. P.; Knapp, C.; Ui, T.; Nagai, K. *Top. Catal.* **2003**, 22, 117.
- (223) Paul, S.; Chu, W.; Sultan, M.; Bordes-Richard, E. *Sci. China: Chem.* **2010**, 53, 2039.